

SUBMITTED TO:  
Anchor QEA, LLC  
1201 3rd Avenue, Suite 2600  
Seattle, WA 98101

BY:  
Shannon & Wilson  
400 N 34th Street, Suite 100  
Seattle, WA 98103

(206) 632-8020  
[www.shannonwilson.com](http://www.shannonwilson.com)

DRAFT

FAULT HAZARD EVALUATION REPORT  
**Dungeness Off-Channel Reservoir**  
SEQUIM, WASHINGTON

Submitted To: Anchor QEA, LLC  
1201 3rd Avenue, Suite 2600  
Seattle, WA 98101  
Attn: David Rice, PE, and Robert Montgomery, PE

Subject: DRAFT FAULT HAZARD EVALUATION REPORT, DUNGENESS  
OFF-CHANNEL RESERVOIR, SEQUIM, WASHINGTON

This report presents the results of our fault hazard evaluation for the Dungeness Off-Channel Reservoir Project in Clallam County, Washington. Shannon & Wilson prepared this report and participated in this project as a subconsultant to Anchor QEA, LLC. Our scope of services for this task was mutually developed over a period of weeks in late 2023 and authorized to proceed via email on December 6, 2023. Budget to perform this fault hazard evaluation used funds reallocated from funds authorized for Phase 2 services under Amendment No. 3, executed June 27, 2023, to our subcontract, dated July 29, 2021.

We appreciate the opportunity to be of service to you on this project. If you have questions concerning this report, or we may be of further service, please contact us.

Sincerely,

SHANNON & WILSON



Christopher D. Kemp

Christopher D. Kemp, LEG  
Senior Geologist

CDK:GJH:SRB/eab:srb:wjp



## EXECUTIVE SUMMARY

The Sequim fault, which intersects the project site, was previously mapped at the ground surface but details of the fault were not previously described. The Sequim fault is approximately coincident with a fault identified in previous geophysical studies that extends up to 46 kilometers (km) from west of the Project site to as far east as the southern Whidbey Island fault zone. A previous seismic reflection geophysical survey indicates the fault has been active in the Quaternary and possibly the Holocene. Holocene and postglacial faults have been documented at or near the ground surface in previous studies about 11 km (7 miles) east and west of the Project site and indicate the site area is tectonically active.

- Two east-northeast-striking scarps on the order of 1 to 2.5 meters (m) (3 to 8 feet [ft]) in height cross the alluvial surface within the Project site. Another two lineaments, one of which intersects the north margin of the Project site, appear as broad undulations on the alluvial surface. Some of these features extend across the glacial till surface east of the Project site. Our mapping is consistent with and builds upon the original mapping by Nelson and others (2007). Based on new mapping and ages of Quaternary alluvial surfaces, we interpret the scarps and lineaments to postdate about 7,600 years before present. Flow modelling and field observations indicate that channels on these alluvial surfaces have been vertically displaced across the most prominent scarp, indicating post-depositional (after 7,600 years ago) surface deformation that we interpret as tectonic in origin.
- Regional stresses and geophysical data suggest the Sequim fault is characterized by right-lateral, oblique reverse slip and south to vertical dip direction. Based on similar strikes, scarp morphologies, and subsurface geophysics, we interpret that the Sequim fault is either an eastern continuation of the 80-km-long North Olympic fault zone (NOFZ) or ruptures together with the NOFZ. Based on the Wells and Coppersmith (1994) surface rupture length-displacement scaling relationship and measured per event slip from paleoearthquakes on the NOFZ, we recommend that 5 m per event net slip be considered for potential future earthquakes on the Sequim fault.
- To assist with reservoir configuration selection, we developed surface deformation hazard zones for the Project site and provide recommendations to address interpreted future magnitude and style of deformation. We recommend locating the reservoir to the south of the interpreted fault zone, similar to reservoir location Option D, to reduce hazard and avoid hazard by avoiding the deformation hazard zones. Locating the reservoir south of the interpreted fault zone would also reduce the fieldwork necessary to further assess the hazard.

1 Introduction .....1

1.1 Scope .....1

1.2 Previous Fault Hazard Assessments for the Project .....2

1.3 Regional Geologic History .....4

1.3.1 Olympic Peninsula .....5

1.3.2 Glacial History .....7

1.3.3 Holocene History .....11

1.4 Tectonic Setting .....13

1.4.1 Sequim Fault .....16

1.4.2 North Olympic Fault Zone .....18

1.4.3 Southern Whidbey Island Fault Zone .....21

2 Methodology .....21

2.1 Lidar Data and Derivative Models .....21

2.2 Alluvial Terrace and Lineament Mapping .....23

2.3 Project Site Subsurface Information .....24

3 Results .....24

3.1 Dungeness River Terrace Mapping .....24

3.2 Subsurface Interpretation .....26

3.3 Geomorphic and Lineament Mapping .....27

3.3.1 Lineaments in the Dungeness River Valley .....28

3.3.2 Lineaments in the Eastern Upland Glacial Till Surface .....29

3.3.3 Lineaments in the Western Upland Glacial Till Surface .....30

3.3.4 Lineaments South of Sequim Bay .....31

3.3.5 Lineaments Near Siebert Creek .....31

4 Discussion and Conclusions .....32

4.1 Geomorphic History of the Dungeness River .....32

4.2 Age and Origin of the Project Site Lineaments .....35

4.3 Characterization of Subsurface Structure .....36

5 Implications and Recommendations .....39

5.1 Displacement Estimates .....39

5.2 Surface Fault Rupture Hazard .....42

5.3 Recommendations.....44

6 References .....47

Exhibits

Exhibit 1-1: Elements of the Cascadia Subduction Zone .....5

Exhibit 1-2: Simplified Geologic Map of the Olympic Peninsula.....6

Exhibit 1-3: Extent of the Juan de Fuca and Puget Lobes of the Cordilleran Ice Sheet .....8

Exhibit 1-4: Ice Thickness of the Vashon Stade Glacial Ice.....9

Exhibit 1-5: Relative Sea Level Curve for the Strait of Juan de Fuca .....10

Exhibit 1-6: Paleochannels of the Dungeness River .....12

Exhibit 1-7: Profiles of the Dungeness River and Paleochannels .....13

Exhibit 1-8: Tectonic Escape of the Olympic Mountains Block .....15

Exhibit 1-9: Comparison of Earthquake Timing Along the North Olympic Fault Zone .....20

Exhibit 3-1: Relative Terrace Elevations Above the Modern Dungeness River Channel .....25

Exhibit 3-2: Daisy Trench Site on the Eastern Lake Creek-Boundary Creek Fault.....32

Exhibit 4-1: Characteristics of the Sequim Fault From Previous Studies .....37

Exhibit 4-2: Microseismicity Cross Section of the Puget Sound and Eastern Strait of Juan de Fuca .....38

Exhibit 5-1: Components of Fault Displacement .....40

Tables

Table 1: North Olympic Fault Zone Components of Slip

Table 2: Sequim Fault Components of Displacement

Table 3: Sequim Fault Surface Rupture Length – Average Displacement Relationships

Table 4: Summary of Deformation Hazard Zones

Table 5: Sequim Fault Seismic Source Parameters

Figures

Figure 1: Regional Location Map

Figure 2: Project Location

Figure 3: Regional Faults

Figure 4: Geologic Map of the Site Area

Figure 5: Magnetic Survey of MacLeod and Others (1977)

Figure 6: Seismotectonic Map of Gower and Others (1985)

Figure 7: Schematic Geologic Map of Johnson and Others (1996)

Figure 8:	Seismic Reflection Line and Cross-Section of Johnson and Others (1996)
Figure 9:	Seismic Tomography Map of Brocher and Others (2001)
Figure 10:	Dungeness River Terrace Map
Figure 11:	A – Project Site Terrace Map B – Project Site Terrace Map (REM Base)
Figure 12:	Cross-Section A-A' with Borings
Figure 13:	Cross-Section B-B' with Borings
Figure 14:	Lineament Mapping Index Map
Figure 15:	Scarp and Lineament Map – Dungeness River Valley and Eastern Upland Surface
Figure 16:	Scarp and Lineament Map – Western Upland Surface
Figure 17:	Scarp and Lineament Map – South of Sequim Bay
Figure 18:	Scarp and Lineament Map – Siebert Creek
Figure 19:	Dungeness River Valley and Eastern Upland Surface Topographic Profiles (6 sheets)
Figure 20:	Surface Flow Modeling
Figure 21:	Alluvial Deposits Fold Profile
Figure 22:	Western Upland Surface Topographic Profiles (2 sheets)
Figure 23:	Siebert Creek Topographic Profile
Figure 24:	Fault Structure Cartoon
Figure 25:	Seismic Sources
Figure 26:	A – Deformation Hazard Zone – Reservoir Option A B – Deformation Hazard Zone – Reservoir Option B C – Deformation Hazard Zone – Reservoir Option C D – Deformation Hazard Zone – Reservoir Option D

## Appendices

Appendix A: Geophysical Report  
Important Information

## ACRONYMS

AD	average displacement
BP	before present
DEM	digital elevation model
CA	California
cal.	calibrated (or calendar)
cm	centimeters
DFDHA	deterministic fault displacement hazard analysis
DNR	Department of Natural Resources
DSHA	deterministic seismic hazard analysis
DSO	Dam Safety Office
DSOD	Division of Safety of Dams
Ecology	Washington State Department of Ecology
FERC	Federal Energy Regulatory Commission
GPS	global position system
H:V	Horizontal to Vertical
IDW	inverse distance weighting
km	kilometers
LCBC	Lake Creek-Boundary Creek
lidar	Light detection and ranging
m	meters
ma	million years ago
MASW	multi-channel analysis of surface waves
mm	millimeters
mi	mile(s)
msl	mean sea level
NOFZ	North Olympic fault zone
NSHMP	National Seismic Hazards Mapping Project
PFDHA	probabilistic fault displacement hazard analysis
PSHA	probabilistic seismic hazard analysis
REM	relative elevation model
SRL	surface rupture length
SWIF	southern Whidbey Island fault zone
Qa	Quaternary alluvium
QFFD	Quaternary Fault and Fold Database
USGS	United States Geological Survey

# 1 INTRODUCTION

This report documents our desktop evaluation of surface fault rupture hazard for the Dungeness Off-Channel Reservoir project (Project), Clallam County, Washington. We understand that the proposed Project would construct an off-channel reservoir, or reservoirs, with approximately 1,400- to 1,600-acre-feet of storage south of Sequim, Washington, on a 319-acre parcel currently owned by the Washington State Department of Natural Resources (DNR). The parcel location is shown in Figures 1 and 2. The reservoir would be gravity-fed and store water diverted from the Dungeness River during periods of high flow. The stored water would be released to meet streamflow and irrigation needs in the late summer. The specific reservoir/embankment location and dimensions have not yet been selected. This evaluation focused primarily on the previously mapped Sequim fault, possibly related topographic lineaments at and near the site, and implications for the Project, which could impact reservoir location, configuration, and embankment design.

Clallam County is the Project Owner. Shannon & Wilson is providing geotechnical engineering services for this Project in accordance with our subcontract to Anchor QEA, LLC, dated July 29, 2021.

## 1.1 Scope

The scope of services to complete this report represents the first step of a phased fault investigation that includes the following:

- Step 1 – Supplemental Desktop Study and Initial Report (this report)
- Step 2 – Detailed Trench Planning (if applicable)
- Step 3 – Trench Excavation (if applicable)
- Step 4 – Final Reporting

Step 1 is considered supplemental to a Seismic-Geologic Site Reconnaissance that was completed in several iterations from April through October 2023.

A phased approach was recommended and implemented so that each step would provide information to tailor subsequent steps and levels of effort based on discoveries and conclusions from the preceding phases.

The scope of services for Step 1, documented in this report, included:

1. Compilation and review of relevant published maps, reports, and papers.
2. Acquisition and processing of publicly available light detection and ranging (lidar) data.

3. Development of a geologic and geomorphic history of site vicinity, to include assessment of paleontological, archaeological, and volcanological information to constrain ages of Quaternary stratigraphy.
4. Interpretation of satellite imagery and derivative lidar products to develop a Quaternary geologic map and assess for Quaternary deformation in the site vicinity.
5. Synthesis of new mapping with existing information.
6. Development of recommendations for future services.
7. Reporting.

This evaluation included desktop study only and did not include field investigations.

## 1.2 Previous Fault Hazard Assessments for the Project

Several previous iterations of varying levels of effort were made to evaluate potential surface fault rupture hazards for the Project. Prior to initiating the Project design, Clallam County engaged PanGEO, Inc. to complete a feasibility-level review of geologic hazards near the site. In their focus on seismic considerations, PanGEO completed a review of available geologic information, an initial site reconnaissance, and a follow-up site reconnaissance with geologists from the U.S. Geological Survey (USGS) (PanGEO, 2020). The USGS geologists reviewed lidar topographic data prior to the follow-up site reconnaissance. This effort focused on traces of the Sequim fault mapped, but not described, by Nelson and others (2007) at and near the Project site (Figure 3). The USGS geologists observed “possible, subtle lineaments, but nothing striking” in the lidar according to PanGEO (2020). The site reconnaissance revealed “no certain evidence of past faulting” and “no suggestion of Holocene movements” (PanGEO, 2020). Based on these assessments, PanGEO (2020) concluded “there is no identifiable evidence of faulting in the project area.”

In 2021, Shannon & Wilson reached out to the USGS to confirm the status of the Sequim fault. The USGS Quaternary Fault and Fold Database (QFFD) lacks information on the Sequim fault but classifies the Sequim fault as a Class A fault (USGS and DNR, 2024). This classification is reserved for faults with demonstrable evidence of tectonic origin and Quaternary activity. We understood that the USGS was considering reclassifying the Sequim fault to Class B based on the assessment they conducted in conjunction with PanGEO (2020). Class B is used when there is evidence that demonstrates the existence of a fault or suggests Quaternary deformation. A Class B fault may not be a source of large earthquakes. To date, the Sequim fault remains a Class A fault in the USGS QFFD.

In August 2021, a Shannon & Wilson geologist and engineer performed a field reconnaissance along the steep bluff west of the Project site and east of the Dungeness River,



as well as the east cut bank of the Highland Irrigation District Main Canal southeast of the Project site. This reconnaissance was conducted to aid the geologic characterization of the site (Shannon and Wilson, 2022). They observed glacial till comprising the majority of the slope up to about 2 to 5 meters (m) (6 to 17 feet [ft]) below the top of the bluff. A 2- to 3-m (6- to 8-ft) thick layer of alluvium was overlying the glacial till with a wavy, undulating contact. They also observed glacial till, stratified sand and silt layers, glacial outwash and alluvium exposed in small cuts in the bluff further north. Small fractures, with offsets on the order of up to a few centimeters (cm) were observed in stratified advance glacial outwash deposits exposed in the Dungeness River bluff on the southwest margin of the site (Figure 3).

In April 2023, Shannon & Wilson geologists completed a Seismic-Geologic Site Reconnaissance, which included review of the background information cited in the PanGEO study, analysis and interpretation of lidar topographic data, and a one-day site reconnaissance visit. The results of the reconnaissance were presented to Clallam County in May 2023; these results are summarized below and also incorporated into this report. Several topographic lineaments (i.e., scarps and apparent warps) observed in the lidar data are consistent with, but not necessarily related to, tectonic deformation. These lineaments were identified in the same location and were approximately colinear with traces of the Sequim fault mapped by Nelson and others (2007) and included in the USGS QFFD (USGS and DNR, 2024). The one-day field reconnaissance focused on confirming the presence of the lineaments on the ground surface and an assessment of the Dungeness River bluff for evidence of faulting. The reconnaissance focused on potential scarps and lineaments, identified using the lidar data, that cross Happy Valley and the alluvial deposits at the site. The reconnaissance included inspection of the Dungeness River bluff west of the site and east of the Dungeness River (Figure 4). No evidence of faulting was observed in the bluff, although we did observe the minor fractures described in Shannon & Wilson, (2022), which we interpret as glaciotectionic (i.e., decompression due to off-loading of glacial weight). The presence of a north-facing scarp on the eastern upland glacial surface in Happy Valley was confirmed, and vertically offset and truncated stream channels were identified across a subtle scarp that crosses the Project site. Based on the April 2023 Seismic-Geologic Site Reconnaissance, Shannon & Wilson interpreted a tectonic origin as being the most likely cause for the lineaments, but recognized alternative origins could not be ruled out. Fundamental observations and groundwork for this report were completed during the Seismic-Geologic Site Reconnaissance and have been incorporated into this report. Additional details specific to the field reconnaissance are described throughout this report where relevant.

Our previous interpretation of geologic units shown in figures and boring logs included in our draft Geotechnical Data Report (Shannon & Wilson, 2022) have been modified from our



2023 interpretation following the work completed for this report. Our reinterpretation is based on further study of the geomorphic and depositional history of Dungeness River. We now interpret all normally consolidated deposits above glacial till as postglacial alluvial fan and fluvial deposits, as opposed to glacial recessional outwash deposits directly overlying glacial till, and alluvial fan deposits overlying glacial outwash deposits (Sections 3.2 and 4.1).

Based on the findings of the Seismic-Geologic Site Reconnaissance completed in 2023, additional investigations were deemed necessary to determine the origin of the lineaments and how factors contributing to the creation of the lineaments may impact reservoir design. The results of the Seismic-Geologic Site Reconnaissance were presented to the Washington State Department of Ecology (Ecology) Dam Safety Office (DSO) in October 2023, along with the proposed scope of work for further evaluation of the lineaments. During this meeting, DSO agreed that additional evaluation of the lineaments is necessary and concurred with the proposed scope of work.

This report represents the findings of the first step of the phased fault evaluation for the Project to constrain the origin and age of the lineaments and, if tectonic, assess the hazard and risk posed to the Project.

Herein, we use metric units, which are more commonly used in descriptions of fault and landform dimensions, displacements, and slip rates. We parenthetically cite imperial units, with the exception of millimeters (mm) per year. Profiles and cross sections depict imperial units (feet) because that is the native unit of measurement inherent in the lidar data from which the profiles were extracted.

### 1.3 Regional Geologic History

The Project area lies within the Dungeness River drainage basin on the northeastern part of the Olympic Peninsula (Figure 2). The earliest geologic map covering the entire Olympic Peninsula was a 1:125,000 scale map (Tabor and Cady, 1978). Preliminary geologic maps covering the Project site at a 1:24,000 scale were released in 1979 for the Carlsborg (Othberg and Palmer, 1979a) and Sequim quadrangles (Othberg and Palmer 1979b). Updated versions of these geologic maps, with additional field data, were released in 1998 and 2000 for the Sequim and Carlsborg quadrangles respectively (Schasse and Logan, 1998; Schasse and Wegmann, 2000). For analyzing scarps found west of the Carlsborg quadrangle, we used the 1:24,000 scale geologic map of the Morse Creek quadrangle (Schasse and Polenz, 2002). A 1:100,000 scale geologic map focused on Port Angeles (Schasse, 2003) was used for locations outside of the quads. The geologic maps generally agree with each other, but we primarily use the most recent Sequim (Schasse and Logan, 1998) and Carlsborg (Schasse and

Polenz, 2002) quadrangle maps when describing the surficial geology near the Project site due to their larger scale and greater detail.

### 1.3.1 Olympic Peninsula

The Olympic Peninsula lies in the forearc of the Cascadia Subduction Zone, an oblique convergent margin off the western coast of the Pacific Northwest, stretching from northern California into southern British Columbia (Exhibit 1-1). Tabor and Cady (1978) provided the foundation for subsequent geologic studies on the Olympic Peninsula by dividing the bedrock geology into two general terranes: the peripheral rocks outlining the Olympic Mountains to the north, east, and south, and the core rocks that make up the core of the Olympic Mountains and extend westward to the Pacific Coast (Exhibit 1-2).

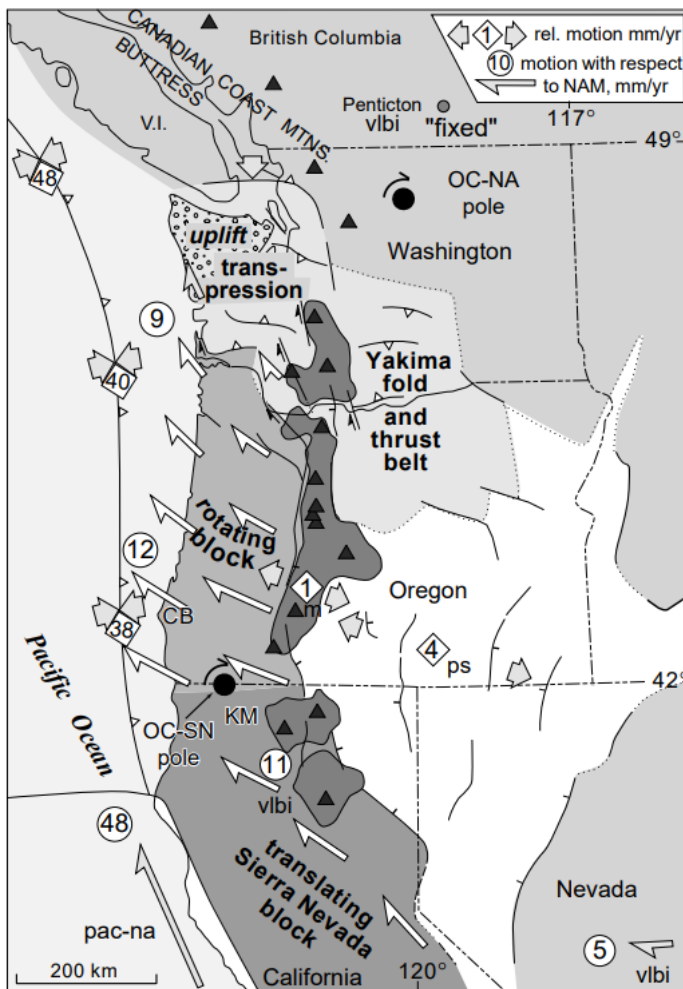


**Exhibit 1-1: Elements of the Cascadia Subduction Zone**

Source: Wells and Simpson (2001)

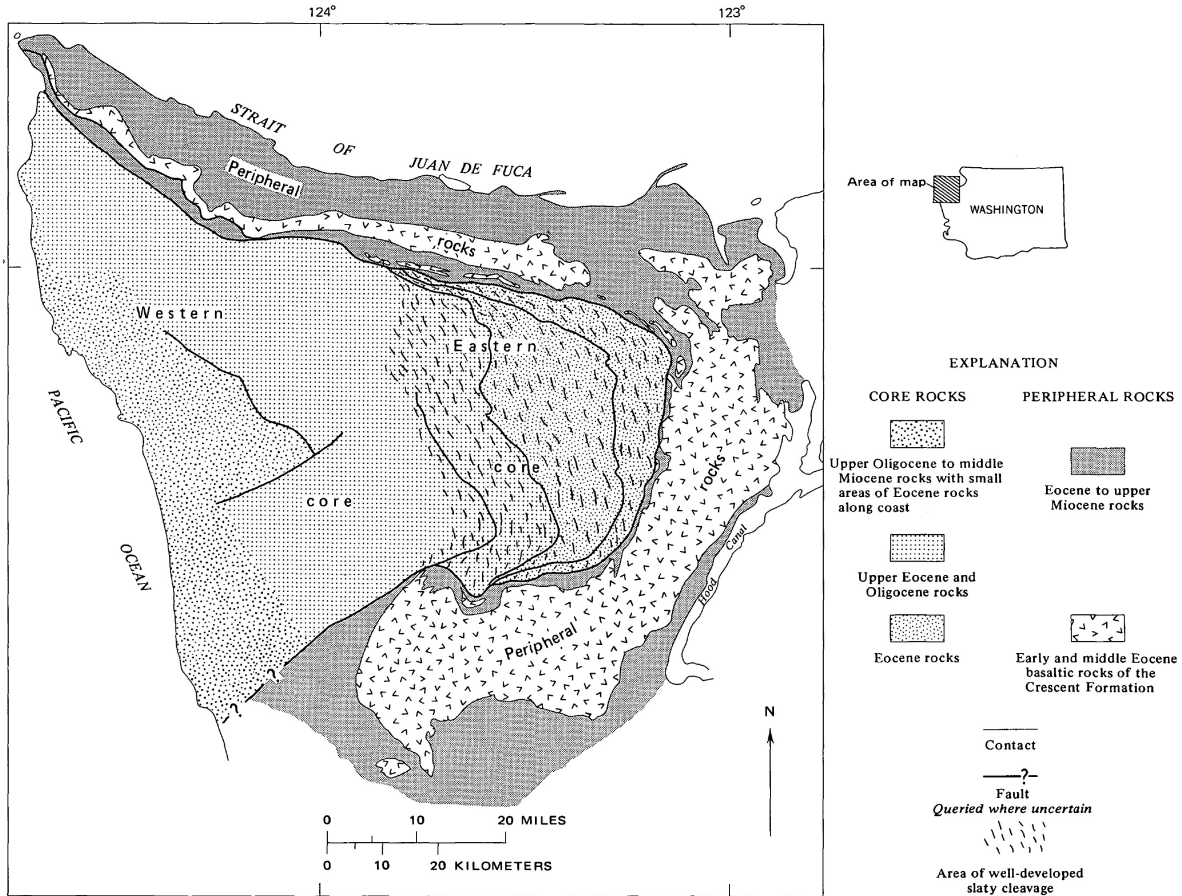


**Exhibit 1-2: Simplified Geologic Map of the Olympic Peninsula**

Source: Tabor and Cady (1978)

The peripheral rocks are composed of the Crescent Formation basalts, which erupted onto the seafloor in the early Eocene, overlain by sedimentary rocks, mostly marine in origin (Tabor and Cady, 1978) (Exhibit 1-2). The origin of the Crescent basalts is not widely agreed upon, but this terrain, sometimes referred to as the “Coast Range” terrain or “Siletzia,” was accreted to North America prior to the initiation of the modern Cascadia Subduction Zone in the middle Eocene, around 42 million years ago (ma) (du Bray and John, 2011; Wells and others, 2014). The peripheral rocks and core rocks are fault contacted by the Hurriganes Ridge Fault, a thrust fault active starting in the late Eocene following the initiation of the Cascadia Subduction Zone (Brandon and others, 1998).

The Crescent Formation forms the northern, eastern, and southern margins of the Olympic Mountains in a crescent shape. Crescent basalt outcrops on the slopes above the Dungeness River beginning approximately 1 kilometer (km) (0.5 mile [mi]) south of the Project site, as well as on Lost Mountain beginning approximately 3 km (2 mi) southwest of the Project site, and on the southern slopes of Bell Hill approximately 3 km east of the Project site (Figure 4). The only other peripheral rocks that outcrop near the Project site, at the crest of Bell Hill and

on its northern slopes, are Eocene- to Miocene-aged sandstone, which is a part of the marine sedimentary rocks overlying the Crescent Formation.

The core rocks are comprised of highly deformed marine sedimentary rocks, the eastern portion interpreted as a western extension of “Siletzia” that was underthrust beneath the Crescent Formation along the Hurricane Ridge Fault, while bedrock to the west has been interpreted as exposed accretionary wedge deposits from the Cascadia Subduction Zone (Brandon and Vance, 1992). These core rocks are exposed in the uppermost reaches of the Dungeness River and its tributaries, beginning approximately 14 km (9 mi) southwest of the Project site.

Both versions of the Sequim and Carlsborg quadrangle maps divide the Dungeness River fan into two units—Quaternary alluvium and Quaternary older alluvium. The raised surfaces on either side of the Dungeness River fan are typically mapped as Vashon glacial till, with occasional Vashon advance and recessional glacial outwash.

The emergence of the Olympic Peninsula above sea level began as early as the middle Miocene between 18 and 16.5 ma (Brandon and Vance, 1998; Shekut and Licht, 2020). The average exhumation rate of the Olympic Peninsula has been estimated at ~0.28 km/ma, while modern erosion rates have been estimated between 0.18 – 0.32 km/ma from two major rivers in the Olympic mountains (Brandon and Vance, 1998). These comparable rates suggest that the mountain range is in a topographic steady state and has been since about 14 ma.

### 1.3.2 Glacial History

During the Quaternary there have been multiple glacial advances and retreats of the Cordilleran ice sheet into and out of the Puget Lowlands and the Strait of Juan de Fuca (Schasse and Logan, 1998; Schasse and Wegmann, 2000; Booth and others, 2004) (see Exhibit 1-3). The Fraser Glaciation is the most recent glaciation, beginning approximately 28,000 years ago and is associated with extensive deposition and erosion obscuring the surficial features left from prior glaciations. The Vashon Stade of the Fraser Glaciation is the period when the Cordilleran ice sheet expanded southwards and crossed the 49th Parallel (i.e., U.S.-Canadian border) approximately 18,700 calibrated (i.e., or calendar) years before present (cal. years BP) (Porter and Swanson, 1998), followed by the postglacial Everson Interstade.

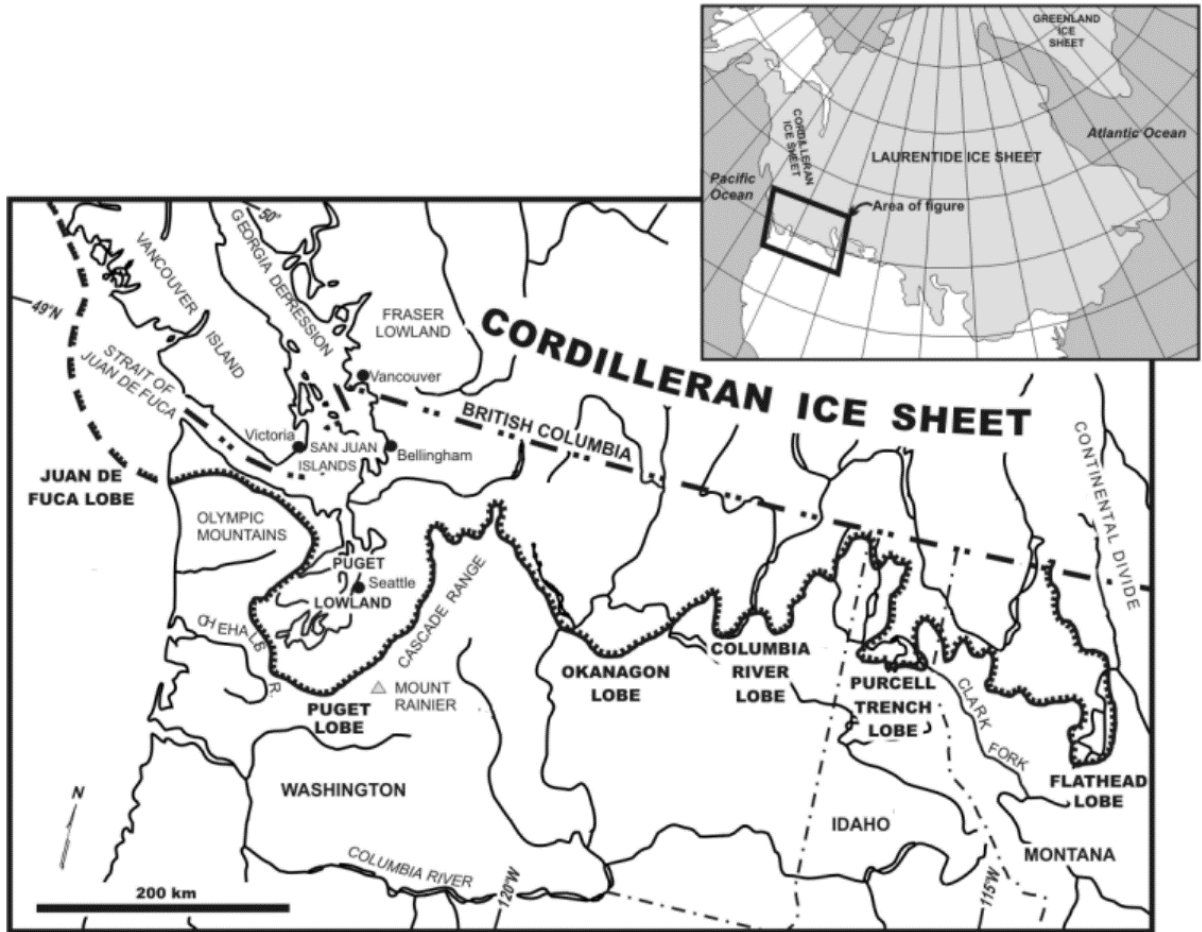
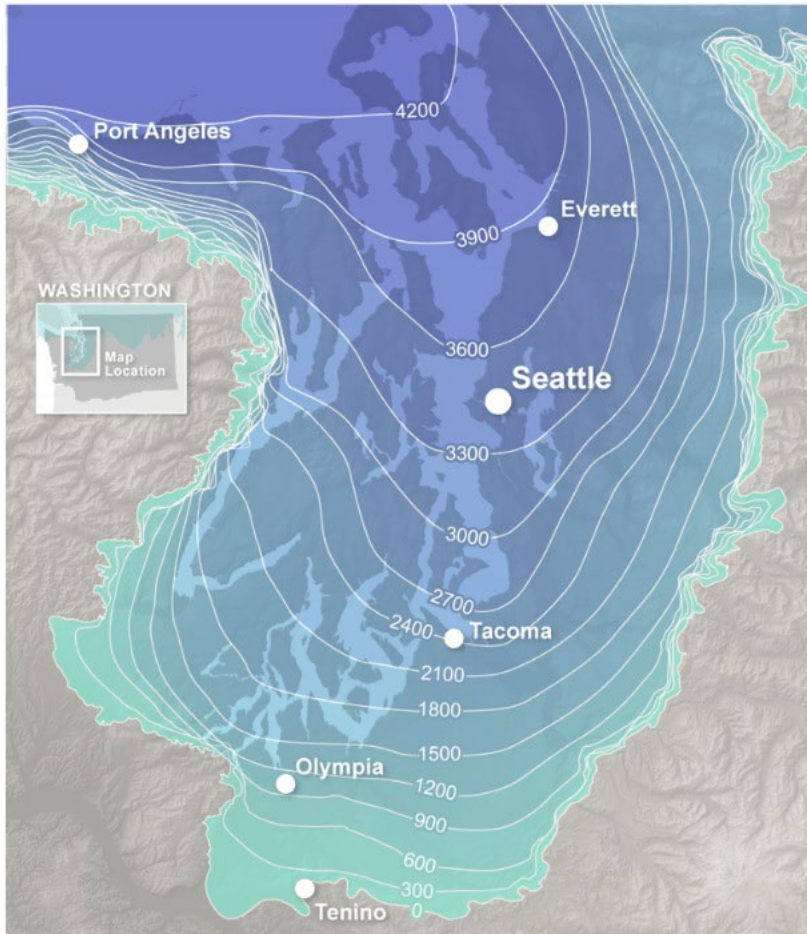


Exhibit 1-3: Extent of the Juan de Fuca and Puget Lobes of the Cordilleran Ice Sheet

Source: Booth and others (2004)





**Exhibit 1-4: Ice Thickness of the Vashon Stage Glacial Ice**

Source: DNR (n.d.)

The ice sheet diverged into two parts with the Puget lobe advancing southwards south over Puget Sound and the Juan de Fuca lobe advancing westward, approximately 16 to 19 km (10 to 12 mi) into the Pacific Ocean beyond Cape Flattery, covering the Strait and the northern Olympic Peninsula (Bretz, 1920) (Exhibit 1-3). Inference from glacial landforms at a point south of the Project site show that the southern margin of the Juan de Fuca lobe reached a maximum elevation of 1,174 m (3,852 ft) above sea level (Thorson, 1980) (Exhibit 1-4). The thickness of the Juan de Fuca lobe has been estimated to be between 1,100 and 1,200 m (3,600 and 3,900 ft) thick near its separation with the Puget lobe (Alley and Chatwin, 1979) (Exhibit 1-4).

The Juan de Fuca lobe reached its maximum extent between 15,670 and 14,900 cal. years BP based on reinterpreted radiocarbon dates from the northwestern Olympic Peninsula near Lake Ozette (Heusser, 1973; Haugerud, 2021). Deglaciation of the Juan de Fuca lobe likely began within a few hundred years of the maximum extent. Postglacial wood ages near Bellingham, Washington, indicate ice-free conditions in the northern Puget Sound by

14,300 cal. years BP (Kovanen and Easterbrook, 2001). The Dungeness River was deglaciated before approximately 13,800 cal. years BP based on radiocarbon dating of Mastodon remains found in a kettle pond on a glacial till surface approximately 1.6 km (1 mi) east of the Project site (Waters and others, 2011) (Figure 4). Seeds and wood found in the pond sediments collected 3 cm (1.2 inches) above the glacial till floor of the pond were also dated, with a maximum age of 12,100 ± 310 cal. years BP (Gustafson, 1979; Petersen, 1983).

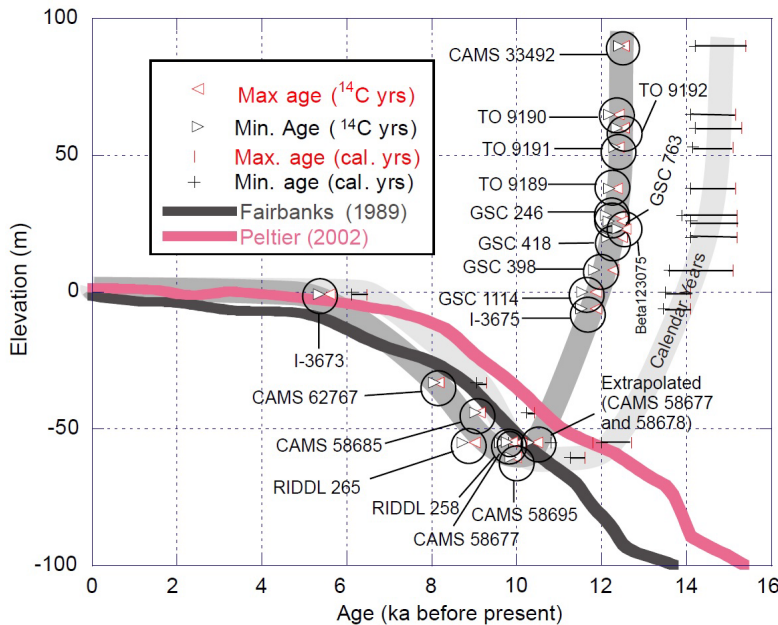


**Exhibit 1-5: Relative Sea Level Curve for the Strait of Juan de Fuca**

Source: Mosher and Hewitt (2004)

Notes: Dark and light gray lines represent the relative sea level curve for the Strait of Juan de Fuca from radiocarbon years and calibrated (i.e., calendar) years, respectively. Pink and black lines represent global eustatic sea level curves in radiocarbon years.

The retreat of the Juan de Fuca and Puget lobes mark the end of the Vashon Stade and the beginning of the Everson Interstade, the period during which the ice sheets were retreating and marine water entered the Puget Lowlands. Isostatic depression of the land surface during glaciation varied locally, and although global sea levels were lower than modern sea level, the relative sea level was at higher elevations in the Puget Lowlands and on the Olympic Peninsula (Exhibit 1-5). Preserved shorelines below intact subglacial landforms on the northwestern coast of the Olympic Peninsula indicate the relative sea level was at most 2 m (6.5 ft) above modern sea level, while near Port Townsend, the highest postglacial shorelines are approximately 52 m (170 ft) above modern sea level, showing a downward tilt to the east due to isostatic depression (Mosher and Hewitt, 2004; Haugerud, 2021). In Victoria, British Columbia, across the Strait of Juan de Fuca, relative sea levels reached a high of 75 ± 2.1 m (246 ft) above modern sea level by approximately 14,500 years ago (Engelhart and others, 2015).

Everson glaciomarine drift has been mapped at elevations up to 23 m (125 ft) above modern sea level in coastal bluffs along the lower reaches of the Dungeness River, overlying Vashon ice contact deposits and glacial till (Schasse and Wegmann, 2000). A shell from a glaciomarine deposit, just north of the Potholes locality in the northern Sequim quadrangle, was radiocarbon dated to between 13,600 and 12,200 years ago, while radiocarbon dates of Everson glaciomarine drift throughout the Puget Lowlands indicate deposition 13,500 to 11,300 years ago (Dethier and others, 1995).

As the glacier advanced westward over the northern Olympic Peninsula, streams emanating from the front of the glacier deposited advance outwash, glacial till beneath the glacier, and carved subglacial bedforms leaving its mark on the landscape. The elongated ridges oriented east-west that are common on the northern Olympic Peninsula and the Project site area are typically flutings or drumlins formed from glacial till or bedrock parallel to the direction of glacial flow. The weight of the glacial ice overriding the landscape resulted in overconsolidation of glacial and pre-glacial sediments as well as isostatic depression of the ground surface beneath the ice. As the glacier retreated, streams emanating from the ice front deposited recessional outwash deposits, burying locally-abandoned blocks of ice and forming kettle landforms. These glacial features, particularly the drumlins and flutes, are common on the upland glacial surfaces east and west of the site (Figure 4). Isostatic rebound drove uplift of the ground surface following thinning and retreat of glacial ice.

### 1.3.3 Holocene History

During the early Holocene, the isostatic rebound of the crust caused the relative sea level to drop to below modern sea level in the Puget Lowland. Proposed sea level lowstands in the greater Strait of Juan de Fuca area include  $-30 \pm 4.9$  m ( $-98 \pm 16$  ft) at about 11,000 years ago (James and others, 2009),  $-58$  m ( $-190$  ft) between about 9,300 and 9,700 years ago (Mosher and Hewitt, 2004) (Exhibit 1-5), and  $-50$  m ( $-164$  ft) between about 9,000 and 11,000 years BP (Linden and Schurer, 1988). A summary of sea level index points near southern Vancouver Island suggest that relative sea level fluctuated between as low as  $-42.7$  m to  $-1.5$  m ( $-140$  to  $-5$  ft) from 12,000 to 6,500 years ago (Engelhart and others, 2015). Relative sea level has been at the same levels as modern sea level since about 4,000 to 5,500 years ago, with crustal uplift of the land generally matching global sea level rise (Linden and Schurer, 1988; Mosher and Hewitt, 2004) (Exhibit 1-5).

The paleo Dungeness River would have been able to establish its channel following deglaciation, with its earliest channels likely graded to the retreating ice front (Noble, 1960). Since deglaciation, the Dungeness River has been eroding and redepositing the glacial deposits, as well as native catchment sediment, into a large alluvial fan with an apex about 3 km (2 miles) south of the Project area and extending radially northward towards the Strait



of Juan de Fuca. The modern Dungeness River has been estimated to transport sediment equivalent to a thickness of greater than 0.5 mm/year, while the paleo-Dungeness River, draining newly deglaciated and unvegetated deposits, would have delivered higher sediment loads during the Everson Interstade (Nelson, 1971; Dethier and others, 1995).

There is evidence for at least three different paleochannels of the Dungeness River incising preserved glacial deposits in the lower Dungeness. These are the Bell, Gierin, and Cassalery paleochannels, which are named after the modern creeks that inhabit these channels, each with a successively gentler gradient (Morgan and others, 1999) (Exhibits 1-6 and 1-7). The Bell paleochannel is interpreted to be graded to a lower sea level than the younger paleochannels, which is consistent with a lower relative sea level (Morgan and others, 1999).

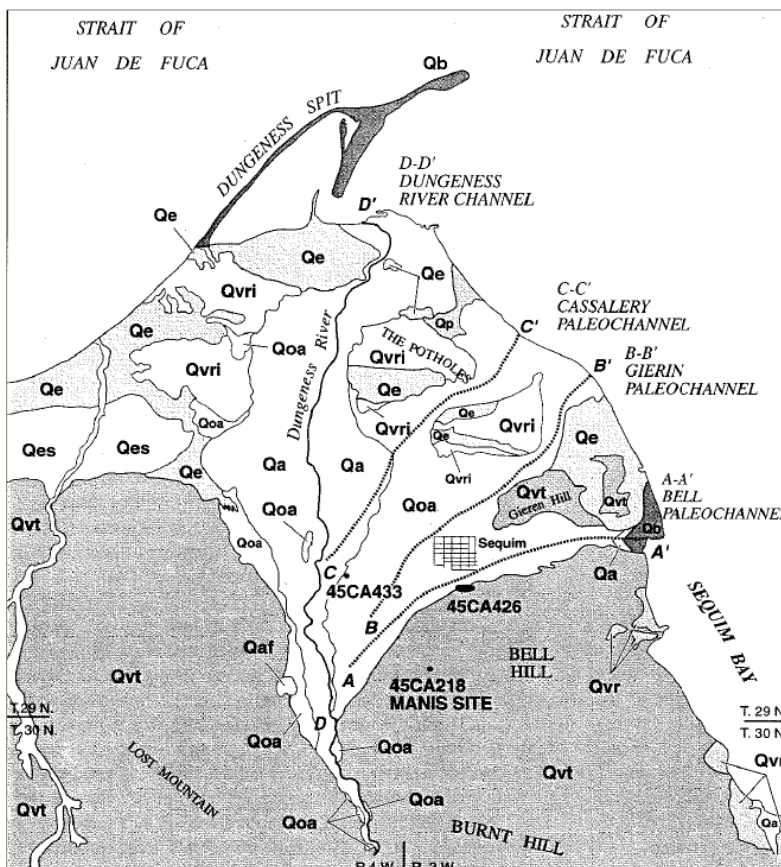


**Exhibit 1-6: Paleochannels of the Dungeness River**

Source: Morgan and others (1999)

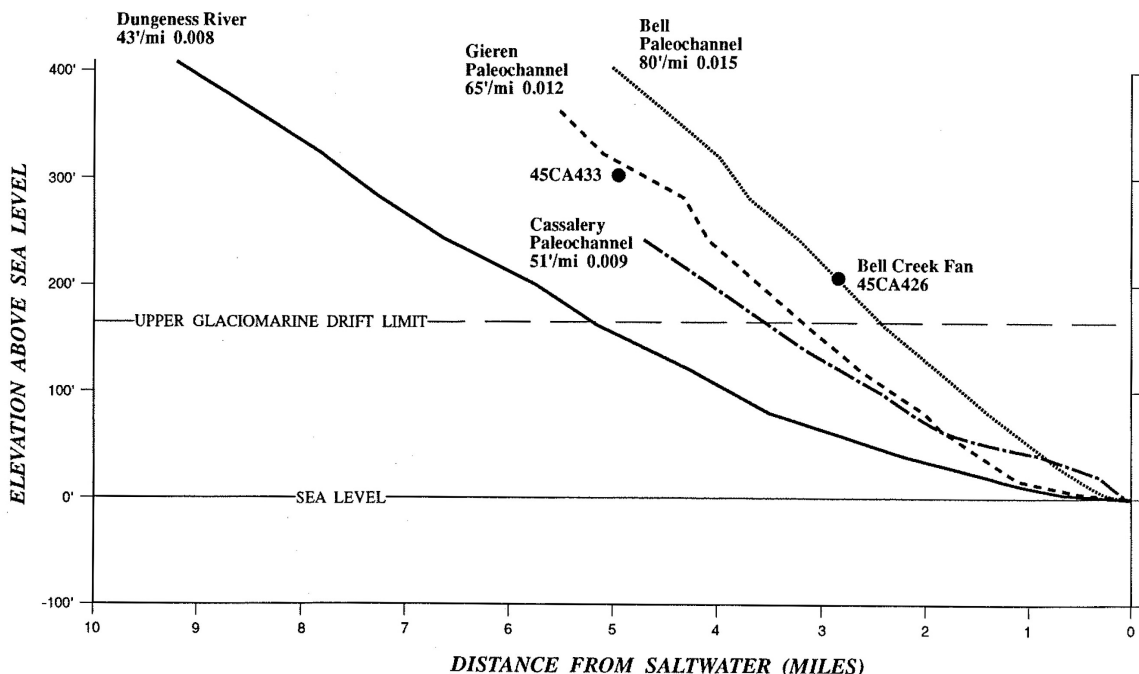


**Exhibit 1-7: Profiles of the Dungeness River and Paleochannels**

Source: Morgan and others (1999)

In the Bell paleochannel, an archaeological investigation excavated three trenches exposing the upper 1.7 m of material underlying a Bell paleochannel surface (Hartmann, 1997) (Figure 4). Trench 2 exposed the following from bottom to top: a 10-cm-thick peat deposit directly overlying fluvial deposits, a layer of Mazama ash, and a 70-cm-thick peat deposit. The fluvial deposits at depth were presumed to be Bell paleochannel deposits. Radiocarbon dates from samples of the peat deposit beneath the Mazama ash suggest deposition between 7,700 and 7,600 cal. years BP, while samples from the peat above the Mazama ash suggest deposition between and 7,400 and 7,000 cal. years BP. Mazama ash was deposited across the Pacific Northwest following an eruption between 7,682 and 7,584 cal. year BP (Egan and others, 2015). The age of the lowest lying peat deposit indicates that the Bell paleochannel was abandoned by the Dungeness River prior to about 7,600 cal. years BP (Morgan and others, 1999). There is no age control for the other paleochannels, but their lower elevations indicate that the Dungeness River occupied them after the Bell paleochannel.

## 1.4 Tectonic Setting

The tectonic setting of the Olympic Peninsula is dominated by the Cascadia Subduction Zone, which is the oblique subduction of the Juan de Fuca plate northeastward beneath the North American plate. This subduction places the Pacific Northwest region into a clockwise rotation, with most of Oregon and southwestern Washington rotating at rates of 0.4 to 1.0° per million years relative to the North American plate (McCaffrey and others, 2007 and

2013). The modern subduction zone initiated in the Eocene, approximately 42 ma (du Bray and John, 2011), resulting in significant uplift, anticlinal doming and deformation within the Olympic Peninsula. Haugerud (2002) and Nelson and others (2017) posit that regional-scale, north-south oriented compression, related to plate-scale clockwise rotation, has caused westward escape of the rigid Olympic Mountains crustal block (Exhibit 1-8). In this model, right-lateral slip would be expected on the northern margin of the block and left-lateral slip would be expected on the southern margin of the block, representing an overprinting on the generally eastward-directed compression imparted by the subduction zone. Studies of active faults along the northern (Nelson and others, 2017; Schermer and others, 2021) and southern (McCroory and others, 2002) margins of the block have demonstrated this model is probable. The North Olympic fault zone (NOFZ) (Figure 3) appears to accommodate the escape of the Olympic Mountains block along its northern margin (Exhibit 1-8), is located as close as 9 km from the site, and is described in Section 1.4.2 below.

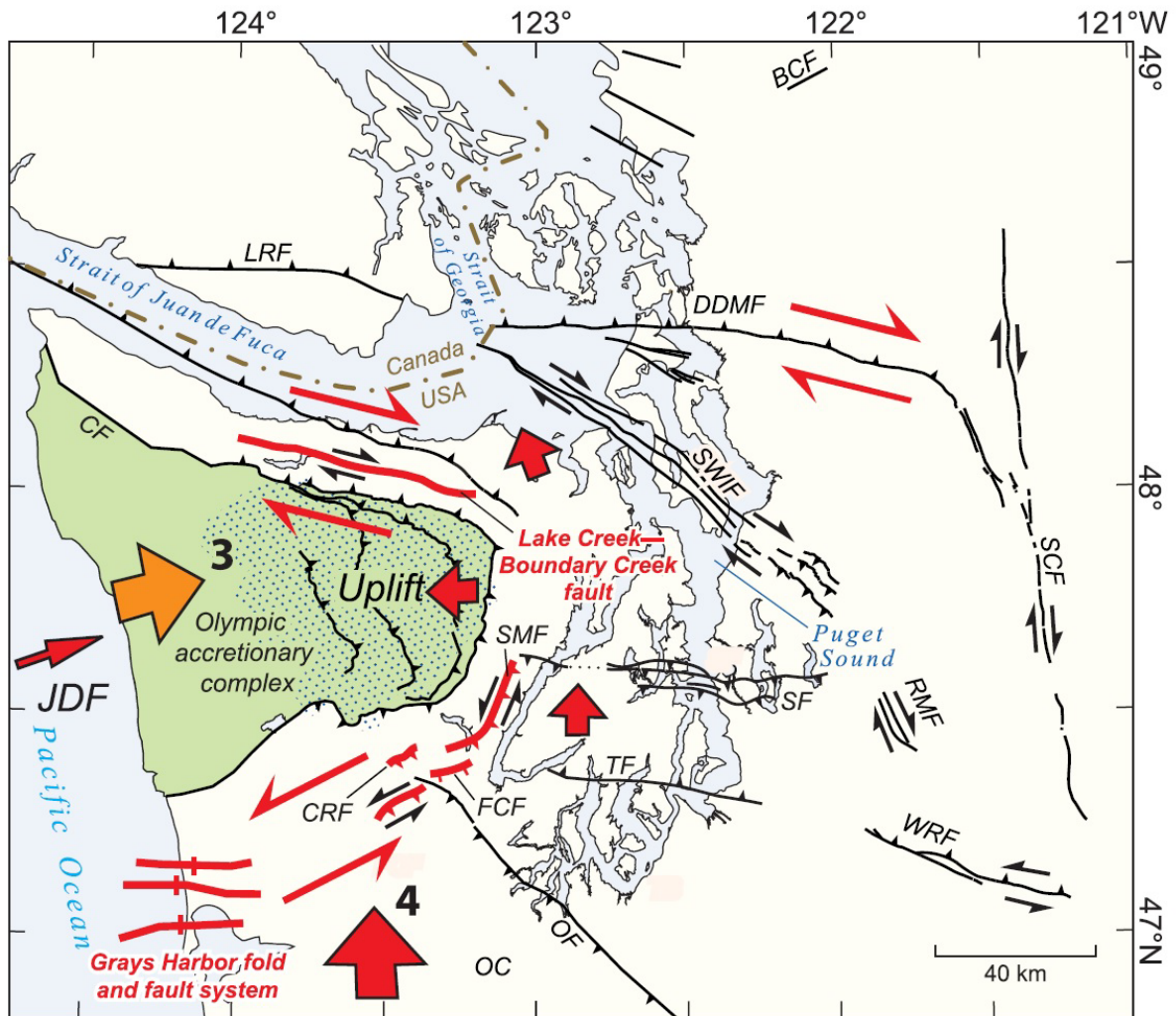


**Exhibit 1-8: Tectonic Escape of the Olympic Mountains Block**

Source: Nelson and others (2017)

The complex geologic history of the Olympic Peninsula has resulted in numerous faults and folds at various orientations throughout the region, which appear on geologic maps surrounding the site (Tabor and Cady, 1978; Schasse and Logan, 1998; Schasse and Wegmann, 2000; Schasse and Polenz, 2002) (Figures 3 and 4). The development and use of global position system (GPS) instrumentation and lidar topographic imaging has allowed for a better understanding of regional stress directions and strain accommodation. Nelson and others (2007 and 2017) recognized that some of these faults, including those within the NOFZ, are reactivated faults that once accommodated oblique left-lateral reverse slip and now accommodate dominantly right-lateral slip within the present stress orientation and tectonic setting.

### 1.4.1 Sequim Fault

The Sequim fault is the closest mapped fault to the Project site that is included in the USGS QFFD (USGS and DNR, 2024) (Figure 3). Prior to its apparent recognition at the ground surface by Nelson and others (2007), which led to its inclusion in the USGS QFFD, the Sequim fault was identified in several geophysical studies and eventually named in the late 20th century. We summarize these studies below:

- USGS (1974 and 1977)
  - Maps of aeromagnetic surveys that represent the earliest imaging of the fault and were used for interpretation in later studies.
  - No report was prepared, nor interpretation of the data is shown on these maps.
- MacLeod and others (1977)
  - Combined USGS (1974 and 1977) aeromagnetic data with marine magnetic and gravity data to interpret crustal structure in the greater Strait of Juan de Fuca region.
  - First publication to depict the Sequim fault in the subsurface, although it was unnamed at that time. The anomaly is labeled "F" in their map (Figure 5).
  - The basis for that fault is a prominent, linear contrast in magnetic data, and to a lesser degree, gravity data, which the authors posit may be a fault or a steep bedrock contact. They delineate the lineament with a queried fault trace.
- Gower (1978)
  - Included a report with interpretation of magnetic and gravity geophysical data (survey not specified) and local geologic mapping at 1:250,000 scale for the greater Puget Sound region. This study was aimed at identifying potential earthquake fault sources.
  - Mapped "inferred structure F" (apparently following anomaly "F" of MacLeod and others, 1977), which was "interpreted as a possible fault" demarcating the northern edge of a magnetic anomaly that bounds Eocene volcanic rocks on the south from Tertiary sedimentary rocks on the north. Apparent down-to-the-north sense of slip was noted.
  - Described a point observation near the south end of Sequim Bay of a fault that strikes N50°W, dips 68° northeast, and offsets post-Fraser glaciation outwash gravel and sand down-to-the-northeast by about 2 m (6.6 ft).
- Gower (1980)
  - Included a report with interpretation of magnetic and gravity geophysical data and a bedrock geologic map and report of the Port Townsend area at 1:100,000 scale.
  - Revised "inferred structure F" trace and description to "interpreted as a fault."
  - Also includes a similar description of the fault identified at Sequim Bay.
- Gower and others (1985)



- Seismotectonic map of the greater Puget Sound region at 1:250,000 scale.
- Defines "probable fault F" with revised and lengthened trace (Figure 6).
- Depicts two northwest-striking faults in the uplands to the west between "probable fault F" and the Lake Creek fault (part of the NOFZ).
- Johnson and others (1996)
  - First description of the yet unnamed Sequim fault as an active fault.
  - Peer-reviewed publication that applied seismic-reflection profile, outcrop, borehole, gravity and magnetic data to assess the southern Whidbey Island fault and nearby structures.
  - Depicted the Sequim fault (unnamed) in similar location to Gower and others (1985) (Figure 7).
  - Crossed and illuminated by Mobil seismic reflection data and tied in with other contemporary gravity, magnetic and borehole data.
  - Fault was described as offsetting top of Crescent Formation by 1,500 m (4,921 ft). Quaternary strata are described as appearing tilted within the zone, "suggesting the fault may be active" (Figure 8). Shannon & Wilson's review of the Johnson and others (1996) information identified additional apparently warped reflectors that suggest deformation of uppermost Quaternary (possible sea floor or Holocene) deposits.
  - They describe the fault dip as ambiguous in the seismic data but interpret two subparallel south-dipping reverse faults from the data, and depict two parallel, 50° south-dipping faults on their cross section (Figure 8).
- Brocher and others (2001)
  - Peer-reviewed publication used seismic tomography to evaluate crustal structure in the Puget Sound region (Figure 9).
  - First to apply the informal name of "Sequim fault" to "Fault F" that had been included on several previous maps.
  - Sequim fault described as an up-to-the-south fault that bounds the northern end of the Port Ludlow uplift, which consists of an area of uplifted Crescent basalt westwardly adjacent to the Kingston arch that appears as a sharp velocity gradient. The Sequim fault also bounds the southern margin of the Port Townsend Basin ("PTB" in Figure 9).
  - Interpreted that the Sequim fault may merge to the east with the southern Whidbey Island fault based on their interpretation of aeromagnetic data in Blakely (1999).
- Van Wagoner and others (2003) and Ramachandran and others (2004)
  - These two studies assess similar datasets and reach similar conclusions for different but overlapping study areas. Their conclusions are synthesized here.

- Used alternative tomography processing techniques to assess the same general data as Brocher and others (2001). (Note that there is co-author overlap between these three studies.)
- The Sequim fault mapped trace is arcuate, convex-south, following seismic tomographic velocity contours defining the Sequim basin, but is in a generally similar location to previously mapped traces defined on small-scale geophysical maps.
- Identifies a low-velocity “Sequim basin” and “Sequim fault.”
- The trace of the Sequim fault depicted as an arcuate fault that is subparallel to the northeast shoreline of the Dungeness River delta. This is in contrast to previously mapped depictions above, which are approximately east-west-striking and have been constrained and mutually confirmed by multiple data types.
- This alternative trace parallels the projection of the N50°W-striking normal fault identified by Gower (1978 and 1980) at the south end of Sequim Bay. Therefore, the “Sequim fault” defined by Van Wagoner and others (2003) and Ramachandran and others (2004) is likely not the same structure defined by other studies above.

The fault was next depicted and named by Nelson and others (2007), where the fault appeared as several traces on a lidar-based USGS map publication. As mapped by Nelson and others (2007), which is directly reflected in the USGS QFFD database, the Sequim fault consists of a 4.5-km-long (2.8-mi) set of four west-southwest-striking fault traces located near the northern part of the Project site in the Dungeness River valley and continues east across Happy Valley and Bell Hill (Figure 3). Nelson and others (2007) include the fault in their map, but without description in the brief summary text. This lack of information is reflected in the USGS QFFD, which classifies the Sequim fault as a Class A Quaternary-active fault, but does not specify any fault parameters (e.g., fault type, strike, dip, and age of movement) other than total fault length.

The USGS QFFD includes short fault traces in Discovery Bay and Port Townsend Bay (Figure 3) that are roughly coincident with the Sequim fault depicted by the geophysical studies above. The QFFD classifies these faults as unnamed Class B “faults in the Strait of Juan de Fuca and Puget Sound.” The USGS provides a database entry that broadly describes the numerous Class B faults in the region, but does not provide any detail with respect to these two sets of faults.

#### 1.4.2 North Olympic Fault Zone

The fault nearest to the Project site with previously documented Holocene rupture is the Lake-Creek Boundary Creek (LCBC) fault, which, combined with the Sadie Creek fault and additional fault scarps to the west, comprise the NOFZ (Figure 3) (Nelson and others, 2017; Schermer and others, 2021). As shown in Figure 3, the easternmost reach of the LCBC fault

is mapped to Siebert Creek, approximately 11 km (7 mi) west of the Project site. The USGS QFFD classifies the LCBC fault as a Class A fault. The LCBC fault may rupture together with the adjoining Sadie Creek fault to the west as a fault zone (total length of approximately 56 km or 35 mi), or each fault may rupture independently (between 14 and 31 km, or 9 and 19 mi) (Exhibit 1-9; Figure 3).

The LCBC fault consists of dozens of short and aligned scarps that typically strike west-northwest and extend 31 km (19 mi) from Lake Crescent to Siebert Creek (Figure 3) (Daisy trench site in Exhibit 1-9 is coincident with Siebert Creek). Nelson and others (2007 and 2017) excavated five trenches across multiple scarps, and based on stratigraphy and age-date modeling, documented three to five Holocene-age (< 11,000 years) earthquakes. Their mapping indicates that these earthquakes occurred along near-vertical faults, and movement largely consisted of right-lateral displacement with a smaller component of normal and reverse offset. Fault scarps typically indicate north-side-up vertical separation, but south-side-up scarps are locally present, further suggesting lateral displacement. Cumulative lateral and vertical offsets yield 4.6 m (15.1 ft) of average slip per event. Radiocarbon dating of material found in earthquake-related deposits suggests a postglacial average recurrence interval of about 3,500 years.

Recent evaluations of lidar and mapping of geomorphic features extend the NOFZ at least another 14 km (9 mi) to the west from the end of LCBC fault (Figure 3). This newly identified fault is the Sadie Creek fault (Nelson and others, 2017; Schermer and others, 2021). Based on trench studies across the Sadie Creek fault and geomorphic mapping of offset drainages that cross the fault, Schermer and others (2021) identified five postglacial earthquakes with a recurrence interval of around 2,400 years that may correlate with events in trenches along the LCBC fault, and a most recent event approximately 1,000 years ago. Trench stratigraphy and landform mapping confirms about 4 m (13.1 ft) of average right-lateral slip per event.



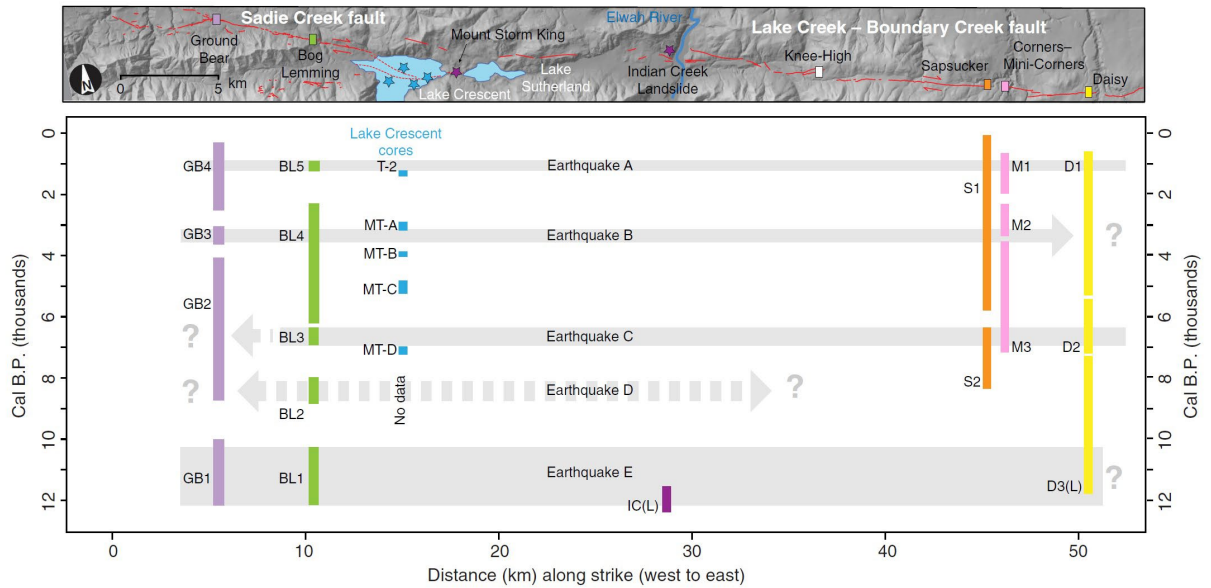


**Exhibit 1-9: Comparison of Earthquake Timing Along the North Olympic Fault Zone**

Source: Schermer and others (2021)

Notes: Vertical bars are color-coded with trench sites shown as polygons and labeled in map; vertical bars represent 95% confidence in earthquakes observed in trenches, gray bands show interpreted full length ruptures of the North Olympic fault zone, blue stars in lake indicate coring locations, and purple stars indicate radiocarbon sample sites on landslides.

Schermer and others (2021) combined the Sadie Creek fault and the LCBC fault studies (Nelson and others, 2017) to interpret ruptures that span the entire 56-km-long (35-mi) fault zone comprising the Sadie Creek fault and the LCBC fault (Exhibit 1-9). They compared radiocarbon ages from earthquake-related deposits mapped in all the trenches and identified sets of overlapping ages. Based on these overlapping ages and similarities along both fault zones of trench stratigraphy and geomorphic fault expression, they estimate that the LCBC fault and the Sadie Creek fault likely ruptured together (at least 56 km or 35 mi) at least twice and as many as four times in the Holocene. Where ages do not overlap between the faults, and given that more earthquakes were mapped in the Sadie Creek fault trenches, they infer that the Sadie Creek and LCBC faults also rupture independently. The faults demonstrate a dominantly dextral component of slip with a horizontal to vertical slip ratio of 10 Horizontal to 1 Vertical (10H:1V) to 6H:1V on steeply dipping faults (Nelson and others, 2017; Schermer and others, 2021). This ratio is consistent with slip required to accommodate escape along the northern margin of the Olympic Mountains block.

Schermer and others (2021) indicate that they have identified additional scarps that extend west beyond the Sadie Creek fault to Clallam Bay (Figure 3). They have not studied these scarps in detail but suggest that these scarps, the Sadie Creek fault, and the LCBC fault comprise the NOFZ with a total combined length of approximately 80 km (50 mi).

### 1.4.3 Southern Whidbey Island Fault Zone

The southern Whidbey Island fault zone (SWIF) comprises a 6- to-11-km-wide, steeply northeast-dipping zone of subparallel faults (Johnson and others, 1996) (Figure 3). The SWIF is characterized by inferred right-lateral strike-slip and reverse senses of slip (Johnson and others, 1996) (Figure 3). Sherrod and others (2008) note that the SWIF has been mapped using borehole data, potential field anomalies, and marine seismic reflection surveys as three subparallel, northwest trending strands extending ~100 km from near Vancouver Island to the northern Puget Lowland. They extend this length at least 30 km southeast and speculate that it continues to a junction with the Seattle fault farther southeast, while Johnson and others (1996) map the SWIF northwestward to potentially merge with faults on southern Vancouver Island. Paleoseismic evidence from Sherrod and others (2008) suggests that there have been at least four earthquakes along the SWIF since deglaciation, with the most recent earthquake occurring less than 2,700 years ago. Brocher and others (2001) suggest that the Sequim fault may intersect the SWIF north of the Port Ludlow uplift (Figure 9).

## 2 METHODOLOGY

This desktop study relied heavily on analysis of lidar topographic data, satellite imagery, and aerial photography. To aid in our evaluation, we supplemented these remote data with site subsurface information including multi-channel analysis of surface waves (MASW) geophysical surveys, sonic borehole logs, and existing geologic mapping. We also relied on field observations from the Seismic-Geologic Site Reconnaissance performed in 2023. This section describes the data and usage of each method.

### 2.1 Lidar Data and Derivative Models

Lidar data have been used extensively for about 25 years to identify evidence of tectonic surface deformation and assist in geologic and geomorphic mapping (Haugerud and others, 2003). These data have been particularly useful in the Pacific Northwest, where dense tree canopy conceals the bare earth surface from aerial imagery, and exposures are limited in the field (Haugerud and Harding, 2001).

We downloaded classified point lidar cloud data from the Olympics North OPSW 2018 and Olympics South OPSW 2019 datasets provided through the DNR Lidar Portal (DNR, 2018 and 2019) and created a bare earth digital elevation model (DEM).

From the bare earth DEM, we derived several additional models. These models include hillshades with various sun azimuths, sun angles, and vertical exaggeration factors. The

two we found most useful for topographic lineament mapping were vertically exaggerated ten times, with the sun azimuth oriented  $0^\circ$  and  $180^\circ$  with the sun angle at  $20^\circ$  and  $45^\circ$ , respectively. However, numerous other exaggerations, azimuths, and angles were developed iteratively to assist with mapping. A slope angle model was commonly used for mapping, which can allow for vertical exaggeration of the landscape by symbolizing specific intervals of angles. A model that combines slope angle with slope aspect (direction slope faces) was utilized to distinguish topographic lineaments that do not follow the glacial topographic fabric.

Topographic and stream longitudinal profiles were extracted from the bare earth DEM, which allowed for visualization of the ground surface in cross section or profile form.

We also created relative elevation models (REM) using the bare earth DEM based for the active Dungeness River channel and the interpreted path of the Bell paleochannel. Unlike DEMs that show absolute elevation above sea level, relative elevation models (REMs) show local vertical relief above a variable base level, typically a river thalweg or water surface elevation. REMs are useful for identifying river-related landforms, such as alluvial terraces and fans, as well as small scale geomorphic features imprinted on river-related landforms (e.g., levees, abandoned channels). To develop the REM models, we followed the inverse distance weighting (IDW) methods outlined by Olson and others (2014), which include the following:

- Extracting elevations along the river centerline at 150-foot spacing.
- Creating a base level elevation model from extracted point elevations using IDW interpolation.
- Generating the REM by subtracting the base level elevation model from the original DEM.

Prompted by the observation of uphill facing topographic scarps in the bare DEM and confirmatory field observations of vertically offset channel thalwegs, we assessed for continuity of surface flow across the alluvial fan surfaces by modeling hydrologic flow routing across the surfaces. Flow routing is a processing step in watershed delineation which describes how surface water moves through terrain, based on a lidar-derived DEM. Flow routing is useful for identifying active or abandoned stream channels; ponds, lakes, and wetlands; and the influence of natural or man-made terrain features on surface water flow. Flow routing requires sequential processing steps, including the following:

- Identifying closed depressions (sinks), such as lakes and ponds.
- Conditioning a DEM to remove both artificial lidar artifacts and real drainage impediments, such as closed depressions and flat areas.

- Delineating the direction of surface water flow from each cell in a DEM.
- Calculating flow accumulation, which describes the number of upstream cells (or geometric area) that contribute flow to each cell in a DEM. Different cutoff values can be applied to a flow accumulation raster to display preferential flow paths through a terrain that have contributing areas larger than the cutoff.

## 2.2 Alluvial Terrace and Lineament Mapping

We used the resulting hillshades, slope maps, REMs, satellite imagery, Project site information, and existing maps, reports, and publications to map alluvial terraces along the modern Dungeness River and topographic lineaments in the site region at a scale of 1:5,000. Alluvial terraces are typically elongated, gently sloping surfaces, separated by steep slope breaks that lie subparallel to and above a modern river and its floodplain. The terrace surfaces represent the remnant floodplains of Dungeness River paleochannels; mapping these terraces was a critical step to understanding the depositional and erosional history of the river to determine relative and absolute timing of terrace formation in relation to the lineaments we observe crossing the surfaces.

Alluvial terraces were mapped east to west across the Dungeness River valley between glacial uplands, and from the apex of the fan about 3 km (2 mi) south of the Project site, to about 500 m (1,500 ft) north of the prominent alluvial fan toe north of U.S. 101. We extended the mapping about 3 km (2 mi) down the Bell paleochannel to include an archaeological study site on that surface that contains radiocarbon age data. While the lower reaches of the Dungeness River and its paleochannels were not mapped in this study, by following terrace contacts from the mapping area downstream, we can estimate in which paleochannels the surfaces are present.

The terrace surfaces were differentiated based primarily on their elevation relative to the modern channel of the Dungeness River, or in the case of the oldest terraces (Qa5 to Qa7), relative to the interpreted Bell paleochannel. The relative elevations were determined based on REMs and cross-sectional profiles. For these oldest surfaces, correlative elevations were determined using topographic profiles oriented perpendicular to the generalized paleochannels. Surface relief and fluvial morphology present in the hillshade were used to visually differentiate surfaces while taking human modification into account, such as buildings, roads, and agriculture. Signs of human modification were determined from a satellite imagery basemap layer curated by Environmental Systems Research Institute, which provides 0.3 m resolution color imagery of the Project area taken on July 28, 2020.

## 2.3 Project Site Subsurface Information

We also assessed subsurface information collected in early phases of the Project to supplement our analysis of surficial data. This information includes nine MASW geophysical surveys (Global Geophysics, 2023) (Appendix A) and logs of sonic core borings complete by Shannon & Wilson for the Project prior to this evaluation (Shannon & Wilson, 2022). Using a seismic source and geophone receivers, the MASW method captures the relationship between surface wave velocity and wavelength to determine the shear wave velocity of media with increasing depth. The data from these measurements are used to model the shear wave velocities of the subsurface, which can be used to interpret rock or soil types, stratigraphic horizons, and their depths (Global Geophysics, 2023). Logs of 4-inch-diameter sonic core borings were assessed to aid in understanding site subsurface stratigraphy and used by Global Geophysics (2023) to interpret the shear wave velocity of the till deposits and the top of the glacial till.

# 3 RESULTS

This section presents the results of each component of our evaluation. Where relevant, we also discuss observations from the Seismic-Geologic Site Reconnaissance performed in April 2023.

## 3.1 Dungeness River Terrace Mapping

Seven generations of alluvial terraces were mapped in the Project area along the Dungeness River, not including the modern channel and its floodplain (Figure 10). These surfaces are numbered from Qa1 to Qa7, with Qa1 being the youngest surface and lowest relative to the modern channel, and Qa7 being the oldest surface and at higher elevations relative to the modern channel. The relative elevations (i.e., vertical distances) of each terrace surface above the modern Dungeness River channel are summarized in Exhibit 3-1. Each surface is characterized by a range of relative elevations, and the range is typically larger for the younger surfaces than the older surfaces due to a higher density of preserved fluvial landforms (e.g., meander bars, levees) in the younger surfaces.

**Exhibit 3-1: Relative Terrace Elevations Above the Modern Dungeness River Channel**

Surface	Relative Age Group	Relative elevations (m) <sup>1</sup>	Relative elevations (ft) <sup>1</sup>	Paleochannel
Qa	Modern	0 – 1.8	0 – 6	Modern Dungeness River
Qa1	Younger	1.8 – 3.6	6 – 12	Dungeness River <sup>2</sup>
Qa2		3.6 – 7.3	12 – 24	Dungeness River <sup>2</sup>
Qa3		7.3 – 10.9	24 – 36	Cassalery and Dungeness River <sup>2</sup>
Qa4	Older	10.9 – 12.1	36 – 40	Cassalery and Matriotti
Qa5		12.1 – 14.0	40 – 46	Gierin
Qa6		14.0 – 15.2	46 – 50	Bell and Gierin
Qa7		14.6 – 16.8	48 – 55	Bell and Gierin

NOTES:

- 1 Relative elevation values can locally vary outside of these ranges.
- 2 Approximately following the modern channel.

We observe several distinguishing characteristics that represent two distinct groups of terraces: a group of four older, higher elevation surfaces comprising Qa7, Qa6, Qa5, and Qa4; and a group of three younger, lower elevation surfaces comprising Qa3, Qa2, and Qa1 that are erosionally inset into the older surfaces (Exhibit 3-1). Our observations to make this distinction are described below:

- The four older surfaces are typically separated from younger surfaces by prominent terrace risers (i.e., a steep slope that separates two terrace surfaces) that exceed the riser heights (i.e., vertical distance between two surfaces) within the two groups (Figures 11A and 11B). The bluff west of the Project leading down to the modern Dungeness River is the best representation of this tall riser.
- Younger surfaces (Qa1 to Qa3) are typically rougher than older surfaces and exhibit common fluvial landforms, such as channel scars, meanders, and oxbow lakes. Older surfaces (Qa4 to Qa7) are characterized by more subdued surface relief with a dense network of small, shallow channels and lack of larger fluvial landforms.
- The older surfaces represent the alluvial deposits that form a distinctive toe to the fan, which is observed as an arcuate slope break in slope where the Dungeness River valley opens to distal portions of the modern fan (Figure 10). The younger surfaces represent an incised gap through this toe and were deposited as inset terraces in a shallowly entrenched cut.

The older terrace surfaces that we mapped extend downstream to and correlate with paleochannels of the Dungeness River described by Collins (2005) (Exhibit 3-1 and Figure 10). We visually assess the correlations of our mapping with the lower Dungeness River and the Gierin, Cassalery, and Matriotti paleochannels. Matriotti Creek is a tributary



of the modern Dungeness River (Collins, 2005) and, based on our interpretation of the lidar data, may have been a paleochannel for the modern Dungeness River.

Remnants of the oldest surface, Qa7, are present between the Bell and Gierin paleochannels and in the lower reaches of both these paleochannels (Figure 10). Qa6 is the most recently active surface present in the Bell paleochannel, and correlative surfaces are likely present in the lower Gierin paleochannel. A small remnant of a terrace is preserved at a higher elevation above the Gierin paleochannel than Qa7, suggesting that perhaps the Gierin paleochannel was occupied by the Dungeness River prior to the Bell paleochannel, as well as after it. The Qa5 surface is only observed along the course of the Gierin paleochannel and is the most recently active surface of the Dungeness River in that channel. The Qa4 surfaces are within the Cassalery and possibly the Matriotti paleochannels, while the Qa3 and Qa2 surfaces were active while the Dungeness River occupied the Cassalery paleochannel, and earlier courses that generally follow the modern Dungeness River. The Qa1 surface was active most recently and likely while the Dungeness occupied the Meadowbrook paleochannel. The modern Dungeness River and its current floodplain are mapped as Qa.

The stratigraphy observed in Trench 2 of the archaeological investigation in the Bell paleochannel (Hartmann, 1997) shows peat deposited on top of fluvial deposits. We correlate the surface where Trench 2 was excavated with the Qa7 alluvial surface (location of trench is labelled T2 in Figure 10). The lower peat deposit was overlying fluvial deposits, which suggests that the Bell paleochannel had been abandoned by 7,600 cal. years BP, and demonstrates all surfaces are middle- to late Holocene in age (Section 1.3.3).

## 3.2 Subsurface Interpretation

Site subsurface information reveal normally consolidated (i.e., not glacially overridden) deposits that we interpret as postglacial alluvial fan and fluvial stream deposits overlying glacial till deposits (Figures 12 and 13).

MASW data image an apparent absence of significant relief in the buried glacial till surface beneath the site. The MASW lines depict an interpreted depth to the glacial till surface based on surface wave velocities that were calibrated using depths to till in borings across the site (Figure 12) (Appendix A). The interpreted depth to till ranges from 0 to 24 m (0 to 80 ft) across the site, with a westward gradient of increasing depth. The top of till is a relatively planar surface, with a few isolated, gradual undulations of about 3 to 6 m over 15 to 60 m (about 10 to 20 ft over 50 to 200 ft). We do not recognize patterns to or alignments of these undulations from either north-south- or east-west-oriented MASW lines, and the undulations do not align with lineaments and scarps observed at the ground surface. The planarity of buried till surface is inconsistent the topography that characterizes the upland

surfaces east and west of the site. Therefore, we interpret this localized variability on the buried till surface to represent channel scour margins caused by fluvial activity, and not buried glacial landforms or tectonic deformation. Line 1 images the most variability, with the till surface locally at or near the ground surface, which we interpret to be caused by its proximity to the margin of the Dungeness River valley and greater distance from the axis of the valley. This higher elevation till surface may represent a shallowly buried strath terrace (i.e., terrace cut into an existing substrate material, as opposed to a terrace deposit) cut into glacial till. A near-surface low-velocity zone is observed on the north side of the north scarp crossing the site. It is best expressed in Lines 2, 5, and 6B and is faintly expressed and limited in depth in Line 3.

Beneath these normally consolidated deposits are glacial till deposits that range from about 13.7 m (45 ft) to at least 21.0 m (69 ft) in thickness (bottom locally not encountered). Glacial advance outwash deposits at least 21.3 m (70 ft) in thickness (bottom not encountered) were encountered locally beneath the glacial till.

Borings across the site demonstrate about 4.6 to 11.3 m (15 to 37 ft) of deposits on top of glacial till, consistent with the glacial till surface imaged by the MASW survey (Appendix A). The borings are spaced too far apart to recognize abrupt changes in elevation of the top of the till surface. The borings encountered primarily coarse alluvium gravel deposits with sand above the glacial till, with fines content on the order of 20% or less, which we interpret as alluvial fan deposits. Finer grained deposits that are locally encountered above the glacial till surface and beneath the coarse alluvium are interpreted as distal fan and floodplain sediments deposited during initial phases of fan progradation.

### 3.3 Geomorphic and Lineament Mapping

This section describes geomorphic scarps and lineaments identified throughout the study area, some of which record apparent ground surface deformation. We do not include all scarps and lineaments throughout the study area in our mapping. Numerous features were interpreted as glacial in origin throughout the mapping process and not included in the discussion. As an exception, we included features that we interpret as glacial in origin but were originally mapped as traces of the Sequim fault mapped by Nelson and others (2017).

The features are located across five areas, each with similar geologic and geomorphic settings, including: (1) alluvial deposits of the Dungeness River valley near the site; (2) the eastern upland glacial till surface (i.e., east of the site in Happy Valley and Bell Hill); (3) the western upland glacial till surface (i.e., north of Lost Mountain); (4) south of Sequim Bay; and (5) near Siebert Creek. Figure 14 labels these areas, shows the locations of topographic



profiles across selected scarps and lineaments, and references four larger-scale maps (Figures 15 through 18) that focus on one or more of the areas listed above.

### 3.3.1 Lineaments in the Dungeness River Valley

Within the alluvial valley of the Dungeness River, we identified two relatively discrete topographic scarps that cross the site and alluvial fan surface, and an area characterized by an undulatory topographic north of these scarps where we define alignments along each of the two crests of the undulations (Figure 15). The scarps and lineaments crossing the alluvial fan surfaces of the Dungeness River valley are subparallel.

Of the two scarps, the northern scarp is more prominent, broad (about 60 m or 197 ft), uphill-facing (i.e., south-facing), strikes east-northeast, and is mapped for a distance of about 880 m (2,887 ft) across the fan surface (Figure 15). This scarp extends beyond the fan across the eastern upland glacial till surface (described in Section 3.3.2) for a total distance of 2,400 m (7,874 ft). The maximum observed height of the scarp in alluvial deposits is about 0.9 m (3 ft) from base to top, with about 2.4 m (8 ft) of vertical separation between adjacent alluvial surfaces (Figure 19, profiles B through F). We note the presence of a possible lineament or scarp on the Qa6 surface on the west side of the valley, where a profile demonstrates a separation of two relatively similar surface gradients separated by a zero-gradient section (Figure 19, profile A). The northern scarp, including the reach on the eastern upland surface, is nearly coincident with the southernmost trace of the Sequim fault mapped by Nelson and others (2007).

Surface flow modeling (described in Section 2.2) indicates that the northern scarp produces a reverse gradient (i.e., topographic divide) across the Qa6 and Qa7 surfaces (Figure 20). Results of the flow modeling show that in the vicinity of roads, modern day surface flow is controlled by ditches and embankments. Based on surface gradients, modern day flow on the Qa6 and Qa7 surfaces follows the paleochannels northeastward to the northern scarp and then abandons the paleochannels to divert eastward in front of the elevated southern face of the central lineament. Flow lines that cross the northern scarp are artificial (i.e., modelling numerically filled the closed depressions to maintain flow). Figure 20 depicts a closed depression at the base of the eastern end of the northern scarp. Aerial imagery suggests this area is more heavily vegetated and may represent moist, fine-grained sediments that have been deposited in the closed depression. There is no evidence, such as an incised cut through the scarp or a consolidated flow path downstream of the sink, that pooling of runoff achieved sufficient height to overtop and erode the scarp so as to allow the reestablishment of flow. We observed vertically offset channels across this scarp during our April 2023 field reconnaissance, consistent with our flow modeling results. Another small,

closed depression is present on the Qa7 surface between the north scarp and the undulation crest to the north.

The southern scarp is less prominent, narrow (about 20 m or 66 ft), downhill-facing (i.e., north-facing), strikes west-southwest, and is mapped for a distance of about 780 m (2,559 ft) within alluvium (Figure 15). The maximum observed height of the scarp in alluvial deposits is about 1.2 m (4 ft) from base to top, with about 0.9 m (3 ft) of vertical separation between adjacent surfaces (Figure 19).

The undulatory topography noted above extends across the alluvial surfaces north of the scarps (Figure 15). The undulations are characterized by a trough-ridge pattern, with axes parallel to the north and south scarps described above. Together with the scarps, the wavelength of features ranges from about 300 to 500 m and about 1.5 to 3 m (5 to 10 ft) in amplitude. The features are best expressed in the REM using the Dungeness River as the baseline elevation (Figure 11B), and they are also evident in topographic profiles (Figure 21). Traces of the Sequim fault mapped by Nelson and others (2007) (Figure 3) on the eastern upland surface project (but are not mapped) into the alluvial deposits where the undulatory topography is observed.

The REM depicts a series of small alluvial fans at the mouth of ravines from the glacial upland onto the Qa6 surface (Figure 20). The alluvial fan at the crest of the southern undulation is asymmetric and lengthened to the north when compared to a more symmetrical alluvial fan further between the northern scarp and the undulations.

### 3.3.2 Lineaments in the Eastern Upland Glacial Till Surface

We identified several lineaments on the upland surface east of the site (Figure 15). The most prominent lineament is a scarp in Happy Valley that appears to represent the eastern extension of the north scarp observed on the alluvial deposits of the Dungeness River valley near the site (see Section 3.3.1). The scarp is about 80 m wide (262 ft), locally uphill facing (i.e., south-facing), strikes east-northeast, and extends for about 1,365 m (4,478 ft) across the glacial till surface. The scarp has a maximum observed height of approximately 3.0 m (10 ft) (Figure 19). Together with the north scarp across the alluvial deposits to the west, the scarp is mapped for a total distance of about 2,400 m (7,874 ft). Brighter, and deeper red color contrasts in color-infrared imagery suggest the scarp represents an impediment to surface and potentially groundwater flow. This color contrast indicates moister conditions, likely attributed to fine-grained soils that have accumulated (i.e., ponded) against the uphill-facing scarp. We observed phreatophyte vegetation at the base of the scarp during our field reconnaissance in April 2023. This scarp is also roughly coincident with the southernmost trace of the Sequim fault mapped by Nelson and others (2007) (Figure 3).

A lineament was identified on both flanks and crossing over Bell Hill, east of and on-strike with the scarp described above (Figure 15). The lineament appears as a swale on the west slope, with no evidence for surface flow or channelization. On the east side of the hill, the lineament shows evidence for channelization, and has eroded into bedrock based on both geologic mapping (Schasse and Logan, 1998) and observations during our April 2023 field reconnaissance. The lineament from both sides of Bell Hill connects over the top the hill, forming a singular, continuous feature that does not appear to represent erosion given the absence of contributing drainage area. We observe no obvious scarp feature in topographic profiles across the lineament (Figure 19, profile P). The total length of this lineament is about 1,780 m (5,840 ft) and is approximately coincident with the easternmost trace of the Sequim fault mapped by Nelson and others (2007) (Figure 3).

Three lineaments are observed north of the prominent scarp described above (Figure 15). The northernmost lineament is curvilinear, oriented generally east-northeast, about 1,230 m (4,035 ft) long, and nearly coincident with a strand of the Sequim fault mapped by Nelson and others (2007). Its profile view depicts a generally positive-relief structure, as opposed to a scarp (Figure 19, profiles O and N), is similar to other curvilinear features that we interpret as glacial in origin, and is consistent with remnants of a subglacial drainage feature (e.g., esker). The southern lineament is generally linear, oriented east-northeast, mapped over a distance of 880 m, and approximately coincident with a trace of the Sequim fault mapped by Nelson and others (2007). It represents a 0.3- to 0.6-m-high scarp in profile view (1 to 2 ft) (Figure 19, profiles L and M).

### 3.3.3 Lineaments in the Western Upland Glacial Till Surface

Numerous lineaments and landforms of glacial origin characterize the upland surface west of the site and active Dungeness River valley (Figure 16). We have not attempted to map the lineaments for which we have high confidence of glacial origin. Instead, we interpreted derivative lidar topographic models (e.g., hillshades, slope, aspect, aspect-slope, local relief), to differentiate glacial landforms from postglacial landforms and to assess for the possibility that scarps recognized in the eastern upland surface and the Dungeness River valley continue to the west. We have mapped several lineaments in the western upland surface. The most prominent of these lineaments is a generally east-west-striking scarp about 4,365 m (14,320 ft) in length and ranging in height up to 1.2 m (4 ft) (Figures 16 and 22, profiles A through D). The scarp is considerably longer than others on the surface, and based on the aspect-slope, appears to obliquely cross the glacial topographic fabric, suggesting a postglacial origin (Figure 16, bottom panel). The western reach of the scarp crosses McDonald Creek, which has an inset apparent strath terrace that appears offset across the mapped scarp (Figure 22, profile A). The scarp has resulted in a zero to negative gradient reach along the strath terrace, and about 3.7 m (12 ft) of offset of the reaches on

either side. The scarp also appears to be expressed crossing a small fan (Figure 16). Other profiles along the feature show a consistent uphill-facing scarp (Figure 22, profiles B through D).

### 3.3.4 Lineaments South of Sequim Bay

Based on a description of 2 m (6 ft) tectonic offset glacial outwash deposits along a northwest-striking fault (Gower, 1978 and 1980; see Section 1.4.1), we evaluated the area south of Sequim Bay for evidence of surface deformation (Figure 17). Similar to other parts of the study area, the area south of Sequim Bay has a strong directional fabric due to glaciation. However, the fabric in this area is oriented generally northwest, in contrast to the east-northeast to west-northwest fabric observed in most other parts of the study area. We identified several lineaments following a northwest trend, some of which may post-date glacial topography. These lineaments are particularly subtle, consist of aligned subtle scarps, drainages, swales, and possible shutter ridges, and can be traced discontinuously for about 4,400 m (14,436 ft) across postglacial erosional topography and Vashon recessional outwash deposits (Figure 17). While these lineaments do not represent compelling surficial evidence suggestive of deformation, the observation by Gower (1978 and 1980) is significant in that it demonstrates Holocene displacement both east and west of the Project site.

### 3.3.5 Lineaments Near Siebert Creek

The Siebert Creek study area was selected to cover the western end of the Lake Creek-Boundary Creek fault of the NOFZ described in Section 1.4.2 to compare scarp morphology of a fault with documented Holocene surface rupture with scarp morphology along the Sequim fault. The fault near Siebert Creek is expressed as a prominent, narrow, uphill-facing (i.e., south-facing) scarp crossing a glacial till surface with a north-northeast-oriented topographic fabric (Figure 18). Where the scarp has not been modified by fluvial erosion, it is approximately horizontal to 0.3 m (1 ft) in height, creating a flat area on the gently north-facing slope, and vertically offset of the uphill and downhill surfaces of up to 2.4 (8 ft) (Figure 23). The scarp strikes west-southwest and was trenched by Nelson and others (2007), where they exposed evidence for two earthquakes in the past approximately 7,000 years, and surficial evidence of right-lateral offset (Exhibit 3-2 and Figure 18). We identify lineaments oriented on-strike with the scarp continuing about 5.2 km (3.2 mi) east beyond where it was mapped by Nelson and others (2007).



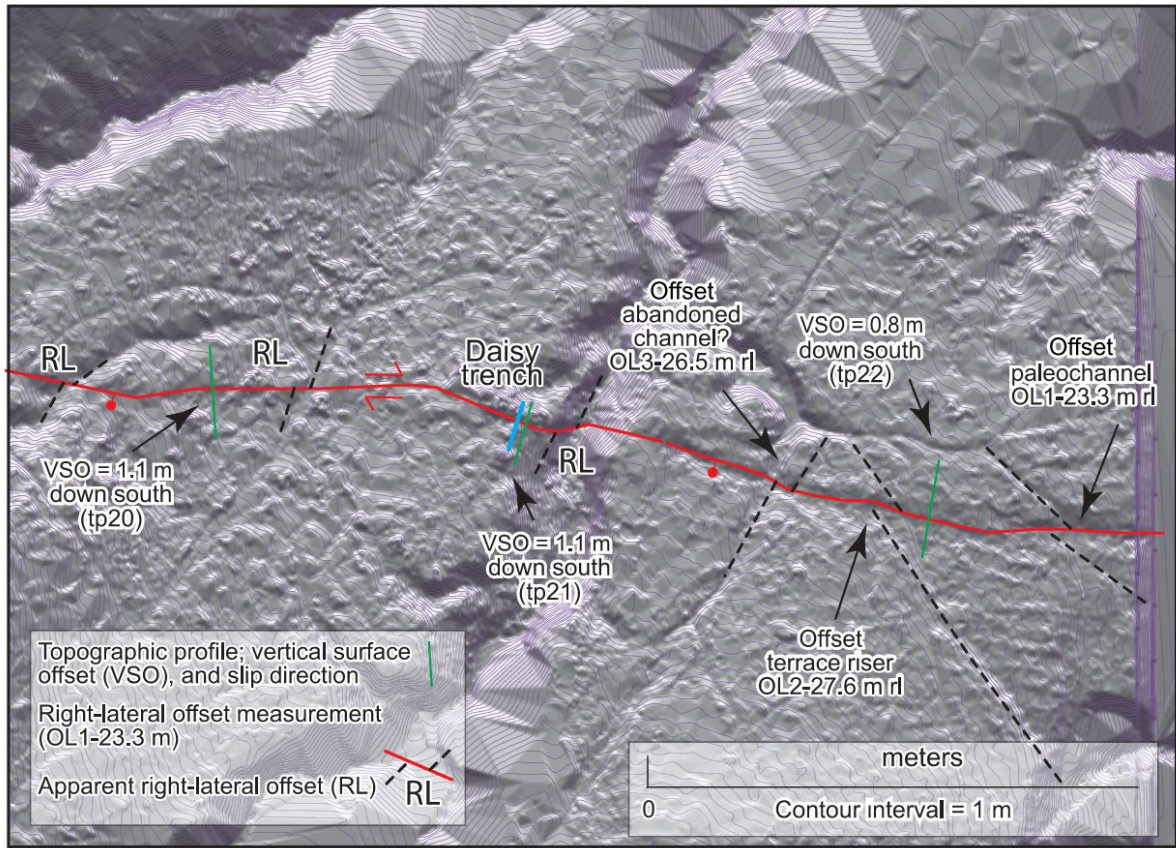


**Exhibit 3-2: Daisy Trench Site on the Eastern Lake Creek-Boundary Creek Fault**

Source: Nelson and others (2017)

## 4 DISCUSSION AND CONCLUSIONS

This section presents our interpretations synthesized from the sections above. We begin with a discussion of the geomorphic and depositional history of the Dungeness River, which provides important age constraints for the lineaments that cross the Dungeness River alluvial fan. We then discuss the relationship between surficial terrace mapping and the lineaments followed by an interpretation of the subsurface structure of the scarps and folds that cross the surfaces.

### 4.1 Geomorphic History of the Dungeness River

The setting and deposits of the Dungeness River record its postglacial erosional and depositional history. This history and the geologic relationships are key factors to understand the origin and age of the scarps and lineaments described in the sections above. Presented below is timeline of key events that place the geomorphic history into context.

- >13,800 years ago
  - Glacial ice of the Juan de Fuca lobe covers the entire study area, with maximum extent between 15,670 and 14,900 years ago (Heusser, 1973; Haugerud, 2020).
  - Glaciation reduces or eliminates pre-glacial topography and leaves a regional topographic fabric of east-west trending flutes, drumlins, and eskers (Collins, 2005). Advance outwash and glacial till have been deposited in the pre-Vashon Dungeness River valley.
  - Climate is cooler and significantly drier than today, with greater seasonal temperature swings (Heusser and others, 1980).
- ~13,800 to ~12,000 years ago
  - Strait of Juan de Fuca is ice-free to Whidbey Island by about 13,595 years ago (Mosher and Hewitt, 2004).
  - Dungeness River valley is ice-free by about 13,800 years ago (Petersen and others, 1983; Waters and others, 2011).
  - The postglacial landscape is recorded in the erosionally-detached uplands east and west of the Project site. This landscape was probably continuous across the present Dungeness River valley with a depression following the pre-Vashon Dungeness River valley (Figures 10 and 12).
  - Relative sea level falls from ~75 m above present (246 ft mean sea level [msl]) to about equivalent with present (Mosher and Hewitt, 2004) (Exhibit 1-5). For reference, the Project site ranges from approximately 115 to 135 m (or 380 to 440 ft msl).
  - The Dungeness River channelizes as sea level falls, grading to present day relative sea level, but is choked with sediment resulting in modest incision into the till deposits that blanket the landscape.
  - Climate warms significantly to a temperature that is only slightly cooler than today, and with similar precipitation (Heusser and others, 1980).
- ~12,000 to ~10,000 years ago
  - Incision accelerates, driven by a combination of a lower eustatic sea level and glacial rebound, equating to a relative sea level about 60 m below present (Mosher and Hewitt, 2004) (Exhibit 1-5). A wetter and slightly cooler climate than modern climate also adds to stream power (Heusser and others, 1980).
  - This lower base level drives significant incision into glacial till deposits (Exhibit 1-7) and channel broadening. This process is recorded by the terrace risers that bound the Dungeness River valley and alluvial surface east and west of the site, and Project subsurface information (MASW profiles and borings), which demonstrate a depth to glacial till of 6 to 24 m (20 to 80 ft). Although there are minor undulations on the top of the buried glacial till, the till surface is consistent with a broad, flat valley that extends to the current risers.
  - The stream has significant power to transport sediment comprised of glacial deposits, and sediment derived from its native catchment.



- Initial deceleration of incision appears to be recorded by the fine-grained alluvial deposits that overlie glacial till in borings (Figures 12 and 13). These likely represent distal fan deposits, which prograded into the mid-Holocene (see below).
- ~10,000 to ~5,000 years
  - Rising relative sea level is driven by a slowing of glacial rebound and rising eustatic sea level (Mosher and Hewitt, 2004). Climate experiences a minor increase in temperature and considerable decrease in precipitation (Heusser and others, 1980).
  - Dungeness River stream power decreases in response to the rising base level and drier climate. The river develops a fan morphology, characteristic of a stream choked with sediment and is dominated by debris flow deposition in flood events, channel abandonment and intermittent side channels. This is recorded by the Qa5, Qa6, and Qa7 mapped terraces, and the coarse but silty deposits encountered in Project borings and observed in the modern Dungeness River bluff. This time frame is consistent with a radiocarbon age of 7,600 cal. years BP in peat overlying the Qa7 surface, indicating that fan deposition had occurred prior to that time (Hartmann, 1997; Morgan and others, 1999). Younger fan surfaces indicate continued fan deposition after 7,600 cal. years BP.
- ~5,000 years ago to present
  - Relative sea level remains at steady elevation into the present (Mosher and Hewitt, 2004). Climate experiences a rebound to conditions similar to today (Heusser and others, 1980).
  - As river achieves equilibrium with climate and steady sea level, the Dungeness River incises through the older alluvial fan deposits (Qa7, Qa6, Qa5, and Qa4) and develops a modern well-graded profile and gently meandering course recorded by the inset younger terrace surfaces.
  - The river, given a modest increase in power due to the factors noted above, incises through the fan it built, leaving the terrace riser between the modern channel deposits and the older fan deposits.

The key takeaways from this timeline are:

1. During a period from about 12,000 to 10,000 years ago, the paleo-Dungeness River incised and planed off the broad valley we see today. This process worked to reset the topography within the valley in contrast to the glacial topography and fabric preserved in the uplands to the east and west. This is an important concept, as it eliminates the possibility that the lineaments that cross the site reflect glacial or recessional topography.
2. The fan deposition that occurred approximately 10,000 to 5,000 years ago includes geologic relationships, supplemented by absolute age dating, to constrain the ages of the fan surfaces, and the lineaments and scarps that cross them.

## 4.2 Age and Origin of the Project Site Lineaments

Based on the timeline and supporting geologic and geomorphic relationships described above, we conclude that the scarps and lineaments crossing the Qa5, Qa6, and Qa7 surfaces at the Project site postdate Vashon glaciation. More specifically, these features postdate about 7,600 cal. years BP, the maximum age of the Qa7 surface, the oldest surface on which the scarps and lineaments are observed. Furthermore, the preponderance of available information leads us to conclude the scarps and lineaments in the Dungeness River valley at and near the site are of tectonic origin, related to surface fault rupture (scarps, or fault scarps) and surface folding above blind faults (lineaments, or fold lineaments) that represent a positive flower structure branching upward from the Sequim fault (Figure 24, described in greater detail in the following section). Below we summarize our observations that support this conclusion:

- The southern fault scarp truncates channels on the Qa6 alluvial surface, which was observed both in the field and through lidar flow path modeling. This demonstrates post-channel deformation of the surface.
- The mapped trace of the Sequim fault, defined in several previous geophysical studies, intersects or projects toward the scarps and lineaments in the Dungeness River valley, and on the upland glacial till surfaces east and west of the site (Section 3.3.1) (Figures 5, 6, 7, and 9). Seismic reflection data document Quaternary activity on the fault and suggest possible deformation of uppermost seafloor sediments.
- A complex zone of subsurface faults is depicted in previous geologic and geophysical structure maps (MacLeod and others, 1977; Gower and others, 1985; Schasse and Logan, 1998; Schasse and Wegmann, 2000), including depictions of the Sequim fault that extend 7 km west of the site. In addition to demonstrating a dense network of faults that may have the capacity to reactivate to accommodate modern stresses (e.g., North Olympic fault as described by Nelson and others, 2017), these faults may also represent a limit to the westward extend of the Sequim fault (Figure 3).
- The presence of documented Holocene surface ruptures on the NOFZ about 12 km west-southwest of the Project site at the Daisy trench site of Nelson and others (2017). Our mapping suggests the NOFZ may continue east of mapping by Nelson and others (2017) to within 8 km southwest of the site.
- Documented 2 m of vertical offset of glacial outwash deposits about 12 km southeast of the site (Gower and others, 1985). Our mapping identified possible lineaments to within 8 km southwest of the Project site that may be related to this offset.
- Both the scarps and lineaments appear to connect with scarps mapped across the eastern upland glacial till surface. Scarps on the glacial till surface have a maximum age of about 13,800 years, which is the maximum age of ice-free conditions on the surface (Waters and others, 2011)

- We map a scarp crossing the western glacial till surface that appears tectonic in origin, deforming an apparent Holocene surface.
- Absence of a reasonable alternative explanation for the presence of the lineaments and their effect on the landscape.
- We speculate that the low-velocity zone observed in MASW surveys at and north of the north scarp may be caused by disturbance of the deposits at the ground surface, where confining stresses are lower.

The Daisy trench on the eastern end of the LCBC fault shows evidence for two ruptures in the past 7,000 years, both of which may have involved rupture on the LCBC and Sadie Creek faults to the west (Exhibit 1-8 and Figure 18). Based on that timing, it is possible that one or both of these events could have ruptured the Sequim fault at the ground surface near the Project site. We interpret that the north and south scarps across Qa5, Qa6, and Qa7 alluvial surfaces have experienced at least one earthquake since about 7,600 cal. years BP based on displacement of alluvial surfaces. The broad zone of deformation that includes the apparent folding to the north suggests multiple events may be recorded in the fan surface. The eastern continuation of the north scarp and greater scarp on the postglacial (i.e., older) eastern upland surface suggests the upland surface has experienced more earthquakes than the alluvial surface, indicating that two or more postglacial events have occurred.

### 4.3 Characterization of Subsurface Structure

Following our conclusion that the scarps and lineaments at the site are tectonic in origin, and apparently related to the Sequim fault, this section discusses the characterization of causative structures. We herein consider the collective scarps and lineaments within the Dungeness River valley and the upland glacial surfaces to the east and west as part of the Sequim fault (Figure 14). It is not clear if the lineaments and offset deposits south of Sequim Bay are somehow related to the Sequim fault. While we identified no compelling surficial evidence suggestive of deformation south of Sequim Bay, the observation by Gower (1978 and 1980) is significant in that it provides documentation of Holocene displacement both east and west (Nelson and others, 2017; Schermer and others, 2021) of the Project site.

The maximum length of the Sequim fault based on previous geophysical structure mapping is at least 46 km (as depicted by Brocher and others, 2001), extending west from the southern Whidbey Island fault to the western edge of their map extent (Figure 9). The map extent ends at roughly the same longitude as the scarp mapped across the western upland glacial surface, and several other more northerly trending structures have been mapped in the area, which may suggest western truncation of the fault.

**Exhibit 4-1: Characteristics of the Sequim Fault From Previous Studies**

Reference	Length (km) [mi]	Dip Angle and Direction	Sense of Slip
MacLeod and others (1977)	31 [19]	Not specified	Down-to-the-north
Gower (1978 and 1980) and Gower and others (1985)	31 [19]	Not specified	Down-to-the-north
Johnson and others (1996)	≥16 [≥10] <sup>1</sup>	54° south <sup>2</sup> 41° south <sup>2</sup> 50° south <sup>3</sup>	Up-to-the-south
Brocher and others (2001)	≥46 [≥29]	70° south	Up-to-the-south

NOTES:

- 1 Limited to the west by map extent.
- 2 Two south-dipping faults interpreted by Johnson and others (1996) on seismic reflection profile (Figure 8).
- 3 Two south-dipping faults on Johnson and others (1996) cross section (Figure 8).

Based on available information, we assume the Sequim fault dips south at depth. The Sequim fault is described as down-to-the-north or up-to-the-south in various publications (Exhibit 4-1). Given that the fault bounds the southern margin of a prominent Tertiary and Quaternary basin (MacLeod and others, 1977; Johnson and others, 1996; Brocher and others, 2001), the dip direction dictates whether the fault has a reverse or normal sense of slip. Interpretation of a seismic reflection profile by Johnson and others (1996) about 20 km east of the site (Figure 8) and a microseismicity profile by Brocher and others (2001) about 30 km east of the site suggest a moderate to steep south dip direction (Exhibit 4-2).

The NOFZ to the west has also been characterized with conflicting dip directions and senses of slip ranging from a north-dipping normal fault to a steeply south-dipping reverse fault (Nelson and others, 2017 and references therein). Faults comprising the NOFZ dip subvertically, north, and south in trench exposures (Nelson and others, 2017; Schermer and others, 2021). It is not uncommon for faults in trench exposures to exhibit a different dip angle, and even direction than the faults at depth. The dip of the NOFZ at depth remains unresolved; however, most scarps demonstrate north-side-up movement (Nelson and others, 2017; Schermer and others, 2023). Displacement estimates discussed in Section 5.1 are most consistent with a 50° dipping fault.

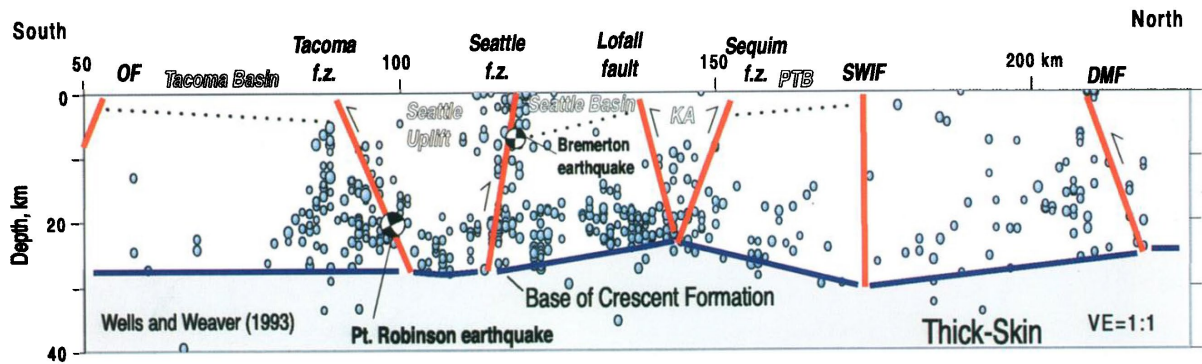


**Exhibit 4-2: Microseismicity Cross Section of the Puget Sound and Eastern Strait of Juan de Fuca**

Source: Brocher and others (2001)

The scarps and folds in the Dungeness River valley appear to represent deformation by a reverse fault based on the following:

- A convex-upward shape of the northern fault scarp (Figure 19, profiles D, E, and F), consistent with normal (i.e., convex) drag and bulldoze zone on a reverse fault (Grasemann and others, 2005).
- Regional north-south compression revealed by GPS surveys (McCaffery and others, 2007 and 2013).
- Observed folding is more common in compressional systems than extensional systems (McCalpin, 2009).
- A 21° change in strike between the dominantly right-lateral NOFZ (10H:1V to 6H:1V) (Schermer and others, 2021) and the Sequim fault. This change in strike would result in a 0.7H:1V to 2.2H:1V displacement ratio for the Sequim fault, assuming a dip ranging from 50° to 70° to the south for both faults (described in greater detail in Section 5.1).
- A south dip, although not particularly well constrained, are depicted by Johnson and others (1996) and Brocher and others (2021) and represent the best surface information to constrain the dip of the fault at depth. A southern dip on a down-to-the-north or up-to-the-south fault translates to reverse slip.

We present three alternative dip direction models in cartoon cross sections of faults and folds in the Dungeness River valley in Figure 24. These non-unique models represent three of a multitude of possibilities and are intended to demonstrate approximate end member configurations of how fault dip at depth may translate to faults in the shallow subsurface (about 1 km or less). Models A and C depict shallow subsurface fault configurations related to near vertical or south-dipping faults at depth. Despite the differences in dip direction, the near surface faults have similar configurations. Model B, which dips north at depth, requires a markedly different configuration of faults in the near surface to maintain a reasonable geometry. We deem Models A and C as more likely than Model B because they more realistically accommodate the apparent normal displacement on the southern fault

scarp and the apparent graben structure adjacently north within a flower-like structure, which are common along strike slip faults in transpressive stress systems (Fossen, 2016). Model B requires a normal fault to branch directly to the ground surface from the north-dipping fault, which is difficult to resolve.

The microseismicity profile in Brocher and others (2001) suggests a seismogenic depth of about 30 km (Exhibit 4-2). The USGS National Seismic Hazard Mapping project developed a grid of seismogenic depth that covers the western U.S. (Zeng and others, 2022), which indicates a depth of about  $34 \pm 2$  km for the Strait of Juan de Fuca region.

## 5 IMPLICATIONS AND RECOMMENDATIONS

The presence of an interpreted Holocene fault crossing or near the site has several implications for the Project that could impact reservoir location, configuration, and embankment design. To assist with these considerations, we provide order-of-magnitude-type displacement and sense of slip estimates. Note that these estimates are not derived from a deterministic or probabilistic fault displacement hazard analysis (DFDHA or PFDHA), which may be warranted to support embankment design. We also make recommendations to assist with reservoir location, configurations and design with respect to fault locations and possible extent of deformation. Reservoir option-specific recommendations are provided for additional work, and seismic source parameters that can be used in an updated probabilistic or deterministic seismic hazard analysis (DSHA or PSHA) are provided.

### 5.1 Displacement Estimates

To develop preliminary estimates of fault displacements, we rely on data gathered from studies of the NOFZ, which appears closely related to, and possibly ruptures with the Sequim fault (described below). The Sequim fault has not been well studied and lacks published slip rate and paleoseismic information. However, the fault shares similar characteristics with the NOFZ, including strike, bounding the northern margin of the Olympic Mountains block, and scarps that share similar morphologies to those mapped in the Dungeness River valley. Based on these similarities, we assume the Sequim fault is capable of producing similar displacements to the NOFZ. Therefore, we rely on previously documented average slip measurements and slip rates of the NOFZ to develop preliminary displacement estimates for the Sequim fault in the Project area. As noted above, these displacements are intended to provide the design team with order-of-magnitude values to assist with reservoir option selection and preliminary embankment design for surface fault



rupture hazard mitigation. We have not performed a DFDHA or PFDHA to produce the estimates below.

An average of 4.6 m of right-lateral slip and 0.4 m of reverse vertical separation per event has been documented on the LCBC fault yielding a 10H:1V displacement component ratio (Nelson and others, 2017). This equates to slightly more than 4.6 m of net slip depending on fault dip. Farther west, on the Sadie Creek fault, an average of 4 m  $\pm$  1 m of right-lateral slip per event is documented, with a 6H:1V displacement component ratio (Schermer and others, 2021). These imply an average vertical separation of about 0.7 m  $\pm$  0.2 m per event, yielding about 4.1 m of net slip per event. Given the continuity of these two faults, and their similar strikes, we make a simplifying assumption that the differences in displacement and sense of slip between the two faults represents composite variability for a single fault.

Herein, we refer to several components of displacement following terms in Exhibit 5-1.

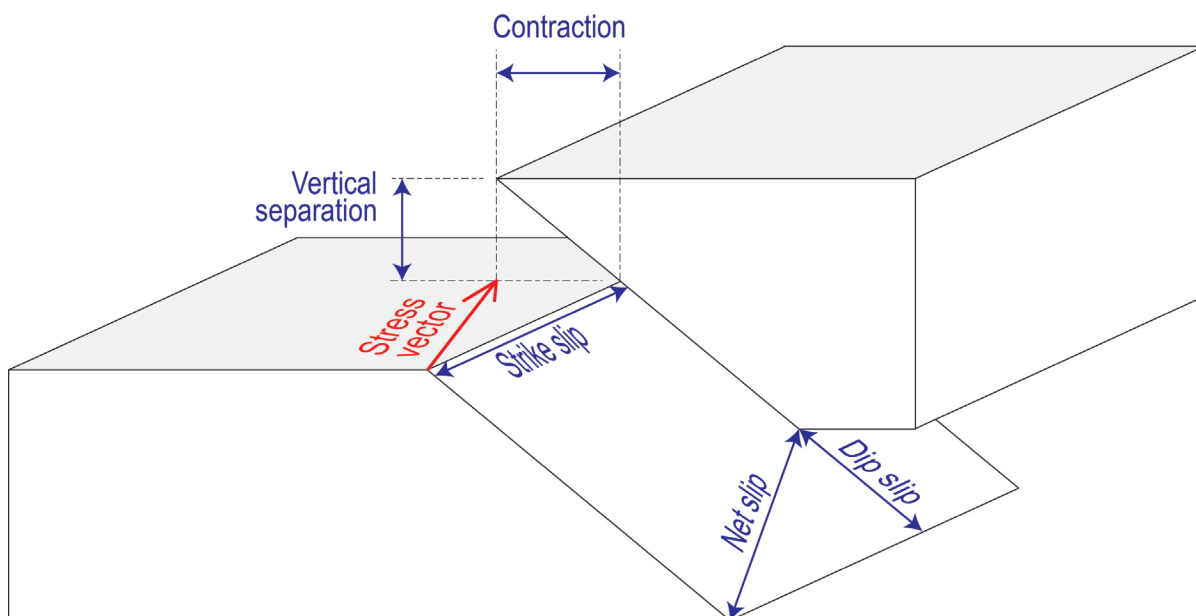


#### Exhibit 5-1: Components of Fault Displacement

Notes: The ratio of strike slip to vertical separation is used to define the horizontal to vertical component displacement ratio.

The NOFZ has an overall strike of about 105° azimuth, and the Sequim fault scarps have an average overall strike of about 85° azimuth (Figure 25). The NOFZ is characterized by dominantly strike-slip and this 21° difference in strike to the Sequim fault, assuming both faults accommodate the same regional stress vector, imparts a considerable reverse component. This approach applies similarly if we assume the faults are structurally connected at depth and the change in strike represents a bend. Changes in slip and displacement ratios due to changes in strike are observed at nearly all scales of faulting (e.g.,

Big Bend of the San Andreas fault in California, local restraining or releasing bends along faults). Therefore, we apply the overall strike of the Sequim fault scarps, as opposed to the general subsurface trace of the fault defined in geophysical studies, to develop preliminary estimates of displacement that apply to the Project site area.

For the NOFZ, we determine a range of stress vector directions from 103° to 113° azimuth based on the strike, range of strike-slip to vertical separation ratios, and range of probable dips (50°, 70°, and 90°) (Table 1). We assume stress vector displacements ranging from 3 to 5 m based on the relationship between measured displacement, fault strike, and displacement ratios (Nelson and others, 2017; Schermer and others, 2021). Note that the vector displacement in Table 1 is nearly equivalent to the horizontal component of displacement because the vertical component of the 10H:1V to 6H:1V is small and implies that the strike of the NOFZ is closely aligned with the stress it accommodates (Table 1). Nelson and others (2017) described both normal and reverse vertical slip on the LCBC fault, while Schermer and others (2021) described primarily reverse vertical slip along the Sadie Creek fault. These inconsistencies in the minor vertical slip components further indicate these faults are oriented to accommodate regional stress. We apply the range of stress vector directions and displacements in Table 1 to the Sequim fault to estimate its displacement components (Table 2).

Comparison of Tables 1 and 2 demonstrates the impact of the change in strike between the NOFZ and the Sequim fault to the displacement components. Whereas the NOFZ is characterized by 10H:1V to 6H:1V displacement component ratios, the Sequim fault ratios range from about 0.7H:1V to 2.3H:1V due to its less ideal alignment with the stress vector acting on the NOFZ.

Displacements and ratios for the Sequim fault assuming a 90° dip could not be determined, because a vertical fault cannot accommodate horizontal contraction. Without observed vertical displacement measurements, as available on the NOFZ, we cannot resolve a vertical component for a vertical fault.

All components of average displacement (AD) per event, which refers to the AD that can be expected anywhere along a rupture, for the Sequim fault are over 1 m (3.2 ft) (Table 2), with the strike slip component ranging from 2.8 to 4.7 m (9 to 15 ft) and the vertical separation component ranging from 1.2 to 6.4 m (4 to 21 ft). The mean AD values determined for a 50° dipping fault range from 3.5 to 3.8 m (11.5 to 12.5 ft) of strike slip, 1.6 to 2.2 m (5.2 to 7.2 ft) of vertical slip, resulting in a displacement ratio of approximately 2H:1V, and yielding net slip up to 4.6 m (15.1 ft) (Table 2). We selected these values because:

- They are most consistent with alluvial surfaces vertically displaced by about 2 to 3 m (7 to 10 ft) upstream and downstream of the north scarp (Figures 15 and 19, profiles D, E, and F). The horizontal component cannot be resolved from our desktop study.
- A dip of 50° is consistent with dip determined by Johnson and others (1996) on their seismic reflection profile and cross section, which represent the best available constraints on fault dip (Figure 8).

The approximately 3 to 5 m (10 to 16 ft) of displacement observed on the NOFZ is uncharacteristically large relative to the length of the fault zone (Table 3). The Wells and Coppersmith (1994) scaling relationship for surface rupture length (SRL) to average displacement (AD) for strike slip faults returns a *mean ± 1 standard deviation* AD range of 0.9 to 2.7 m (1.3 m or 4.2 ft mean AD), assuming a 56-km-long (35-mi-long) SRL for the combined LCBC fault and Sadie Creek faults, and 0.9 to 4 m (1.9 m or 6.2 ft mean AD) for an 80-km-long (50-mi-long) SRL for the NOFZ. These displacements fall either outside or narrowly within the *mean + 1 standard deviation* values of AD with respect to SRL (Table 3).

Therefore, we find it possible that the Sequim fault either (1) represents an eastern extension of the NOFZ along the northern margin of the Olympic Mountains block that, whether directly or through a series of stepping faults or stepovers, extends east to the SWIF; or, (2) the NOFZ and Sequim fault are separate structures that can produce independent ruptures, or combine in larger multi-fault earthquakes. In Figure 25, we present the seismic source model of the most recent USGS National Seismic Hazard Maps, along with two sources (western NOFZ and Sequim fault) that should be considered for future Project site-specific DSHA or PSHA and DFDHA or PFDHA.

The California Department of Water Resources Division of Safety of Dams (DSOD) inspection protocol for fault displacement hazard (CA DSOD, 2018) uses *mean AD +0.5 standard deviation* for dams in high (probable loss of at least one life) to extremely high (probable loss of at least one life and inundation of 1,000 people) hazard classes with fault slip rates of 1.1 to 8.9 mm/year (the NOFZ slip rate is 1.3 to 2.3 mm/year [Schermer and others, 2021]). The *mean AD +0.5 standard deviation* for a combined rupture of the Sequim fault and NOFZ as shown in Figure 25 results in 4.4 m (14 ft) (Table 3), which is generally consistent with the displacement values that we prefer above.

## 5.2 Surface Fault Rupture Hazard

Based on available information that point to the presence of Holocene faults and folds at and near the Project site, we interpret that surface fault rupture is a hazard for the site and developed zones to assist with the selection of reservoir location, configuration, and embankment design.

There is little regulatory guidance to follow for surface fault rupture or deformation hazards. Instead, facility owners are expected to sufficiently address the potential for rupture hazard through site-specific investigation. Ecology's DSO has developed guidelines for assessing the seismic stability of dams (DSO, 1993). The DSO seismic guidelines focus on overtopping due to shaking-induced, acceleration-induced, or liquefaction-induced embankment failure. The DSO guidelines do not provide regulatory guidance for surface fault rupture hazard. They note that embankment cores, filler zones, and drainage features have been used to accommodate potential surface fault rupture. Similarly, the Federal Energy Regulatory Commission (FERC) guidelines for evaluation of earthquake shaking hazards (Idriss and others, 2018) do not provide guidance to address surface fault rupture hazard. The California DSOD (2018) provides guidance on design fault displacements based on hazard classes, but little guidance to address surface fault rupture hazard.

In light of the lack of regulatory guidance, and due to the lack of exposures and well-constrained fault locations, we have developed deformation hazard zones for the Project that are based on qualitative observations. Maps of these zones are provided for each the four reservoir options that have been considered during Project design development (Figures 26A through D). Below, we describe the basis for each of the three types of zones:

- Primary Deformation Zone
  - The relative prominence of the north scarp compared with other deformation on the alluvial surface and the uplands to the east suggests this fault carried the majority of slip in the past earthquake or earthquakes. Therefore, we define a primary deformation zone that encompasses the trace defined at the base of the north scarp (Figure 26A to 26D).
  - It is possible that all primary displacement could occur along a single plane within this zone or be distributed throughout the zone. Secondary faults and deformation are also possible within this zone.
  - The primary deformation zone extends 250 ft north of the north scarp trace and encompasses the width of the north scarp, plus an additional 50 ft to capture uncertainty. The location of reverse faults within a scarp can be difficult to constrain because the fault itself can be obscure within a bulldoze zone of colluvium, folded stratigraphy, and/or post-seismic scarp colluvium.
  - The zone extends 100 ft to the south of the north scarp trace into an area between the north and south scarps that appears undeformed. This southern part of the zone is intended to capture uncertainty in the location of potential future primary and secondary deformation.
- Secondary Deformation Zone
  - The southern scarp appears to represent an antithetic, secondary structure and likely carries secondary deformation during earthquakes. The south scarp is narrower and

- displaces the alluvial surface a smaller amount than the north scarp (Figures 15 and 19) and we observed no evidence of deformation to the south of this zone.
- This zone extends along the trace defined at the base of the south scarp (Figures 26A to 26D).
  - The zone extends 100 ft to the north of the south scarp trace into an area between the north and south scarps that appears undeformed. The zone is intended to capture the potential for uncertainty in the location of potential future primary and secondary deformation.
  - The south scarp buffer extends 200 ft south of the south scarp trace to encompass the width of the scarp, plus an additional 50 ft to capture uncertainty.
- Distributed Secondary Deformation Zones
    - These zones are located between the north and south scarps, and north of the north scarp.
    - The zones are intended to encompass areas of potential future secondary surface fault rupture and folding.
    - These zones may experience deformation due to folding or secondary faulting in potential future earthquakes.
  - Low probability of deformation zone
    - This zone extends across the Project site south of the south scarp where we see no evidence of past surface deformation but cannot preclude the possibility of future rupture or deformation.

### 5.3 Recommendations

Based on the geologic and geomorphic findings of this study, the development of preliminary displacement estimates, and delineation of surface fault rupture and surface deformation hazards above, we have developed several recommendations to assist with the Project.

In Table 4, we provide a recommendation for potential fault displacement to be considered for each deformation hazard in preliminary design that is based on a primary net slip of 5 m, which is consistent with the displacement estimated for a combined rupture of the NOFZ and Sequim fault (Table 3 and Section 5.1), and with the upper uncertainty bracket for average displacement measured in paleoearthquakes on the NOFZ (Section 5.1). Final design should incorporate the results of a DFDHA or PFDHA considering the seismic source parameters in Table 5.

Based on the relatively large displacements recommended for three of these zones, we identify several paths forward for the Project to address surface fault rupture hazard. These

paths are presented in ascending order of viability based on our understanding of design capability and Project goals:

1. Design the reservoir and embankments to accommodate the displacements described above. Without further information, estimated displacements from a DFDHA will likely remain similar to those in Section 5.1. A PFDHA may result in lower estimated fault displacement depending on the return period selection for the Project. However, the high to extremely high hazard class of the proposed Project would likely require a relatively long return period be selected, in which case displacements will likely remain large.
2. Excavate trenches to assess for the presence of faulting in the primary, secondary, and distributed secondary deformation zones (Figures 26A through 26D). If, for example, the area north of the north scarp was found to be devoid of faulting, the embankment could be designed for broad folding, as opposed several feet of vertical and horizontal discrete fault displacement at any location. Given the thickness of what we expect to be massive, structureless alluvial deposits beneath the site, there is a low probability that we could identify continuous stratigraphy to assess for faulting without excavating excessively deep trenches (on the order of 30 ft or more).
3. Excavate off-site trenches (e.g., base of scarp on the upland surface) that could provide information on displacements in paleoearthquakes. This would require ideal conditions and excellent preservation of offsets to develop site-specific per-event displacements. Based on magnitude of scarp heights across alluvial surfaces near the site, we believe it would be unlikely that offsets identified in an off-site trench would result in a significant reduction in displacement.
4. Avoid the primary, secondary, and distributed secondary deformation zones.

Given these general paths, we recommend pursuing the fourth option, which appears viable for reservoir Option D. For the portion of the proposed Option D embankment located within the secondary deformation zone, we recommend the following alternatives:

1. The guidelines for displacement in the secondary deformation zone in Table 4 be followed for preliminary design.
2. A subsurface investigation is performed to assess for the presence or absence of faulting.
  - The proposed Option D footprint does not cross the south scarp but does intersect the secondary hazard zone buffer south of the scarp. It is possible there is no faulting south of the mapped trace within this buffer portion of the zone.
  - As in any trenching investigation, there is a probability for not encountering laterally continuous stratigraphy in a trench excavated to assess for faulting. However, the alluvial deposits in the Option D area are shallower, which would limit the size and depth of the excavation, and the glacial till beneath the alluvium could be assessed for faulting.



- Should faulting be identified, or the deposits cannot be used to assess faulting, the preliminary design would default to the displacements recommended for the secondary deformation zone in Table 4.
3. The reservoir and embankment be located and designed to avoid the zone altogether. If the reservoir and embankment avoid the primary, secondary and distributed secondary deformation hazard zones, excavation of fault trenches to further evaluate the faults would not be necessary during the design phase of the project, in our opinion.

Below are additional recommendations the Project should consider:

- A site-specific DSHA or PSHA that incorporates rupture combinations of the Sequim fault, LCBC fault, Sadie Creek fault, and western NOFZ should be performed prior to final design of the reservoir.
  - Table 5 presents preliminary seismic source parameters for the Sequim fault and various rupture combinations that may be used in the analysis. Figure 25 presents the trace of our proposed Sequim fault source, the existing LCBC and Sadie Creek fault source from the USGS National Seismic Hazard Model (Petersen and others, 2024), and our proposed western NOFZ (which we have not characterized except for the length based on Schermer and others, 2021). For the western NOFZ, we recommend applying the same parameters as used for the LCBC and Sadie Creek fault source from the USGS National Seismic Hazard Model.
  - This additional source beneath the Project site is likely to have a significant effect on ground motions. Additionally, our interpretation of a south-dipping fault at depth will induce hanging wall effect (i.e., elevated ground motion) to the analysis (Donahue and Abrahamson, 2014).
  - The reservoir should be designed to accommodate probable ground movement and ground motions associated with rupture of the faults.
- We recommend reservoir excavation slopes be periodically observed during construction by a Washington State Licensed Engineering Geologist with experience in paleoseismic trench studies.
  - Inspection of the walls for faulting and the possibility that displacements could exceed those described above should be assessed.
  - This recommendation for inspection of the excavation slopes is applicable to any reservoir constructed on the site, even if the reservoir is located in the low probability of deformation zone. Given the presence of apparent Holocene faulting adjacent to this zone, inspection should be made to look for deformation that may not be visible at the ground surface.

## 6 REFERENCES

- Alley, N.F. and Chatwin, S.C., 1979, Late Pleistocene history and geomorphology, southwestern Vancouver Island, British Columbia: *Canadian Journal of Earth Sciences*, v. 16, no. 9, p. 1645-1657.
- Blakely, R.J.; Wells, R.E.; and Weaver, C.S., 1999, Puget Sound aeromagnetic maps and data: U.S. Geological Survey Open-File Report 99-514, available: <https://pubs.usgs.gov/of/1999/of99-514/>.
- Booth, D.B.; Troost, K.G.; Clague, J.J.; and others, 2004, The Cordilleran ice sheet: *Developments in Quaternary Sciences*, v. 1, p. 17-43.
- Brandon, M.T. and Vance, J.A., 1992, Tectonic evolution of the Cenozoic Olympic subduction complex, Washington State, as deduced from fission track ages for detrital zircons: *American Journal of Science*, v. 292, October 1992, p. 565-636.
- Brandon, M.T.; Roden-Tice, M.K.; and Garver, J.I., 1998, Late Cenozoic exhumation of the Cascadia accretionary wedge in the Olympic Mountains, northwest Washington State: *Geological Society of America Bulletin*, v. 110, no. 8, p. 985-1009.
- Bretz, J.H., 1920, The Juan de Fuca lobe of the Cordilleran ice sheet: *The Journal of Geology*, v. 28, no. 4, p. 333-339.
- Brocher, T.M.; Parsons, T.; Blakely, R.J.; and others, 2001, Upper crustal structure in Puget Lowland, Washington: Results from the 1998 seismic hazards investigation in Puget Sound: *Journal of Geophysical Research: Solid Earth*, v. 106, no. B7, p. 13541-13564.
- California Department of Water Resources, Division of Safety of Dams (DSOD), 2018, Division of Safety of Dams inspection and reevaluation protocols: Sacramento, Calif., September 28, 83 p.
- Collins, B.D. and Sheikh, A.J., 2005, Historical reconstruction, classification, and change analysis of Puget Sound tidal marshes: Olympia, Wash., Washington State Department of Natural Resources, June, 120 p.
- Dethier, D.P.; Pessl Jr, F.; Keuler, R.F.; and others, 1995, Late Wisconsinan glaciomarine deposition and isostatic rebound, northern Puget lowland, Washington: *Geological Society of America Bulletin*, v. 107, no. 11, p. 1288-1303.
- Donahue, J.L. and Abrahamson, N.A., 2014, Simulation-based hanging wall effects: *Earthquake Spectra*, v. 30, no. 3, p. 1269-1284.

- du Bray, E.A. and John, D.A., 2011, Petrologic, tectonic, and metallogenic evolution of the Ancestral Cascades magmatic arc, Washington, Oregon, and northern California: *Geosphere*, v. 7, no. 5, p. 1102-1133.
- Egan, J.; Staff, R.; and Blackford, J., 2015, A high-precision age estimate of the Holocene Plinian eruption of Mount Mazama, Oregon, USA: *The Holocene*, v. 25, no. 7, p. 1054-1067.
- Engelhart, S.E.; Vacchi, M.; Horton, B.P.; and others, 2015, A sea-level database for the Pacific coast of central North America: *Quaternary Science Reviews*, v. 113, p. 78-92.
- Idriss, I.M.; Archuleta, R.J.; and Abrahamson, N.A., 2018, Chapter 13 – evaluation of earthquake ground motions, *in* Engineering Guidelines for the Evaluation of Hydropower Projects: Washington, D.C., Federal Energy Regulatory Commission (FERC), May 30, 100 p.
- Fossen, Haakon, 2016, *Structural geology* (3rd ed.): Cambridge, U.K., Cambridge University Press, 463 p.
- Global Geophysics, 2023, Report for multichannel analysis of surface wave survey for the proposed Dungeness off-channel reservoir, Sequim, Wa: Report (unpublished) prepared by Global Geophysics, Monroe, Wash., for Anchor QEA, LLC, Seattle, Wash., January 6, 11 p.
- Gower, H.D., 1978, Tectonic map of the Puget Sound region, Washington, showing locations of faults, principal folds and large-scale Quaternary deformation: U.S. Geological Survey, Open-File Report 78-426, 22 p., 1 sheet, 1:250,000 scale.
- Gower, H.D., 1980, Bedrock geologic and Quaternary tectonic map of the Port Townsend area, Washington: U.S. Geological Survey, Open-File Report 80-1174, 19 p., 1 sheet, 1:100,000 scale.
- Gower, H.D.; Yount, J.C.; and Crosson, R.S., 1985, Seismotectonic map of the Puget Sound region, Washington: U.S. Geological Survey, Miscellaneous Investigations Series, Map I-1613, 1 sheet, 1:250,000 scale.
- Grasemann, B.; Martel, S.; and Passchier, C., 2005, Reverse and normal drag along a fault: *Journal of Structural Geology*, v. 27, no. 6, p. 999-1010.
- Gustafson, C.E.; Gilbow, D.W.; and Daugherty, R.D., 1979, The Manis mastodon site: Early man on the Olympic Peninsula: *Canadian Journal of Archaeology*, no. 3, p. 157-164.

- Hartmann, G.D., 1997, A cultural resources survey of the proposed SR 101: Sequim bypass wetlands mitigation area, Clallam County, Washington: Cheney, Wash., Archaeological and Historical Services, Eastern Washington University, Short Report DOT97-16, 8 p.
- Haugerud, R.A., 2002, Lidar evidence for Holocene surface rupture on the Little River fault near Port Angeles, Washington [abstract]: *Seismological Research Letters*, v. 73, no. 2, p. 248.
- Haugerud, R.A. and Harding, D.J., 2001, Some algorithms for virtual deforestation (VDF) of LIDAR topographic survey data: *International Archives of Photogrammetry Remote Sensing and Spatial Information Sciences*, v. 34, no. 3/W4, p. 211-218.
- Haugerud, R.A.; Harding, D.J.; Johnson, S.Y.; and others, 2003, High-resolution lidar topography of the Puget Lowland, Washington: *GSA Today*, v. 13, no. 6, p. 4-10.
- Haugerud, R.A., 2021, Deglaciation of the Puget Lowland, Washington in Waitt, R.B.; Thackray, G.D.; and Gillespie, A.R., eds., *Untangling the quaternary period: A legacy of Stephen C. Porter*: Boulder, Colo., The Geological Society of America, Special Paper 548, p. 279-298.
- Harding, D.J. and Berghoff, G.S., 2000, Fault scarp detection beneath dense vegetation cover: Airborne lidar mapping of the Seattle fault zone, Bainbridge Island, Washington State, *in American Society of Photogrammetry and Remote Sensing Annual Conference*, Washington, D.C., 2000, Proceedings: Baton Rouge, La., ASPRS, 10 p.
- Heusser, C.J., 1973, Environmental sequence following the Fraser advance of the Juan de Fuca lobe, Washington: *Quaternary Research*, v. 3, no. 2, p. 284-306.
- Heusser, C.J.; Heusser, L.E.; and Streeter, S.S., 1980, Quaternary temperatures and precipitation for the north-west coast of North America: *Nature*, v. 286, no. 5774, p. 702-704.
- James, T.; Gowan, E.J.; Hutchinson, I.; and others, 2009, Sea-level change and paleogeographic reconstructions, southern Vancouver Island, British Columbia, Canada: *Quaternary Science Reviews*, v. 28, no. 13-14, p. 1200-1216.
- Johnson, S.Y.; Potter, C.J.; Miller, J.J.; and others, 1996, The southern Whidbey Island fault: an active structure in the Puget lowland, Washington: *Geological Society of America Bulletin*, v. 108, no. 3, p. 334-354.
- Kovanen, D.J. and Easterbrook, D.J., 2001, Late Pleistocene, post-Vashon, alpine glaciation of the Nooksack drainage, North Cascades, Washington: *Geological Society of America Bulletin*, v. 113, no. 2, p. 274-288.

- Linden, R.H. and Schurer, P.J., 1988, Sediment characteristics and sea-level history of Royal Roads anchorage, Victoria, British Columbia: *Canadian Journal of Earth Sciences*, v. 25, no. 11, p. 1800-1810.
- MacLeod, N.S.; Tiffin, D.L.; Snively Jr, P. D.; and others, 1977, Geologic interpretation of magnetic and gravity anomalies in the Strait of Juan de Fuca, US–Canada: *Canadian Journal of Earth Sciences*, v. 14, no. 2, p. 223-238.
- McCaffrey, R.; Qamar, A.I.; King, R.W.; and others, 2007, Fault locking, block rotation and crustal deformation in the Pacific Northwest: *Geophysical Journal International*, v. 169, no. 3, p. 1315-1340.
- McCaffrey, R.; King, R.W.; Payne, S J.; and others, 2013, Active tectonics of northwestern US inferred from GPS-derived surface velocities: *Journal of Geophysical Research: Solid Earth*, v. 118, no. 2, p. 709-723.
- McCalpin, J.P., 2009, Paleoseismology in extensional tectonic environments: *International Geophysics*, v. 95, p. 171-269.
- McCrorry, P.A.; Foster, D.S.; Danforth, W.W.; and others, 2002, Crustal deformation at the leading edge of the Oregon Coast Range block, offshore Washington (Columbia River to Hoh River): U.S. Geological Survey, Professional Paper 1661-A, Washington DC, US Government Printing Office, 47 p.
- Mosher, D.C. and Hewitt, A.T., 2004, Late Quaternary deglaciation and sea-level history of eastern Juan de Fuca Strait, Cascadia: *Quaternary International*, v. 121, no. 1, p. 23-39.
- Morgan, V.E.; Holstine, C.E.; Gundy, B.J.; and others, 1999, The SR-101 Sequim bypass archaeological project: mid- to late-Holocene occupations on the northern Olympic Peninsula, Clallam County, Washington: Cheney, Wash., Eastern Washington University, Reports in Archaeology and History, v. 1.
- Nelson, L.M., 1971, Sediment transport by streams in the Snohomish River basin, Washington: October 1967-June 1969: U.S. Department of the Interior, Geological Survey, Water Resources Division, 44 p.
- Nelson, A.R.; Personius, S.F.; Buck, J.B.; and others, 2007, Field and laboratory data from an earthquake history study of scarps of the Lake Creek–Boundary Creek fault between the Elwha River and Siebert Creek, Clallam County, Washington: U.S. Geological Survey, Scientific Investigations Map 2961, 2 sheets.

- Nelson, A.R.; Personius, S.F.; Wells, R.E.; and others, 2017, Holocene earthquakes of magnitude 7 during westward escape of the Olympic Mountains, Washington: Bulletin of the Seismological Society of America, v. 107, no. 5, p. 2394-2415.
- Noble, J.B., 1960, A preliminary report on the geology and ground-water resources of the Sequim-Dungeness area, Clallam County, Washington: Lacey, Wash., State of Washington, Department of Conservation, Division of Water Resources, 43 p.
- Olson, P.L.; Legg, N.T.; Abbe, T.B.; and others, 2014, A methodology for delineating planning-level channel migration zones: Lacey, Wash., Washington Department of Ecology, Publication no. 14-06-025, p. 1-83.
- Othberg, K.L. and Palmer, Pamela, 1979a, Preliminary surficial geologic map of the Carlsborg quadrangle, Clallam County, Washington: Washington Division of Geology and Earth Resources, Open File Report 79-20, 1 Sheet, Scale 1:24,000.
- Othberg, K.L. and Palmer, Pamela, 1979b, Preliminary surficial geologic map of the Sequim quadrangle, Clallam County, Washington: Washington Division of Geology and Earth Resources, Open File Report 79-18, 1 Sheet, Scale 1:24,000.
- PanGEO, Inc., 2020, Geotechnical engineering feasibility report review Dungeness off-line storage facility, River Road, Clallam County, Washington: Report prepared by PanGEO, Seattle, Wash., File no. 20-122, for Clallam County Department of Public Works, Port Angeles, Wash., December, 15 p.
- Petersen, K.L.; Mehringer, P.J.; and Gustafson, C.E., 1983, Late-glacial vegetation and climate at the Manis mastodon site, Olympic Peninsula, Washington: Quaternary Research, v. 20, no. 2, p. 215-231.
- Petersen, M.D.; Shumway, A.M.; Powers, P.M.; and others, 2024, The 2023 US 50-state national seismic hazard model: Overview and implications: Earthquake Spectra, v. 40, no. 1, p. 5-88.
- Porter, S.C. and Swanson, T.W., 1998, Radiocarbon age constraints on rates of advance and retreat of the Puget lobe of the Cordilleran ice sheet during the last glaciation: Quaternary Research, v. 50, no. 3, p. 205-213.
- Ramachandran, K.; Dosso, S.E.; Zelt, C.A.; and others, 2004, Upper crustal structure of southwestern British Columbia from the 1998 seismic hazards investigation in Puget Sound: Journal of Geophysical Research: Solid Earth, v. 109, no. B9, 14 p.
- Schasse, H.W., 2003, Geologic Map of the of the Washington Portion of the Port Angeles Quadrangle: Washington Department of Natural Resources, Division of Geology and Earth Resources Open File Report 2003-6.



- Schasse, H.W. and Logan R.L., 1998, Geologic map of the Sequim 7.5-minute quadrangle, Clallam County, Washington: Washington Division of Geology and Earth Resources, Open File Report 98-7, -28 p., 2 plates, scale 1:24,000.
- Schasse, H.W., and Polenz, M., 2002, Geologic Map of the Morse Creek 7.5-Minute Quadrangle, Clallam County, Washington: Washington Department of Natural Resources, Division of Geology and Earth Resources Open File Report 2002-8.
- Schasse, H.W., and Wegmann, K.W., 2000, Geologic map of the Carlsborg 7.5-minute quadrangle, Clallam County, Washington: Washington Division of Geology and Earth Resources, Open File Report 2000-7, p. 1 - 33, 2 plates, scale 1:24,000.
- Shekut, Samuel and Licht, Alexis, 2020, Late middle Miocene emergence of the Olympic Peninsula shown by sedimentary provenance: *Lithosphere*, v. 2020, no. 7040598, p. 1-20.
- Shannon and Wilson, Inc., 2022, Phase 1 geotechnical data report, Dungeness off-channel reservoir, Sequim, Washington: Report prepared by Shannon and Wilson, Seattle, Wash., for Anchor QEA, LLC, Seattle, Wash., January, 264 p.
- Sherrod, B.L.; Blakely, R.J.; Weaver, C.S.; and others, 2008, Finding concealed active faults: Extending the southern Whidbey Island fault across the Puget Lowland, Washington: *Journal of Geophysical Research: Solid Earth*, v. 113, no. B5, 25 p.
- Schermer, E.R.; Amos, C.B.; Duckworth, W.C.; and others, 2021, Postglacial  $M_w$  7.0–7.5 Earthquakes on the North Olympic Fault Zone, Washington: *Bulletin of the Seismological Society of America*, v. 111, no. 1, p. 490-513.
- Tabor, R.W. and Cady, W.M., 1978, Geologic map of the Olympic Peninsula, Washington: U.S. Geological Survey, Miscellaneous Investigations Series Map I-994, 2 sheets, scale 1:125,000.
- Thorson, R.M., 1980, Ice-sheet glaciation of the Puget lowland, Washington, during the Vashon Stade (late Pleistocene): *Quaternary Research*, v. 13, no. 3, p. 303-321.
- U.S. Geological Survey, 1974, Aeromagnetic map of part of the Puget Sound area, Washington: USGS Numbered Series, Open-File Report 74-1106, 1 sheet.
- U.S. Geological Survey, 1977, Aeromagnetic map of northern and eastern parts of the Puget Sound area, Washington: USGS Numbered Series, Open-File Report 77-34, 1 sheet.
- U.S. Geological Survey and Washington Department of Natural Resources (USGS and DNR), 2024, Quaternary fault and fold database for the United States: Available: <https://www.usgs.gov/natural-hazards/earthquake-hazards/faults>, accessed January 2024.

- Van Wagoner, T.M.; Crosson, R.S.; Creager, K.C.; and others, 2002, Crustal structure and relocated earthquakes in the Puget Lowland, Washington, from high-resolution seismic tomography: *Journal of Geophysical Research: Solid Earth*, v. 107, no. B12, p. ESE-22-1–ESE-22-23.
- Washington State Department of Ecology, Dam Safety Office (WA DSO), 1993, Dam safety guidelines part IV: Dam design and construction: Lacey, Wash., WA DSO, Report no. 92-55D, July, 178 p.
- Washington Department of Natural Resources (DNR), 2018, Washington lidar portal (Olympics North OPSW 2018): Available: <https://lidarportal.dnr.wa.gov/>.
- Washington Department of Natural Resources (DNR), 2019, Washington lidar portal (Olympics South OPSW 2019): Available: <https://lidarportal.dnr.wa.gov/>.
- Washington State Department of Natural Resources (DNR), n.d., How did the Puget Lowland form?: Available: <https://wa100.dnr.wa.gov/puget-lowland/how-did-the-puget-lowland-form>.
- Washington Geological Survey, 2023, Surface geology, 1:24,000-GIS data, January 2023 (version 3.2): Washington Geological Survey Digital Data Series DS-10, available: [https://ngmdb.usgs.gov/Prodesc/proddesc\\_102466.htm](https://ngmdb.usgs.gov/Prodesc/proddesc_102466.htm).
- Waters, M.R.; Stafford Jr, T.W.; McDonald, H.G.; and others, 2011, Pre-Clovis mastodon hunting 13,800 years ago at the Manis site, Washington: *Science*, v. 334, no. 6054, p. 351-353.
- Wells, D.L. and Coppersmith, K.J., 1994, New empirical relationships among magnitude, rupture length, rupture width, rupture area, and surface displacement: *Bulletin of the Seismological Society of America*, v. 84, no. 4, p. 974-1002.
- Wells, R.; Bukry, D.; Friedman, R.; and others, 2014, Geologic history of Siletzia, a large igneous province in the Oregon and Washington Coast Range: Correlation to the geomagnetic polarity time scale and implications for a long-lived Yellowstone hotspot: *Geosphere*, v. 10, no. 4, p. 692-719.
- Wells, R.E., and Simpson, R.W., 2001, Northward migration of the Cascadia forearc in the northwestern U.S. and implications for subduction deformation: *Earth, Planets, and Space*, v. 53, p. 275–283.
- Zeng, Y.; Petersen, M.D.; and Boyd, O.S., 2022, Data release for the lower seismogenic depth model of western U.S. earthquakes: U.S. Geological Survey data release, available: <https://doi.org/10.5066/P9NSNPV8>.

**Table 1: North Olympic Fault Zone Components of Slip**

Horizontal Slip per Event Scenario	Fault dip (°) <i>input assumed</i>	Horizontal component (unitless) <i>input documented</i>	Vertical component (unitless) <i>input documented</i>	Contractional component (unitless) <i>derived</i>	Fault strike-stress vector angle of incidence (°) <i>derived</i>	Strike of fault (° azimuth) <i>input documented</i>	Stress vector (° azimuth) <i>derived</i>	Strike slip per event (m) <i>input documented</i>	Vertical separation per event (m) <i>derived</i>	Contraction per event (m) <sup>1</sup> <i>derived</i>	Dip slip per event (m) <i>derived</i>	Net slip per event (m) <i>derived</i>	Stress vector displacement per event (m) <i>derived</i>
Mean - uncertainty	50	10.0	1	0.8	5	105	110	3.0	0.3	0.3	0.4	3.0	3.01
Mean - uncertainty	50	6.0	1	0.8	8	105	113	3.0	0.5	0.4	0.7	3.1	3.03
Mean - uncertainty	70	10.0	1	0.4	2	105	107	3.0	0.3	0.1	0.3	3.0	3.00
Mean - uncertainty	70	6.0	1	0.4	3	105	108	3.0	0.5	0.2	0.5	3.0	3.01
Mean - uncertainty	90	10.0	1	0.0	0	105	105	3.0	0.3	0.0	0.3	3.0	3.00
Mean - uncertainty	90	6.0	1	0.0	0	105	105	3.0	0.5	0.0	0.5	3.0	3.00
Mean	50	10.0	1	0.8	5	105	110	4.0	0.4	0.3	0.5	4.0	4.01
Mean	50	6.0	1	0.8	8	105	113	4.0	0.7	0.6	0.9	4.1	4.04
Mean	70	10.0	1	0.4	2	105	107	4.0	0.4	0.1	0.4	4.0	4.00
Mean	70	6.0	1	0.4	3	105	108	4.0	0.7	0.2	0.7	4.1	4.01
Mean	90	10.0	1	0.0	0	105	105	4.0	0.4	0.0	0.4	4.0	4.00
Mean	90	6.0	1	0.0	0	105	105	4.0	0.7	0.0	0.7	4.1	4.00
Mean + uncertainty	50	10.0	1	0.8	5	105	110	5.0	0.5	0.4	0.7	5.0	5.02
Mean + uncertainty	50	6.0	1	0.8	8	105	113	5.0	0.8	0.7	1.1	5.1	5.05
Mean + uncertainty	70	10.0	1	0.4	2	105	107	5.0	0.5	0.2	0.5	5.0	5.00
Mean + uncertainty	70	6.0	1	0.4	3	105	108	5.0	0.8	0.3	0.9	5.1	5.01
Mean + uncertainty	90	10.0	1	0.0	0	105	105	5.0	0.5	0.0	0.5	5.0	5.00
Mean + uncertainty	90	6.0	1	0.0	0	105	105	5.0	0.8	0.0	0.8	5.1	5.00

**Table 2: Sequim Fault Components of Displacement**

Horizontal slip per event scenario	Fault dip (°) input assumed	Horizontal component (unitless) derived	Vertical component (unitless) derived	Contractional component (unitless) derived	Fault strike-stress vector angle of incidence (°) derived	Strike of fault (° azimuth) input - documented	Stress vector (° azimuth) derived from NOFZ (Table 1)	Strike slip per event (m) derived	Vertical separation per event (m) derived	Contraction per event (m) <sup>1</sup> derived	Dip slip per event (m) derived	Net slip per event (m) derived	Stress vector displacement per event (m) derived from NOFZ (Table 1)
Mean - uncertainty	50	2.3	1	1.0	20	85	105	2.8	1.2	1.0	1.6	3.2	3
Mean - uncertainty	50	2.1	1	1.1	22	85	107	2.8	1.3	1.1	1.8	3.3	3
Mean - uncertainty	50	1.9	1	1.2	23	85	108	2.8	1.4	1.2	1.9	3.3	3
Mean - uncertainty	50	1.8	1	1.3	25	85	110	2.7	1.5	1.3	2.0	3.4	3
Mean - uncertainty	50	1.6	1	1.4	28	85	113	2.6	1.7	1.4	2.2	3.4	3
Mean - uncertainty	70	1.0	1	1.0	20	85	105	2.8	2.8	1.0	3.0	4.1	3
Mean - uncertainty	70	0.9	1	1.1	22	85	107	2.8	3.1	1.1	3.3	4.3	3
Mean - uncertainty	70	0.8	1	1.2	23	85	108	2.8	3.3	1.2	3.5	4.4	3
Mean - uncertainty	70	0.8	1	1.3	25	85	110	2.7	3.5	1.3	3.7	4.6	3
Mean - uncertainty	70	0.7	1	1.4	28	85	113	2.6	3.9	1.4	4.1	4.9	3
Mean	50	2.3	1	1.4	20	85	105	3.8	1.6	1.4	2.1	4.3	4
Mean	50	2.1	1	1.5	22	85	107	3.7	1.8	1.5	2.3	4.4	4
Mean	50	1.9	1	1.6	23	85	108	3.7	1.9	1.6	2.5	4.4	4
Mean	50	1.8	1	1.7	25	85	110	3.6	2.0	1.7	2.6	4.5	4
Mean	50	1.6	1	1.9	28	85	113	3.5	2.2	1.9	2.9	4.6	4
Mean	70	1.0	1	1.4	20	85	105	3.8	3.8	1.4	4.0	5.5	4
Mean	70	0.9	1	1.5	22	85	107	3.7	4.1	1.5	4.4	5.8	4
Mean	70	0.8	1	1.6	23	85	108	3.7	4.4	1.6	4.7	5.9	4
Mean	70	0.8	1	1.7	25	85	110	3.6	4.6	1.7	4.9	6.1	4
Mean	70	0.7	1	1.9	28	85	113	3.5	5.2	1.9	5.5	6.5	4
Mean + uncertainty	50	2.3	1	1.7	20	85	105	4.7	2.0	1.7	2.7	5.4	5
Mean + uncertainty	50	2.1	1	1.9	22	85	107	4.6	2.2	1.9	2.9	5.5	5
Mean + uncertainty	50	1.9	1	2.0	23	85	108	4.6	2.4	2.0	3.1	5.5	5
Mean + uncertainty	50	1.8	1	2.1	25	85	110	4.5	2.5	2.1	3.3	5.6	5
Mean + uncertainty	50	1.6	1	2.3	28	85	113	4.4	2.8	2.3	3.6	5.7	5
Mean + uncertainty	70	1.0	1	1.7	20	85	105	4.7	4.7	1.7	5.0	6.9	5
Mean + uncertainty	70	0.9	1	1.9	22	85	107	4.6	5.2	1.9	5.5	7.2	5
Mean + uncertainty	70	0.8	1	2.0	23	85	108	4.6	5.5	2.0	5.8	7.4	5
Mean + uncertainty	70	0.8	1	2.1	25	85	110	4.5	5.8	2.1	6.1	7.6	5
Mean + uncertainty	70	0.7	1	2.3	28	85	113	4.4	6.4	2.3	6.9	8.2	5

Notes:  
1 - Contraction cannot be accommodated on a vertical fault; because this parameter is necessary to derive additional components, we do not include a 90° for the Sequim fault.

**Table 3: Sequim Fault Surface Rupture Length—Average Displacement Relationships**

Scenario	Scaling Relationship	SRL (km)	Average Displacement (m)			
			Mean - 1 standard deviation	Mean	Mean + 0.5 standard deviation	Mean + 1 standard deviation
Sequim fault (USGS QFFD)	WC94 SS SRL-AD	7	0.1	0.2	0.2	0.3
Sequim fault (East upland, Dungeness River valley, west upland traces)	WC94 SS SRL-AD	14	0.1	0.3	0.4	0.6
Sequim fault (Brocher and others, 2001)	WC94 SS SRL-AD	46	0.5	1.1	1.5	2.2
Lake Creek-Boundary Creek fault +Sadie Creek fault (56 km)	WC94 SS SRL-AD	56	0.6	1.3	1.9	2.7
North Olympic fault zone (80 km)	WC94 SS SRL-AD	80	0.9	1.9	2.7	4.0
Sequim fault + Lake Creek-Boundary Creek fault +Sadie Creek fault (56 km)	WC94 SS SRL-AD	102	1.2	2.4	3.5	5.1
Sequim fault (46 km) + North Olympic fault zone (80 km)	WC94 SS SRL-AD	126	1.5	3.1	4.4	6.4
<i>Average displacements below represent the range of measured net slip per event measured on the Lake Creek-Boundary Creek and Sadie Creek faults (<math>4 \pm 1</math> m) (Nelson and others, 2017; Schermer and others, 2021). These average displacement values were determined by iteratively adjusting the surface rupture length to yield the mean average displacement equivalent to the observed average net slip per event measurements.</i>						
Surface rupture length to produce 3 m average displacement = 124 km	WC94 SS SRL-AD	124	1.4	3.0	4.3	6.3
Surface rupture length to produce 4 m average displacement = 164 km	WC94 SS SRL-AD	164	1.9	4.0	5.8	8.4
Surface rupture length to produce 5 m average displacement = 203 km	WC94 SS SRL-AD	203	2.4	5.0	7.2	10.5

**Table 4: Summary of Deformation Hazard Zones**

Hazard Zone	Recommended Displacement <sup>1</sup> to Assume for Preliminary Design				Sense of Slip		Distribution of Slip
	Horizontal		Vertical		Horizontal	Vertical	
	(m)	(ft)	(m)	(ft)			
Primary deformation zone	4.1 to 4.5	<b>13.5 to 14.8</b>	2.1 to 2.8	<b>6.9 to 9.2</b>	Right-lateral	North-side-up	Single slip surface to distributed through zone
Secondary deformation zone <sup>2</sup>	2.1 to 2.3	<b>6.8 to 7.4</b>	1.1 to 1.4	<b>3.5 to 4.6</b>	Right-lateral	South-side-up	Single slip surface to distributed through zone
Distributed secondary deformation zone <sup>3</sup>	1.0 to 1.1	<b>3.4 to 3.7</b>	0.5 to 0.7	<b>1.7 to 2.4</b>	Right-lateral	Variable	Narrow zone (~5-10 ft) to distributed through zone
Low probability of deformation zone	-- deformation not expected --						

Notes:

1. Based on 5 m of primary net displacement with 1.5H:1V to 2.5H:1V horizontal to vertical slip ratio
2. 50% of primary displacement; CA DSOD (2018) utilizes 25%
3. 25% of primary displacement; CA DSOD (2018) utilizes 25%



**Table 5: Sequim Fault Seismic Source Parameters**

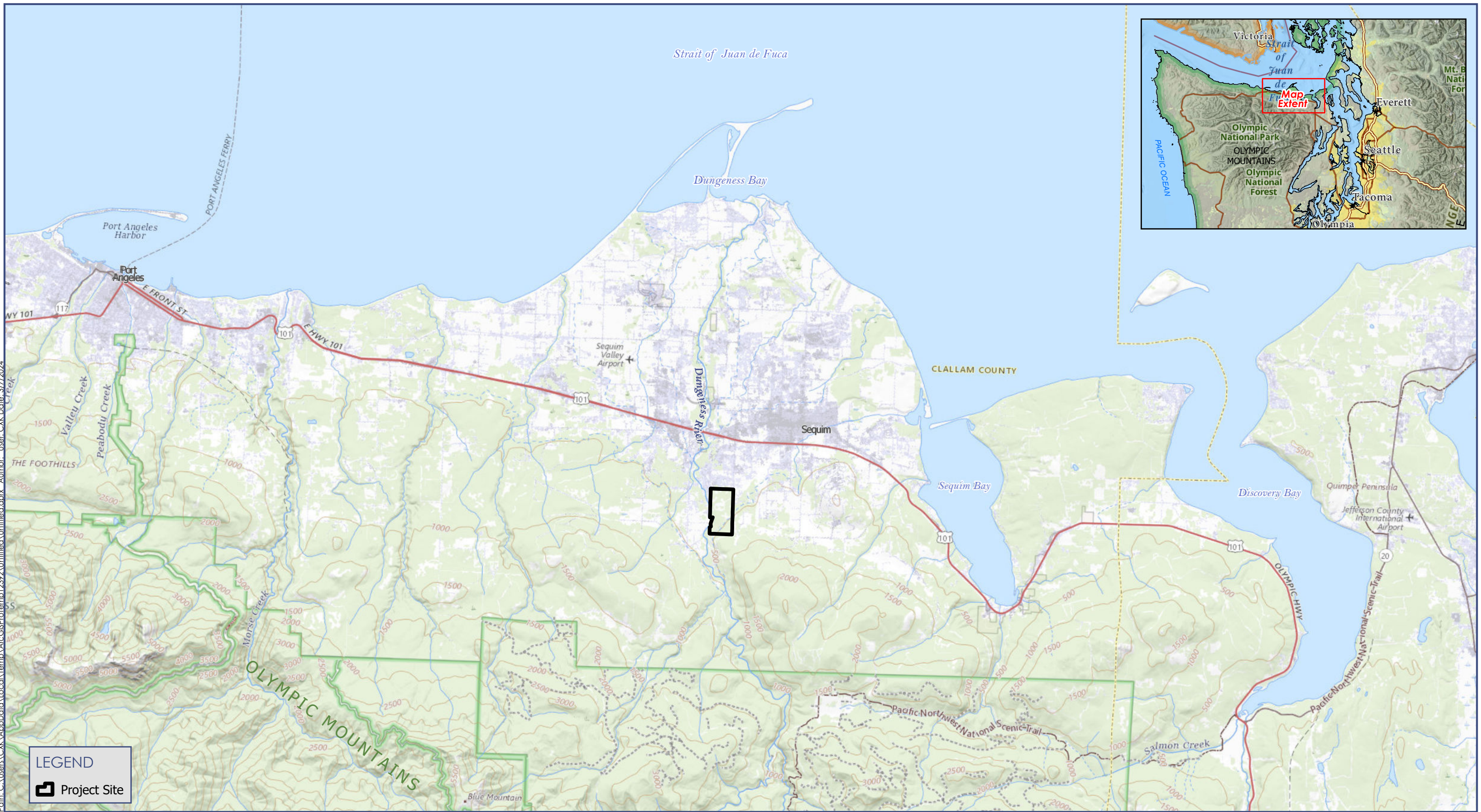
Slip rate (mm/yr)	Length (km)	Dip Direction	Dip Angle (°)	Mechanism	Rake (°)	Top of Rupture (km)	Bottom of Rupture (km)
1.3 [0.5]	14 [0.2]	North [0.1]	50 [0.5]	Reverse [0.2]	90 [0.2]	0 [0.9]	30 [0.5]
2.3 [0.5]	46 [0.4]	South [0.6]	70 [0.3]	Right lateral [0.3]	180 [0.3]	0.5 [0.1]	36 [0.5]
	126 [0.4]	Vertical [0.3]	90 [0.2]	Right lateral-reverse [0.5]	135 [0.5]		

Notes:

Rake is defined as degrees from horizontal (left-lateral = 0°)

mm/yr = millimeters per year; km = kilometers;





Path: C:\Users\CXK\AppData\Local\Temp\ArcGISProTemp\2392\Untitled1\Map\prj\prj\_3172024... Author: User\_CXK Date: 3/17/2024

0 2  
Kilometers  
0 2  
Miles  
104680







Path: C:\Users\CXK\AppData\Local\Temp\ArcGISProTemp\2392\Untitled1\Map\Map.aprx - Author: User, CXX Date: 3/17/2024

**LEGEND**

Project Site

0 1,000  
Meters

0 3,000  
Feet

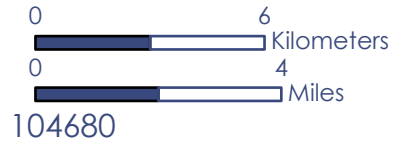
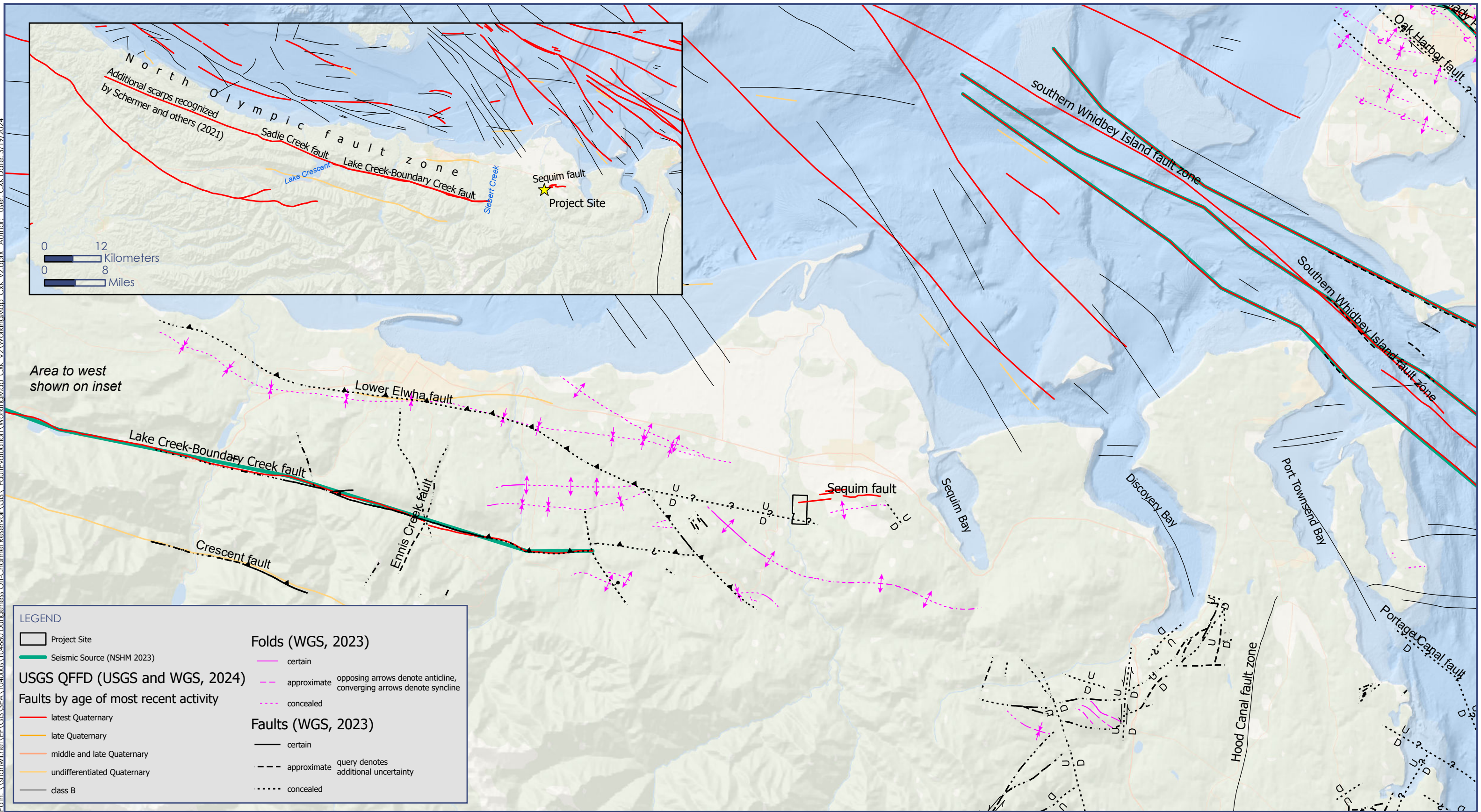
104680

Notes:

1. LiDAR is courtesy of WA DNR, WA Geologic Society and the USGS; Olympics North OPSW 2018 and Olympics South OPSW 2019.





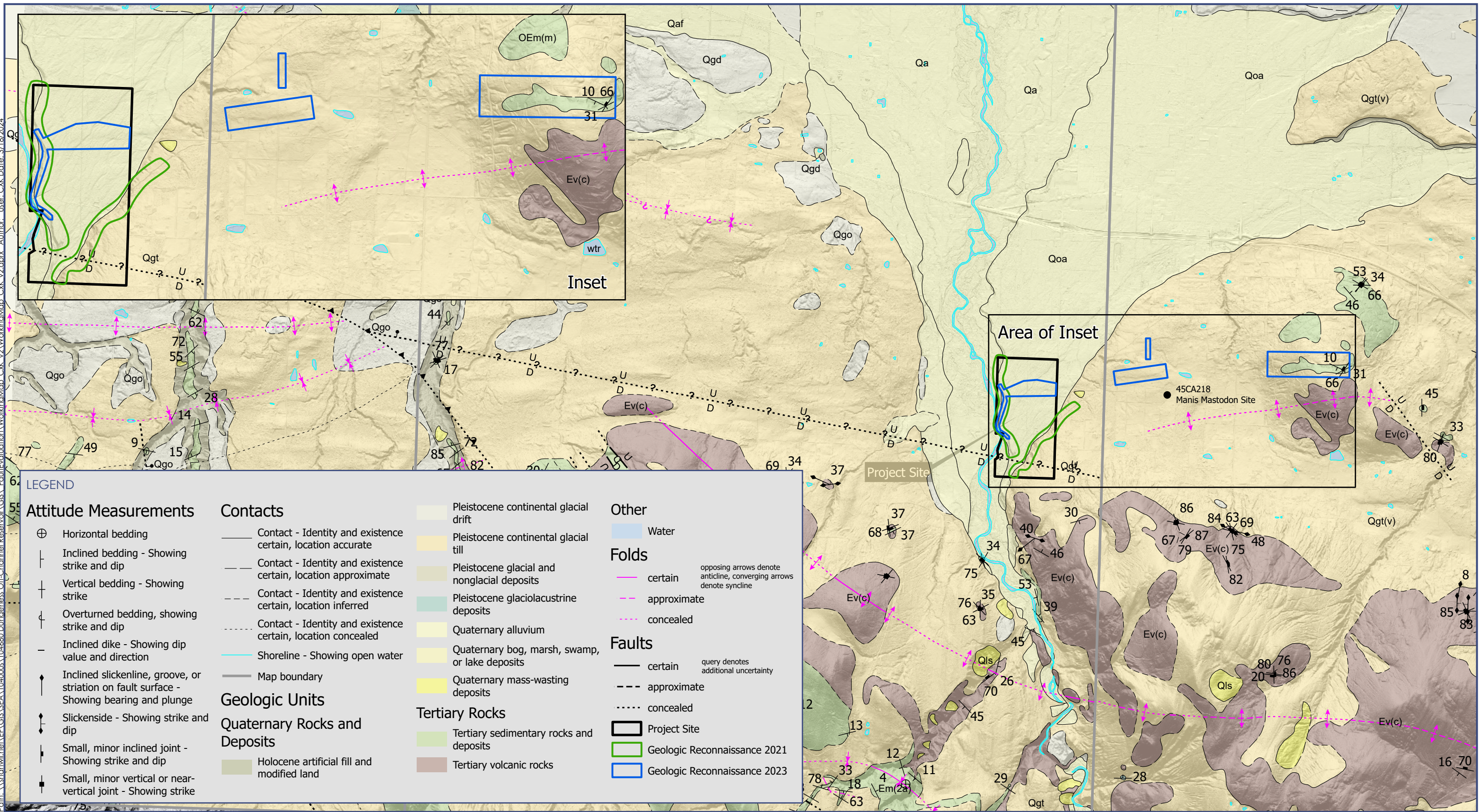


**Notes:**  
1. LiDAR is courtesy of WA DNR, WA Geologic Society and the USGS; Olympics North OPSW 2018 and Olympics South OPSW 2019.



Path: \\shannonwilson\EE\GIS\SFA\104680\Dungeness Off-Channel Reservoir\GIS\FaultEvaluation\WorkingMap\_CxK\_v2.aprx Author: User\_CXK Date: 3/19/2024

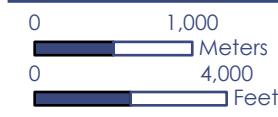




Path: \\shannonwilson\GIS\SEA\104680\Dungeness Off-Channel Reservoir\GIS\FaultEvaluation\WorkingMap\_CxK\_v2.aprx Author: User: CXK Date: 3/18/2024

**LEGEND**

<p><b>Attitude Measurements</b></p> <ul style="list-style-type: none"> <li>⊕ Horizontal bedding</li> <li>  Inclined bedding - Showing strike and dip</li> <li>+ Vertical bedding - Showing strike</li> <li>⊥ Overturned bedding, showing strike and dip</li> <li>- Inclined dike - Showing dip value and direction</li> <li>↗ Inclined slickenline, groove, or striation on fault surface - Showing bearing and plunge</li> <li>↘ Slickenside - Showing strike and dip</li> <li>↖ Small, minor inclined joint - Showing strike and dip</li> <li>↗ Small, minor vertical or near-vertical joint - Showing strike</li> </ul>	<p><b>Contacts</b></p> <ul style="list-style-type: none"> <li>— Contact - Identity and existence certain, location accurate</li> <li>- - - Contact - Identity and existence certain, location approximate</li> <li>- · - · - Contact - Identity and existence certain, location inferred</li> <li>- · · · - Contact - Identity and existence certain, location concealed</li> <li>— Shoreline - Showing open water</li> <li>— Map boundary</li> </ul>	<p><b>Geologic Units</b></p> <ul style="list-style-type: none"> <li>— Holocene artificial fill and modified land</li> </ul>	<p><b>Quaternary Rocks and Deposits</b></p> <ul style="list-style-type: none"> <li>— Pleistocene continental glacial drift</li> <li>— Pleistocene continental glacial till</li> <li>— Pleistocene glacial and nonglacial deposits</li> <li>— Pleistocene glaciolacustrine deposits</li> <li>— Quaternary alluvium</li> <li>— Quaternary bog, marsh, swamp, or lake deposits</li> <li>— Quaternary mass-wasting deposits</li> </ul>	<p><b>Tertiary Rocks</b></p> <ul style="list-style-type: none"> <li>— Tertiary sedimentary rocks and deposits</li> <li>— Tertiary volcanic rocks</li> </ul>	<p><b>Other</b></p> <ul style="list-style-type: none"> <li>— Water</li> </ul>	<p><b>Folds</b></p> <ul style="list-style-type: none"> <li>— certain</li> <li>- - - approximate</li> <li>- · · · concealed</li> </ul> <p>opposing arrows denote anticline, converging arrows denote syncline</p>	<p><b>Faults</b></p> <ul style="list-style-type: none"> <li>— certain</li> <li>- - - approximate</li> <li>- · · · concealed</li> </ul> <p>query denotes additional uncertainty</p>	<p><b>Project Site</b></p> <ul style="list-style-type: none"> <li>— Project Site</li> <li>— Geologic Reconnaissance 2021</li> <li>— Geologic Reconnaissance 2023</li> </ul>
----------------------------------------------------------------------------------------------------------------------------------------------------------------------------------------------------------------------------------------------------------------------------------------------------------------------------------------------------------------------------------------------------------------------------------------------------------------------------------------------------------------------------------------------------------------------------------------------------------------------------	-------------------------------------------------------------------------------------------------------------------------------------------------------------------------------------------------------------------------------------------------------------------------------------------------------------------------------------------------------------------------------------------------------------------------------------------------------	-----------------------------------------------------------------------------------------------------------------------------	------------------------------------------------------------------------------------------------------------------------------------------------------------------------------------------------------------------------------------------------------------------------------------------------------------------------------------------------------------------------------------------------------------------------------------	-------------------------------------------------------------------------------------------------------------------------------------------------------------	-------------------------------------------------------------------------------	------------------------------------------------------------------------------------------------------------------------------------------------------------------------------------------------------------------	------------------------------------------------------------------------------------------------------------------------------------------------------------------------------------	-----------------------------------------------------------------------------------------------------------------------------------------------------------------------------



104680

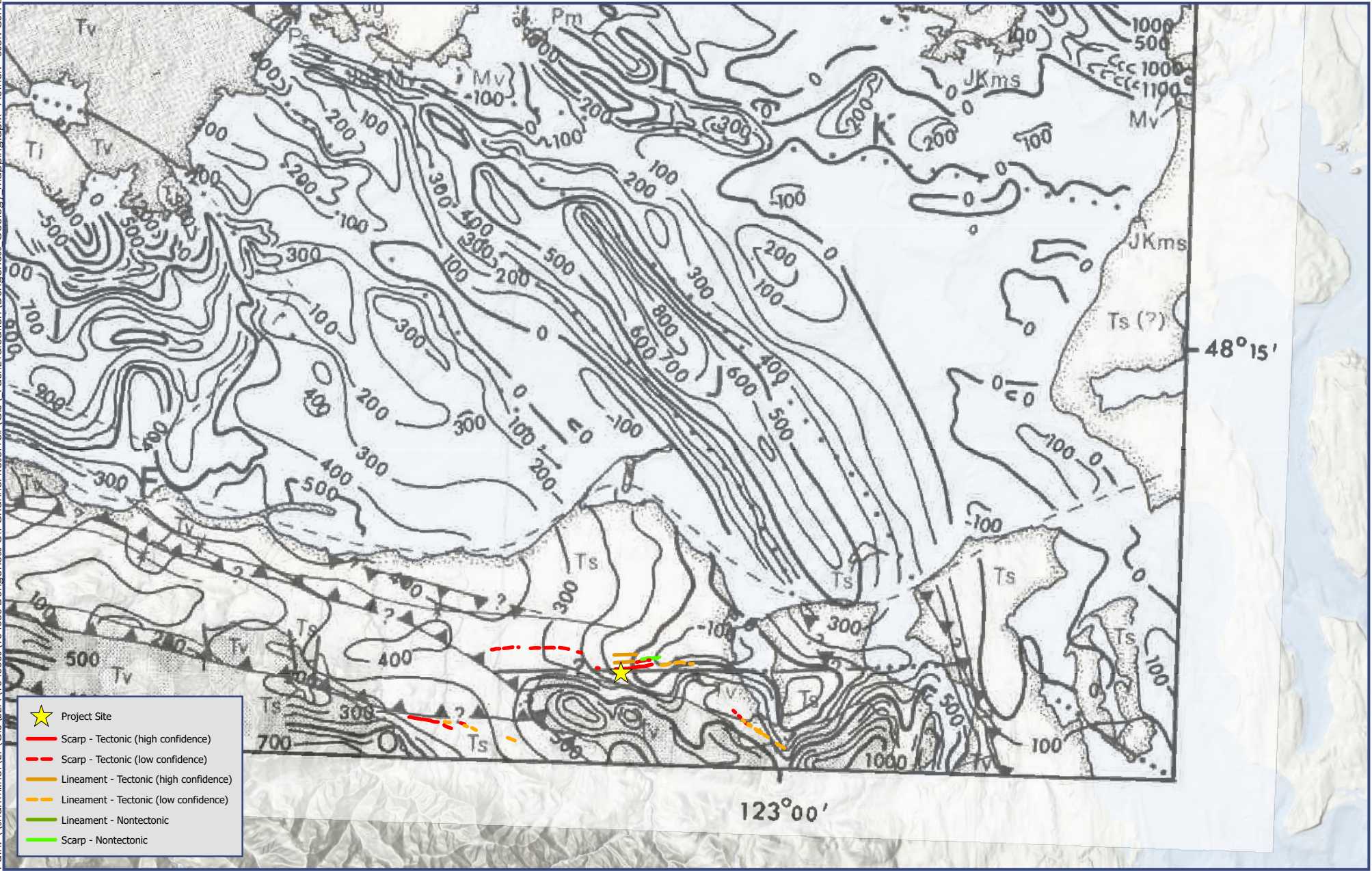
**Notes:**

- LiDAR is courtesy of WA DNR, WA Geologic Society and the USGS; Olympics North OPSW 2018 and Olympics South OPSW 2019.
- Geology from: Washington Geological Survey, 2023, Surface geology, 1:24,000-GIS data, January 2023; Washington Geological Survey Digital Data Series DS-10, version 3.2.

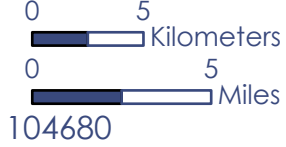




Path: \\shannonwilson\GIS\SEA\104680\Dungeness Off-Channel Reservoir\GIS\FaultEvaluation\Dungeness\_Geology\_Mapping.aprx Author: User: G.H Date: 3/1/2024



- Project Site
- Scarp - Tectonic (high confidence)
- Scarp - Tectonic (low confidence)
- Lineament - Tectonic (high confidence)
- Lineament - Tectonic (low confidence)
- Lineament - Nontectonic
- Scarp - Nontectonic



- Notes:
1. Overlying map from MacLeod and others (1977).
  2. Basemap service layer credits: CHS, Esri, Garmin, NaturalVue, Airbus, USGS, NGA, NASA, CGIAR, NCEAS, NLS, OS, NMA, Geodatas, and the GIS user community.



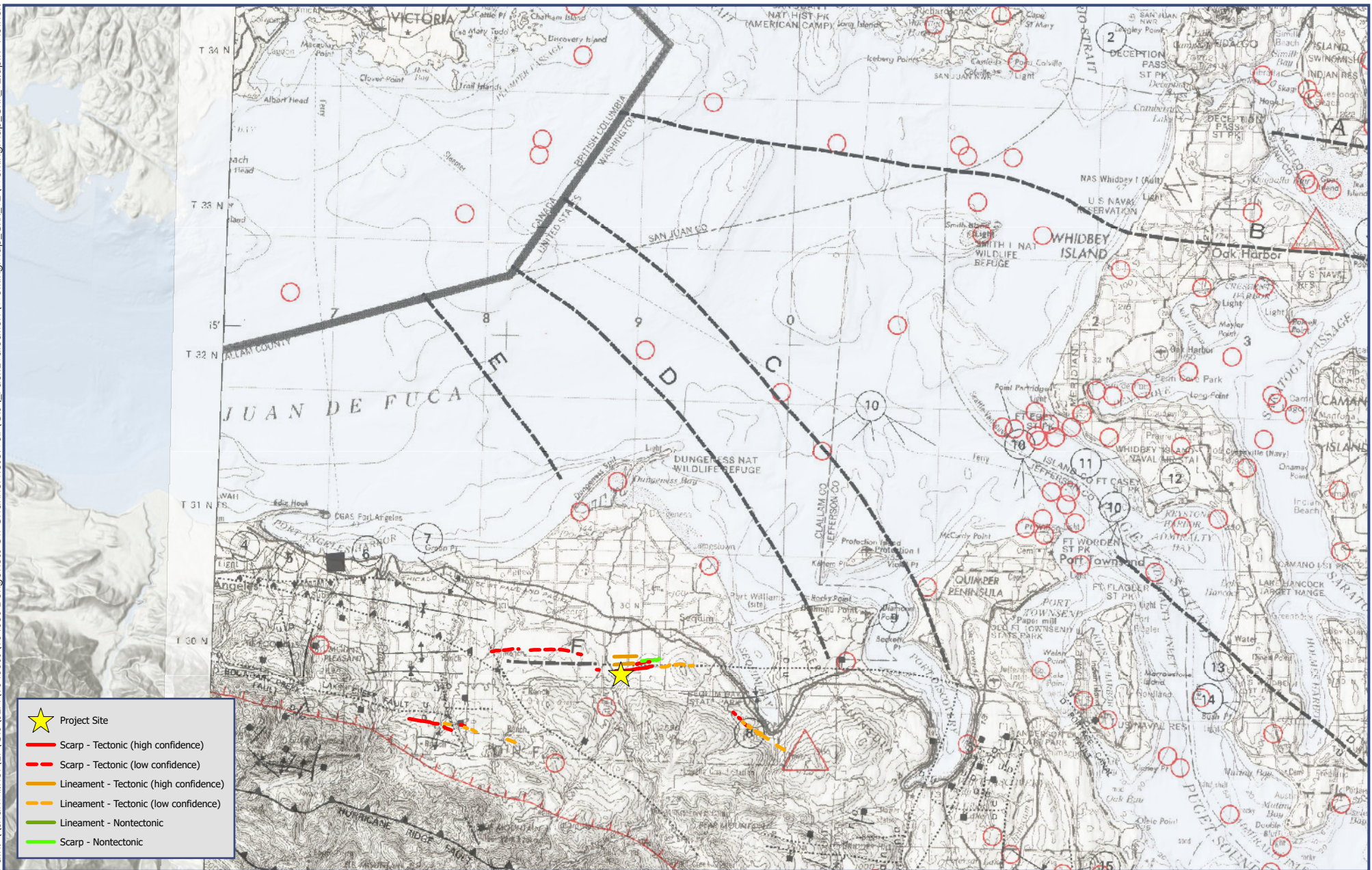
**MAGNETIC SURVEY OF MACLEOD AND OTHERS (1977)**

March 2024

**Figure 5**



Path: \\shamwil\nef\GIS\SEA\1040005\104680\Dungeness Off-Channel Reservoir\GIS\FaultEvaluation\WorkingMap\_Cxk\_v2\WorkingMap\_Cxk\_v2.aprx Author: User: CKX Date:



104680

Notes:

1. Overlying map from Gower and others (1985).
2. Basemap service layer credits: CHS, Esri, Garmin, NaturalVue, Airbus, USGS, NGA, NASA, CGIAR, NCEAS, NLS, OS, NMA, Geodatas, and the GIS user community.



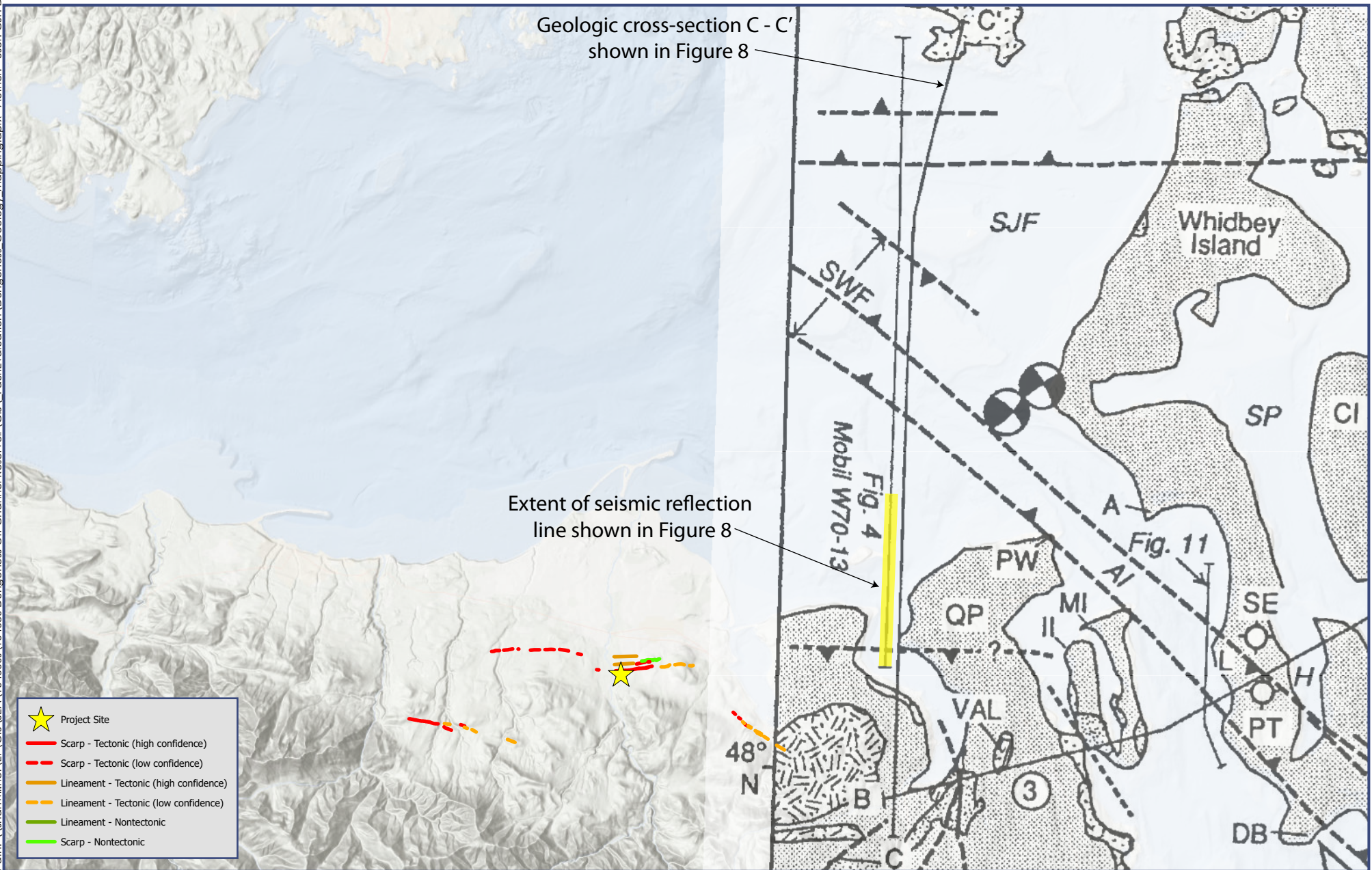
SEISMOTECTONIC MAP OF PORT GOWER AND OTHERS (1985)

March 2024

Figure 6



Path: \\shannonwilson\GIS\SEA\1040003\104680\Dungeness Off-Channel Reservoir\GIS\FaultEvaluation\Dungeness\_Geology\_Mapping.aprx Author: G.H Date: 3/1/2024



- Project Site
- Scarp - Tectonic (high confidence)
- Scarp - Tectonic (low confidence)
- Lineament - Tectonic (high confidence)
- Lineament - Tectonic (low confidence)
- Lineament - Nontectonic
- Scarp - Nontectonic

Notes:

1. Overlying map from Johnson and others (1996).
2. Basemap service layer credits: CHS, Esri, Garmin, NaturalVue, Airbus, USGS, NGA, NASA, CGIAR, NCEAS, NLS, OS, NMA, Geodatas, and the GIS user community.



**SCHEMATIC GEOLOGIC MAP OF JOHNSON AND OTHERS (1996)**

March 2024

**Figure 7**



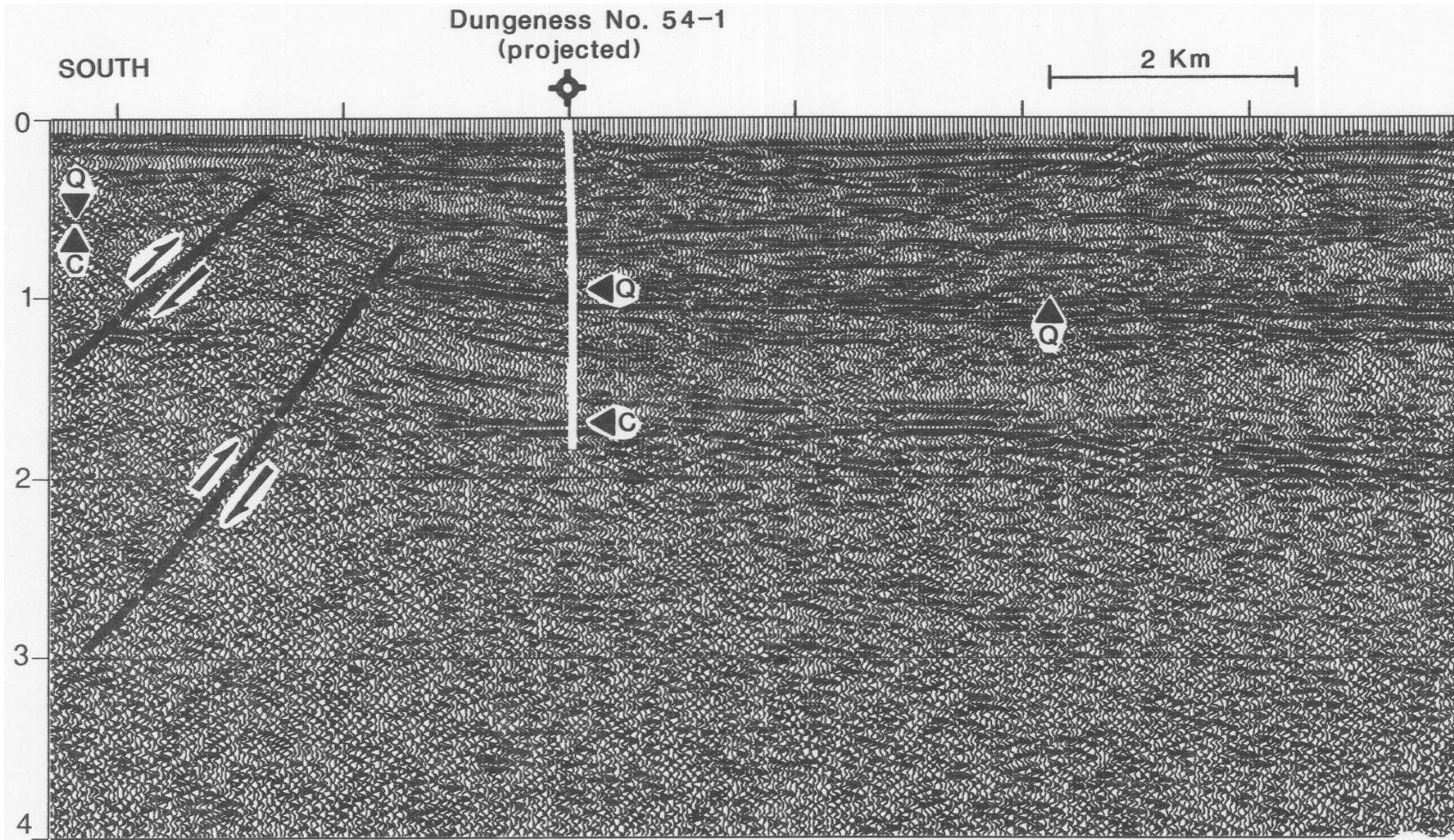


Figure 5. Mobil seismic-reflection line W70-13 (unmigrated) across the eastern Strait of Juan de Fuca (Fig. 2). Arrows indicate base of Quaternary deposits (Q), top of Crescent Formation (C), and top of pre-Tertiary rock (pT). Figure 10 shows overlapping geologic cross section (C-C'). Stratigraphy from Standard Dungeness No. 1-54 borehole (McFarland, 1983) is projected onto line from 14 km to west. Faults are inferred to have experienced both vertical offset (indicated by arrows) and lateral offset. Vertical exaggeration is ~1:1 at depths of 1-3 km (~1-2.3 s TWT) based on velocities reported by Johnson et al. (1994, Fig. 5) from the Standard Engstrom (Fig. 4) borehole.

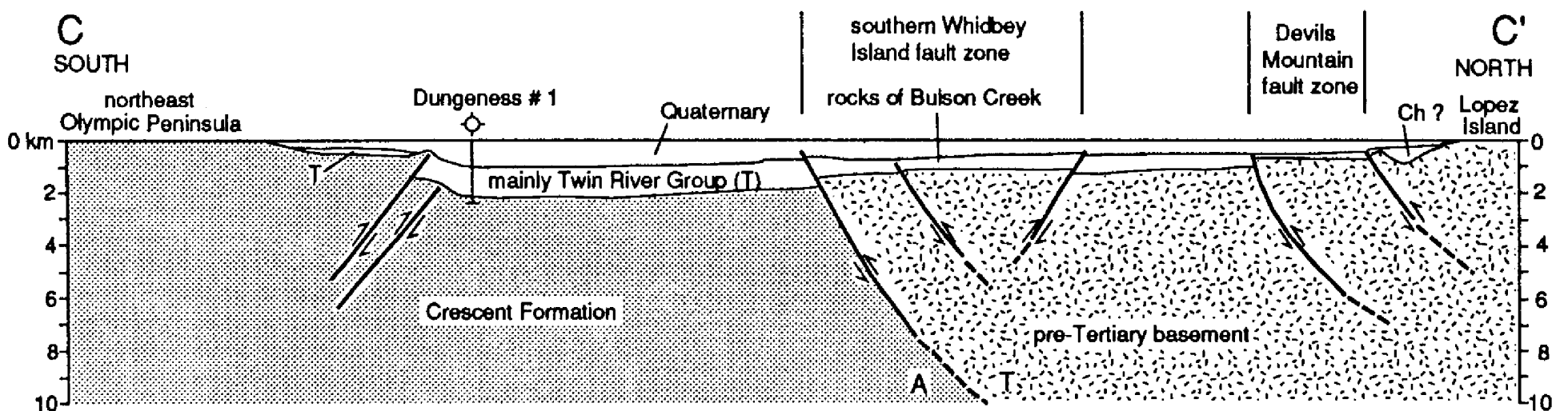
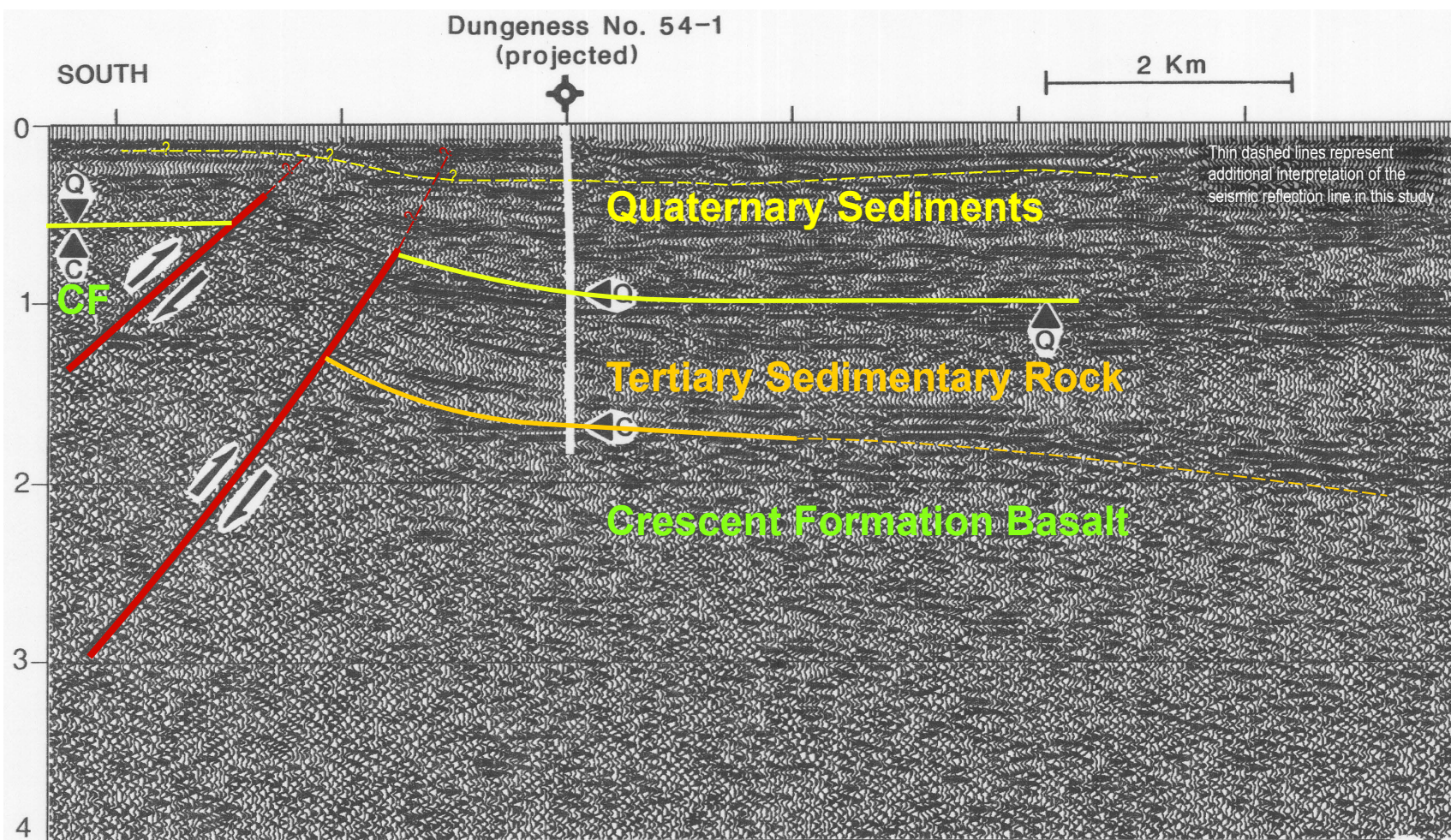


Figure 10. Geologic cross sections across the south Whidbey Island area. Section lines shown in Figure 2. Many faults (heavy solid lines) are inferred to have undergone both vertical offset (indicated by arrows) and lateral offset. T = lateral offset toward viewer; A = lateral offset away from viewer. Boreholes projected onto cross sections from various distances, as shown in Figure 2.

Notes:

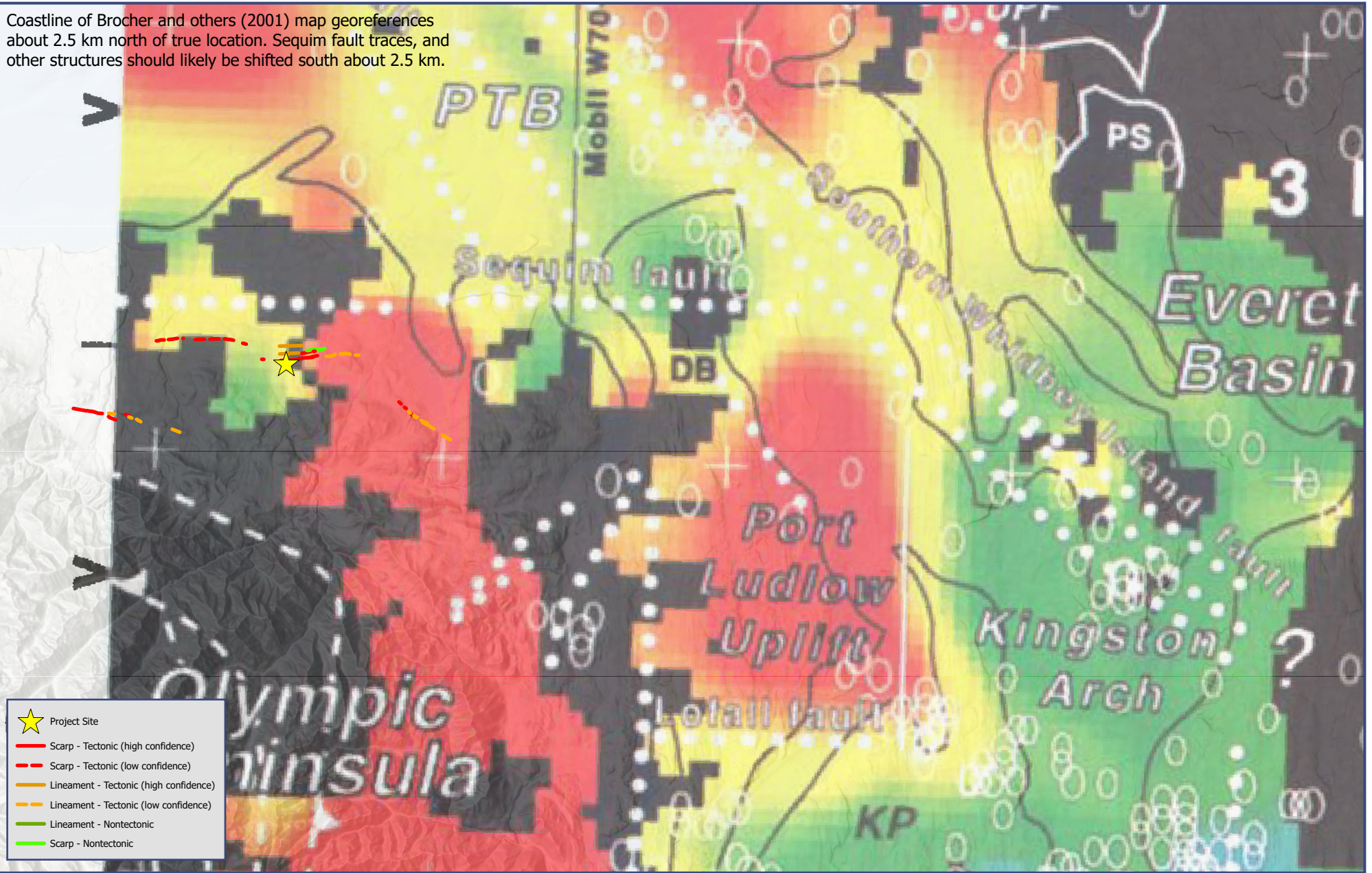
1. Modified from Figure 5 and Figure 10c from Johnson and others (1996).

March 2024



Coastline of Brocher and others (2001) map georeferences about 2.5 km north of true location. Sequim fault traces, and other structures should likely be shifted south about 2.5 km.

Path: C:\Users\CXK\AppData\Local\Temp\ArcGISProTemp\2392\Unfiled\Unfiled.aprx Author: User: CXK Date: 3/17/2024



0 5 Miles

104680

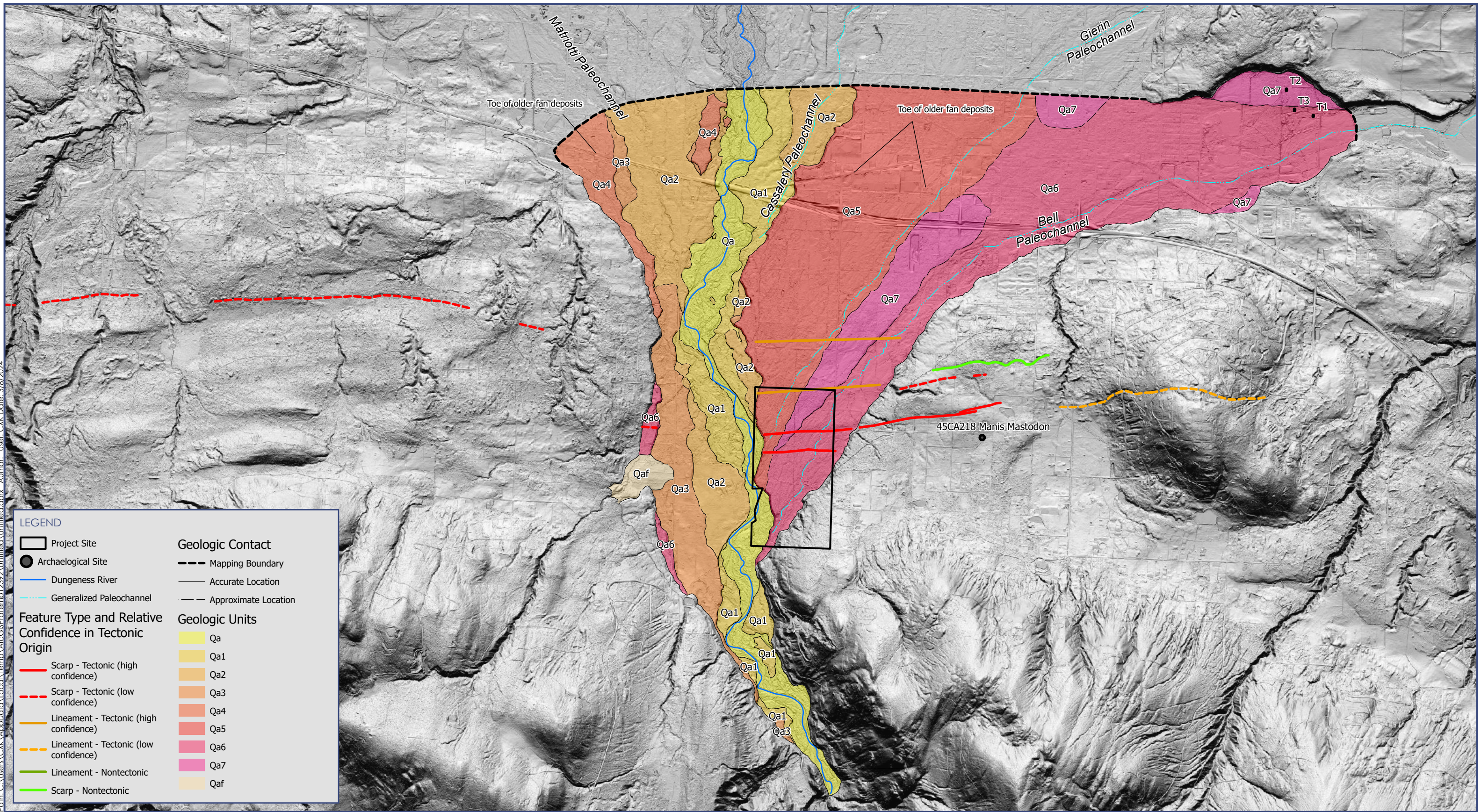
**Notes:**

1. Overlying map from Brocher and others (2001).
2. Basemap service layer credits: CHS, Esri, Garmin, NaturalVue, Airbus, USGS, NGA, NASA, CGIAR, NCEAS, NLS, OS, NMA, Geodatas, and the GIS user community.



**SEISMIC TOMOGRAPHY MAP OF BROCHER AND OTHERS (2001)**  
March 2024  
Figure 9





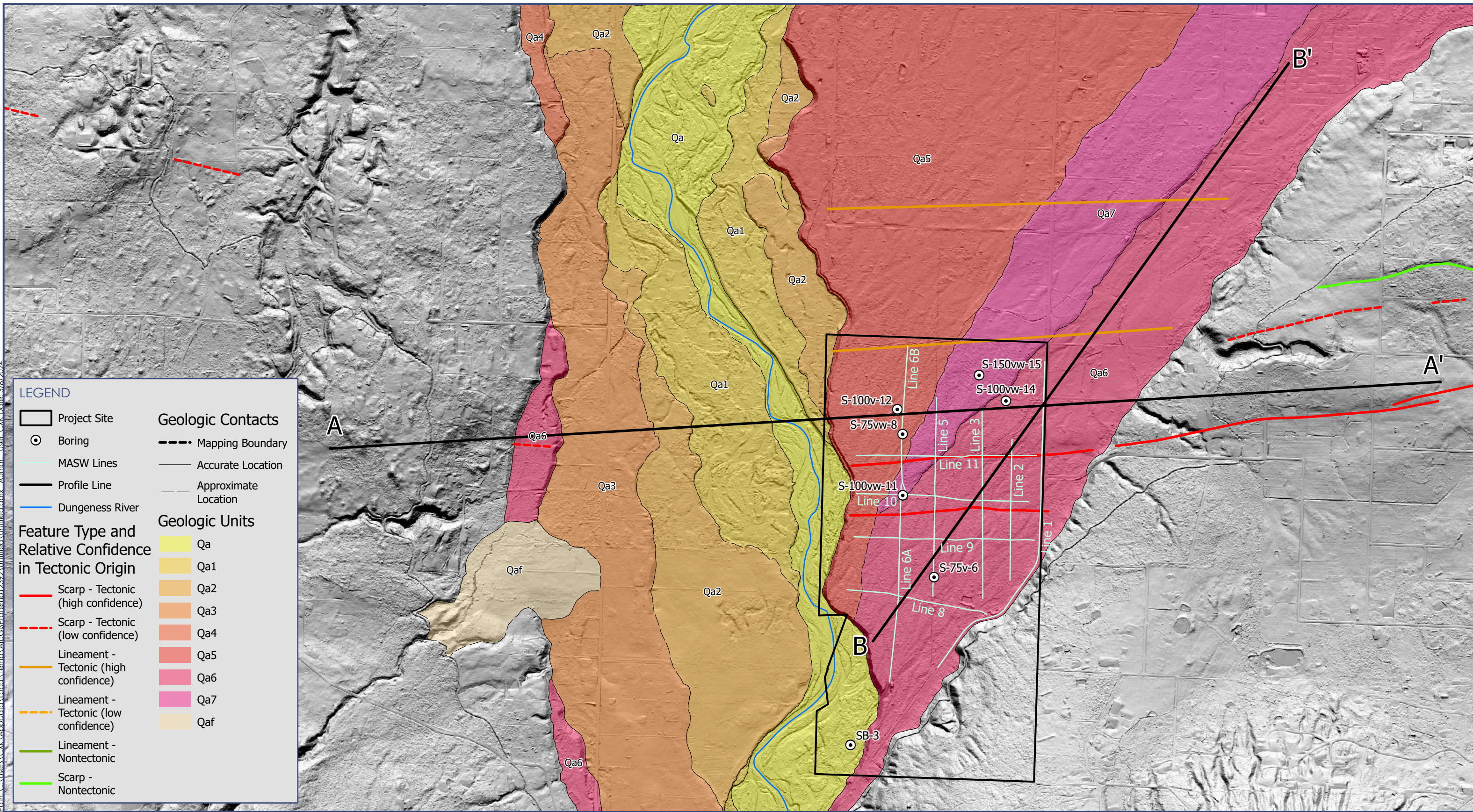
Path: C:\Users\CXK\AppData\Local\Temp\ArcGIS\Temp\2392\Unfiled\Unfiled.aprx - Author: User, CXK Date: 3/8/2024



Notes:  
1. LiDAR is courtesy of WA DNR, WA Geologic Society and the USGS; Olympics North OPSW 2018 and Olympics South OPSW 2019.



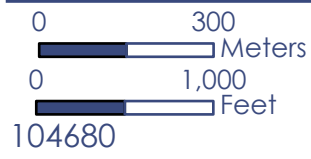




Path: C:\Users\CYK\AppData\Local\Temp\ArcGISProTemp\12392\Unfiled\Unfiled.aprx - Author: User, CYK, Date: 3/8/2024

**LEGEND**

	Project Site	<b>Geologic Contacts</b>	
	Boring		Mapping Boundary
	MASW Lines		Accurate Location
	Profile Line		Approximate Location
	Dungeness River		
<b>Feature Type and Relative Confidence in Tectonic Origin</b>		<b>Geologic Units</b>	
	Scarp - Tectonic (high confidence)		Qa
	Scarp - Tectonic (low confidence)		Qa1
	Lineament - Tectonic (high confidence)		Qa2
	Lineament - Tectonic (low confidence)		Qa3
	Lineament - Nontectonic		Qa4
	Scarp - Nontectonic		Qa5
			Qa6
			Qa7
			Qaf

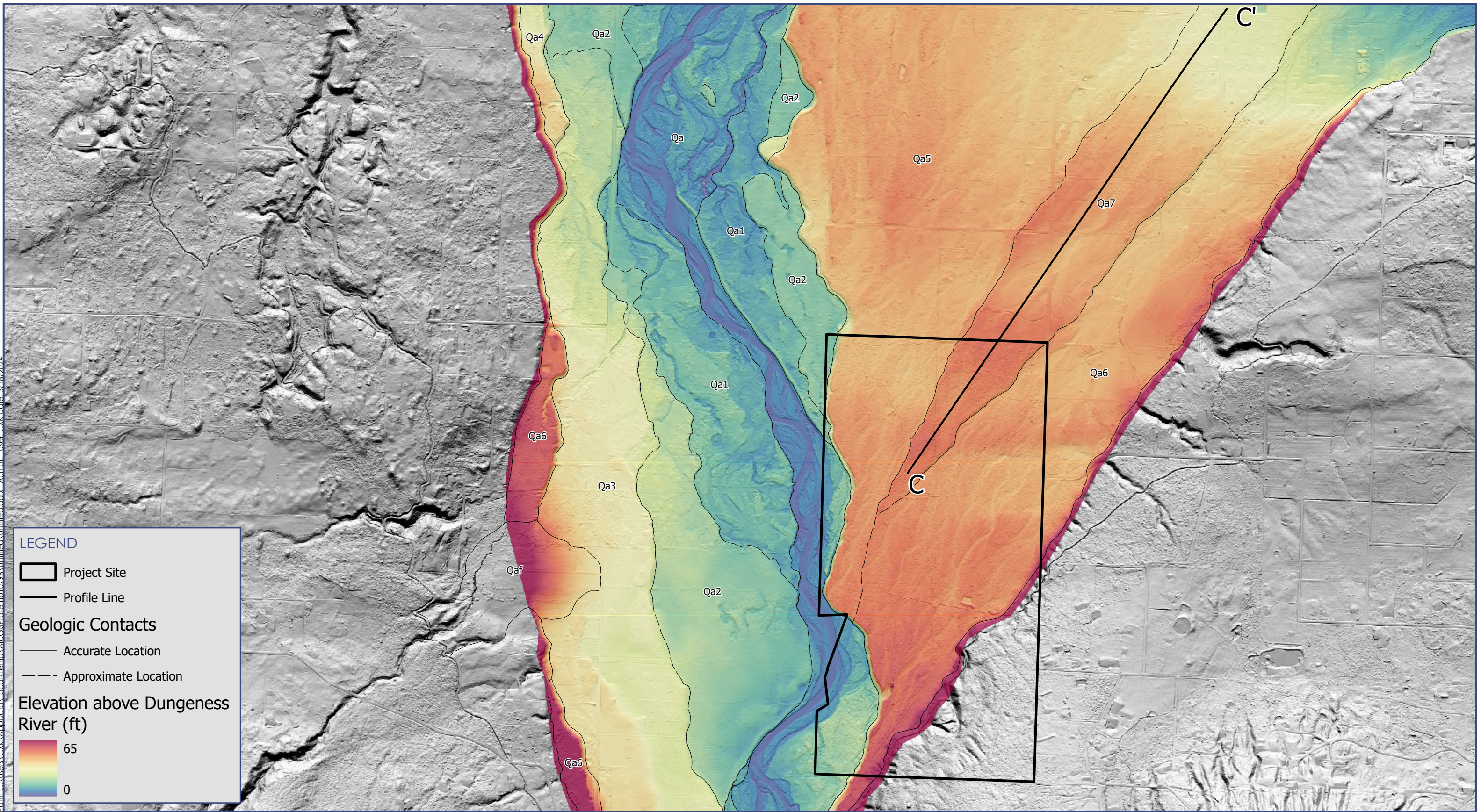


**Notes:**

- LiDAR is courtesy of WA DNR, WA Geologic Society and the USGS; Olympics North OPSW 2018 and Olympics South OPSW 2019.
- Reservoir options A & D are displayed







Path: C:\Users\CJK\AppData\Local\Temp\ArcGISProTemp\0796\Untitled1\Untitled1.aprx - Author: User, CJK Date: 3/18/2024

**LEGEND**

- Project Site
- Profile Line

**Geologic Contacts**

- Accurate Location
- Approximate Location

**Elevation above Dungeness River (ft)**

65
0

0 300  
0 1,000  
104680

Notes:

1. LiDAR is courtesy of WA DNR, WA Geologic Society and the USGS; Olympics North OPSW 2018 and Olympics South OPSW 2019.





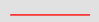
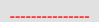
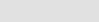
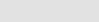
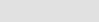


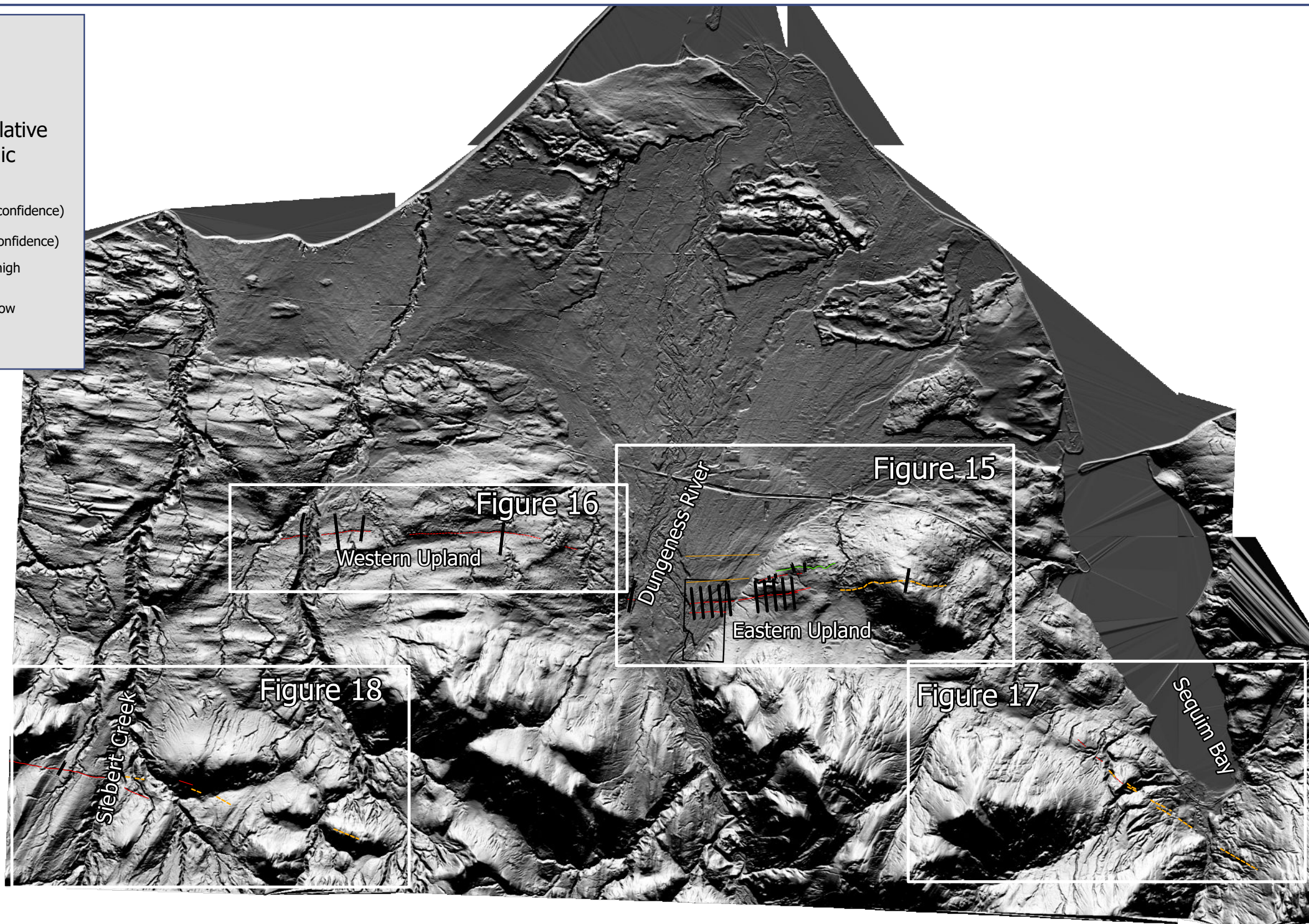




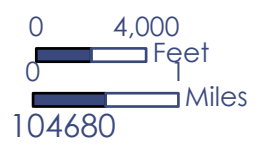


LEGEND

-  Project Site
-  Profile Lines
- Feature Type and Relative Confidence in Tectonic Origin**
-  Scarp - Tectonic (high confidence)
-  Scarp - Tectonic (low confidence)
-  Lineament - Tectonic (high confidence)
-  Lineament - Tectonic (low confidence)
-  Scarp - Nontectonic



Path: \\shannonwilson\EE\GIS\SFA\104680\Dungeness Off-Channel Reservoir\GIS\FaultEvaluation\WorkingMap\_CxK.aprx Author: User: CXK Date: 3/8/2024

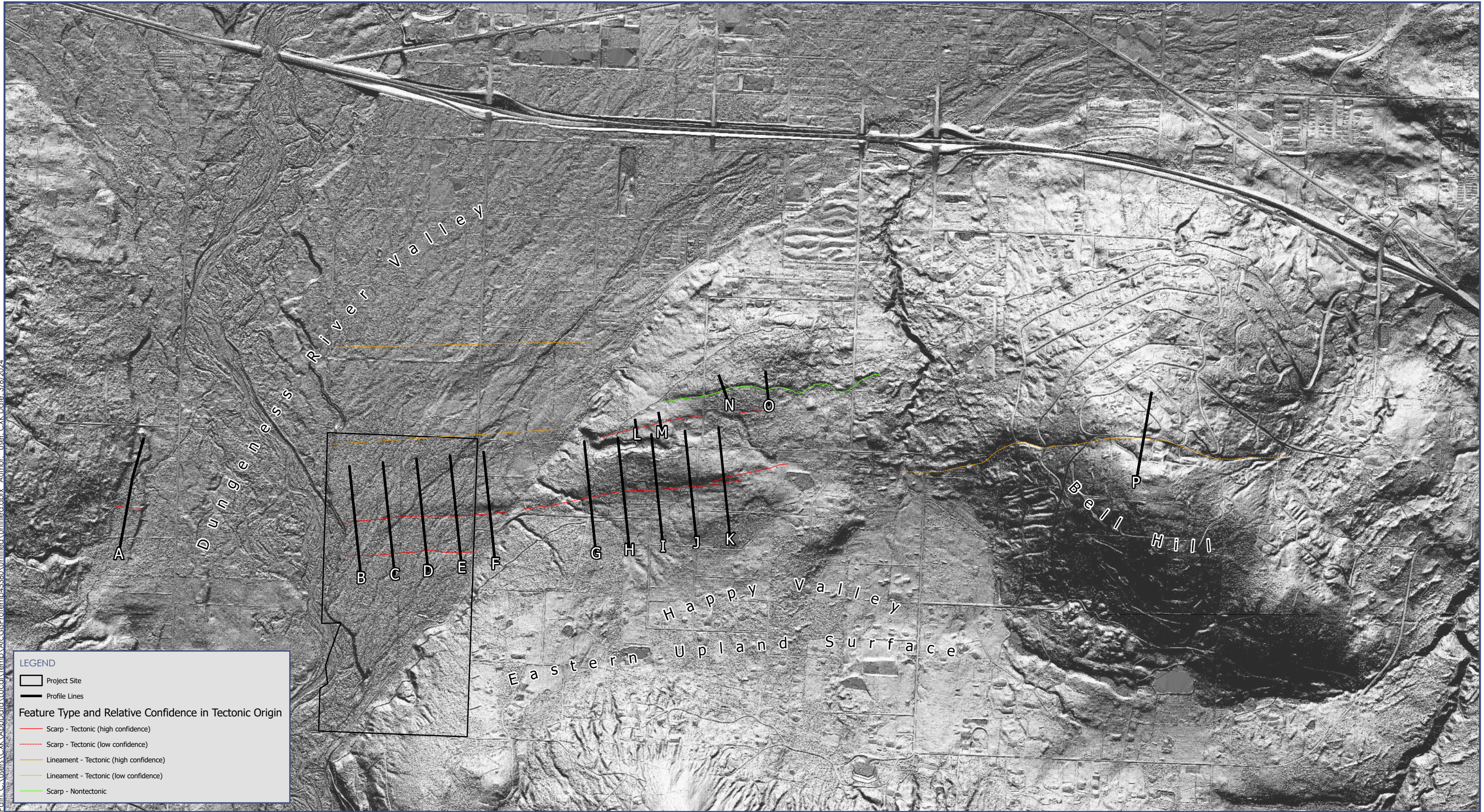


Notes:

1. LiDAR is courtesy of WA DNR, WA Geologic Society and the USGS; Olympics North OPSW 2018 and Olympics South OPSW 2019.
2. Reservoir options A & D are displayed







Path: C:\Users\CXK\AppData\Local\Temp\ArcGISProTemp\45980\Unfiled\Unfiled.aprx - Author: User, CXK Date: 3/8/2024

**LEGEND**

Project Site

Profile Lines

**Feature Type and Relative Confidence in Tectonic Origin**

- Scarp - Tectonic (high confidence)
- Scarp - Tectonic (low confidence)
- Lineament - Tectonic (high confidence)
- Lineament - Tectonic (low confidence)
- Scarp - Nontectonic

0 1,600 Feet

104680

Notes:  
1. LiDAR is courtesy of WA DNR, WA Geologic Society and the USGS; Olympics North OPSW 2018 and Olympics South OPSW 2019.

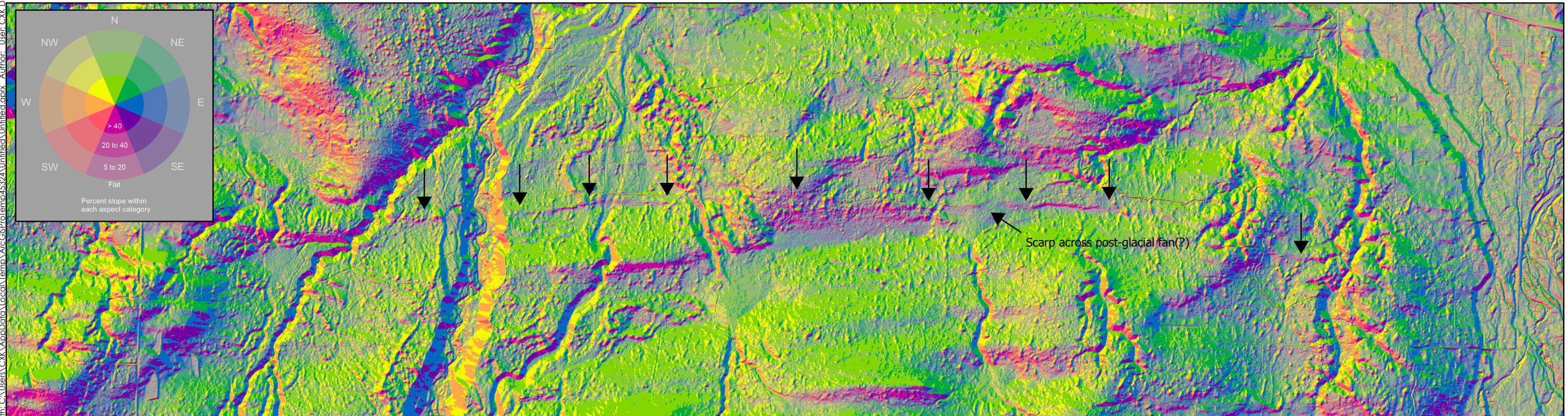
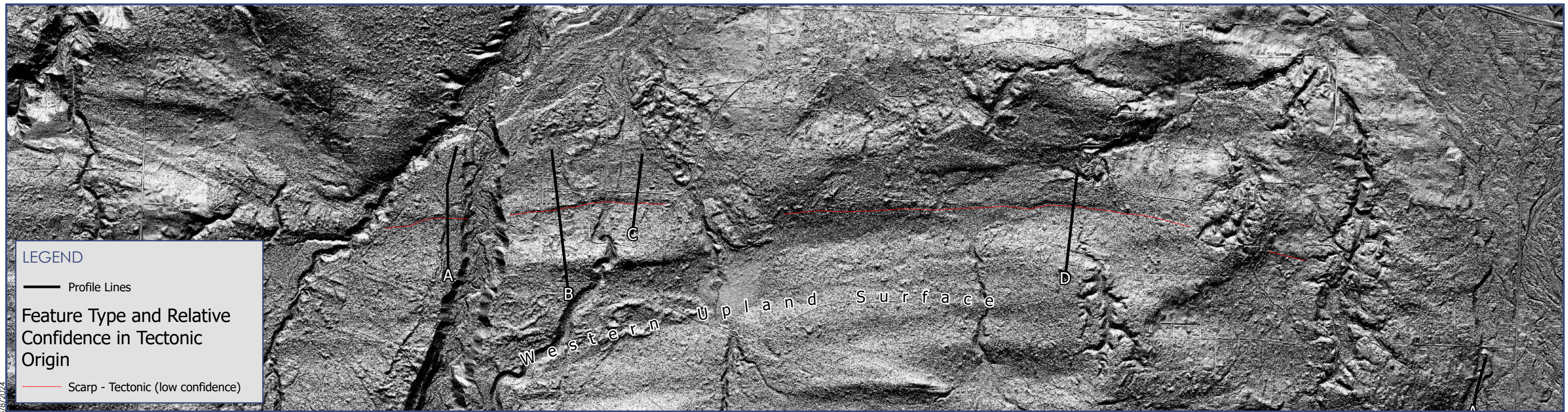


**SCARP AND LINEAMENT MAP-DUNGENESS RIVER VALLEY AND EASTERN UPLAND SURFACE**

March 2024

**Figure 15**





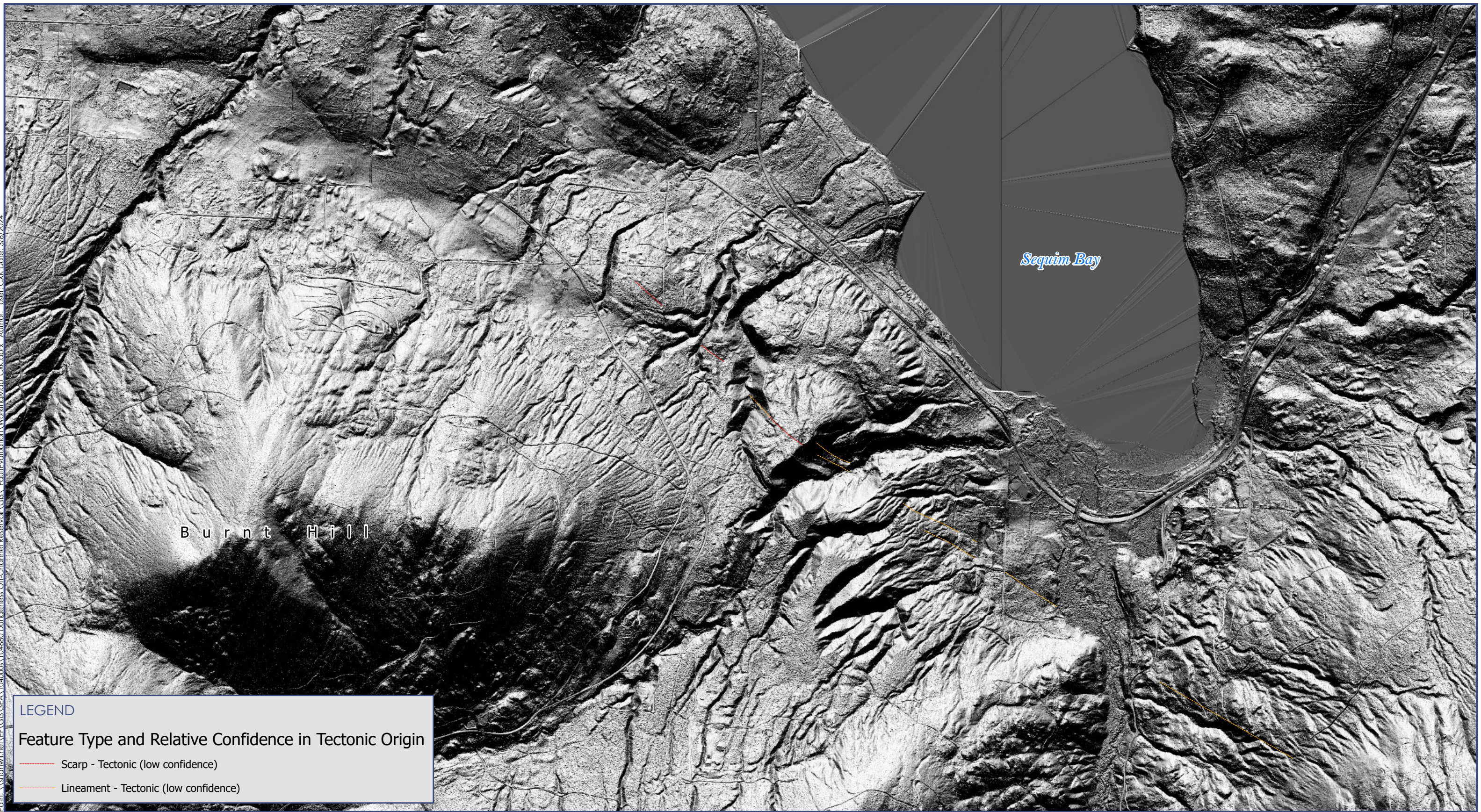
0 2,000 Feet

104680

Notes:  
1. LiDAR is courtesy of WA DNR, WA Geologic Society and the USGS; Olympics North OPSW 2018 and Olympics South OPSW 2019.







Path: \\shannonwilson\GIS\SEA\104680\Dungeness Off-Channel Reservoir\GIS\FaultEvaluation\WorkingMap\_CXK.aprx Author: User: CXK Date: 3/8/2024

**LEGEND**

**Feature Type and Relative Confidence in Tectonic Origin**

- Scarp - Tectonic (low confidence)
- Lineament - Tectonic (low confidence)

0 500  
Meters

0 1,600  
Feet

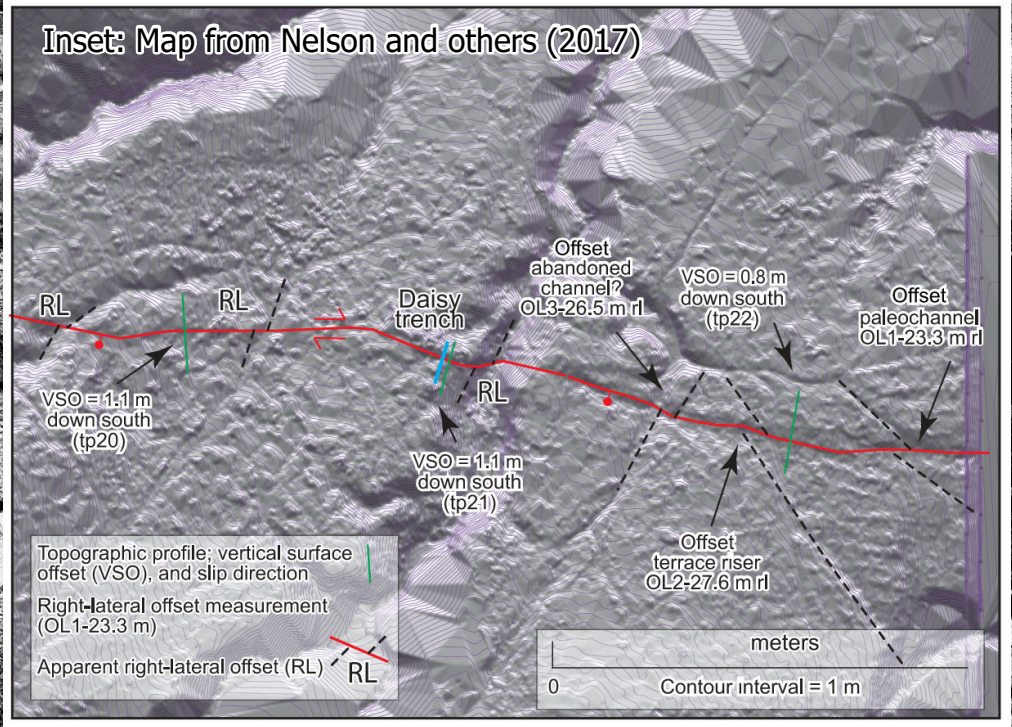
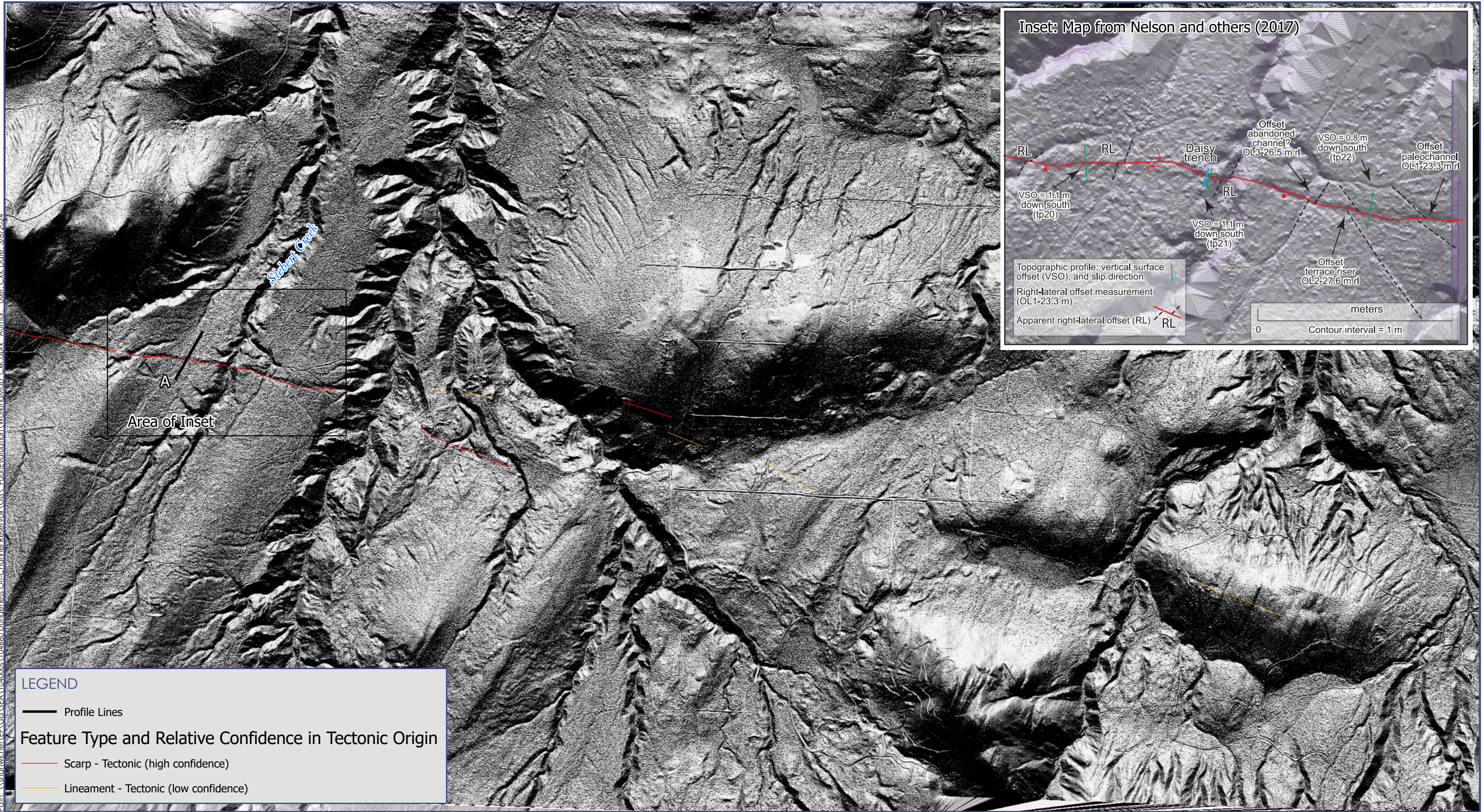
104680

Notes:

1. LiDAR is courtesy of WA DNR, WA Geologic Society and the USGS; Olympics North OPSW 2018 and Olympics South OPSW 2019.







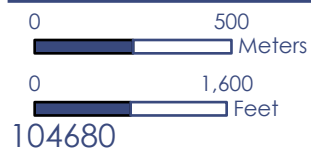
**LEGEND**

— Profile Lines

**Feature Type and Relative Confidence in Tectonic Origin**

— Scarp - Tectonic (high confidence)

— Lineament - Tectonic (low confidence)

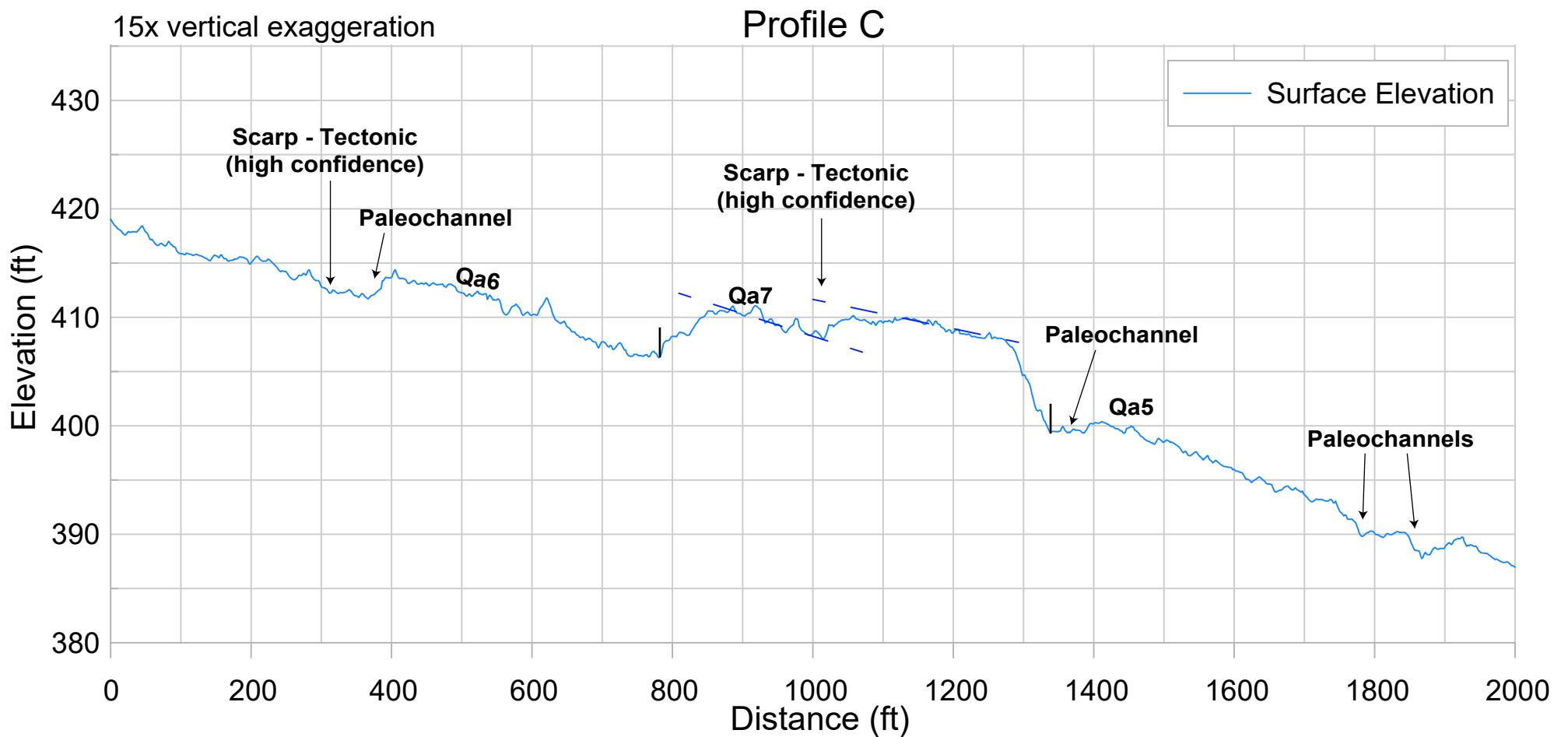
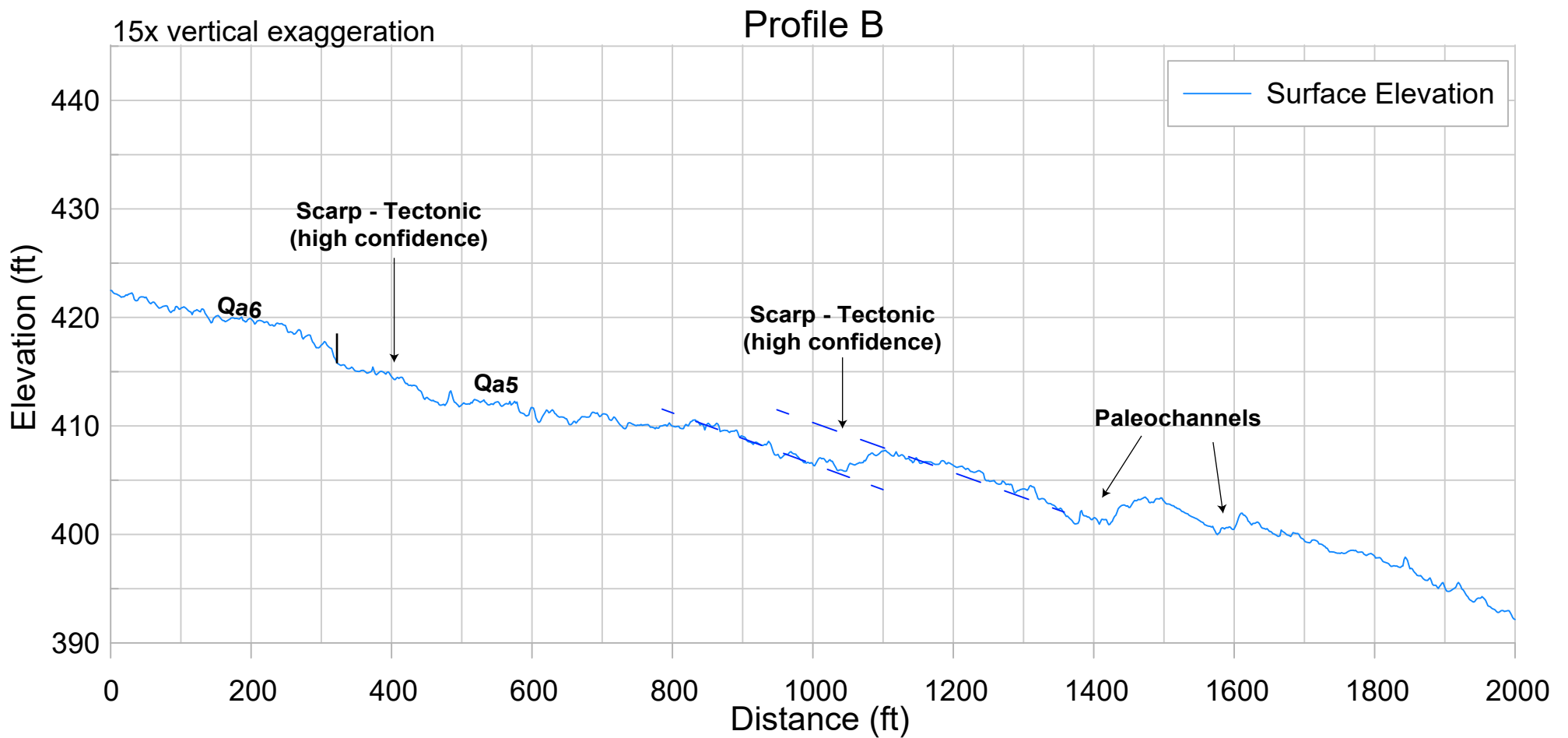
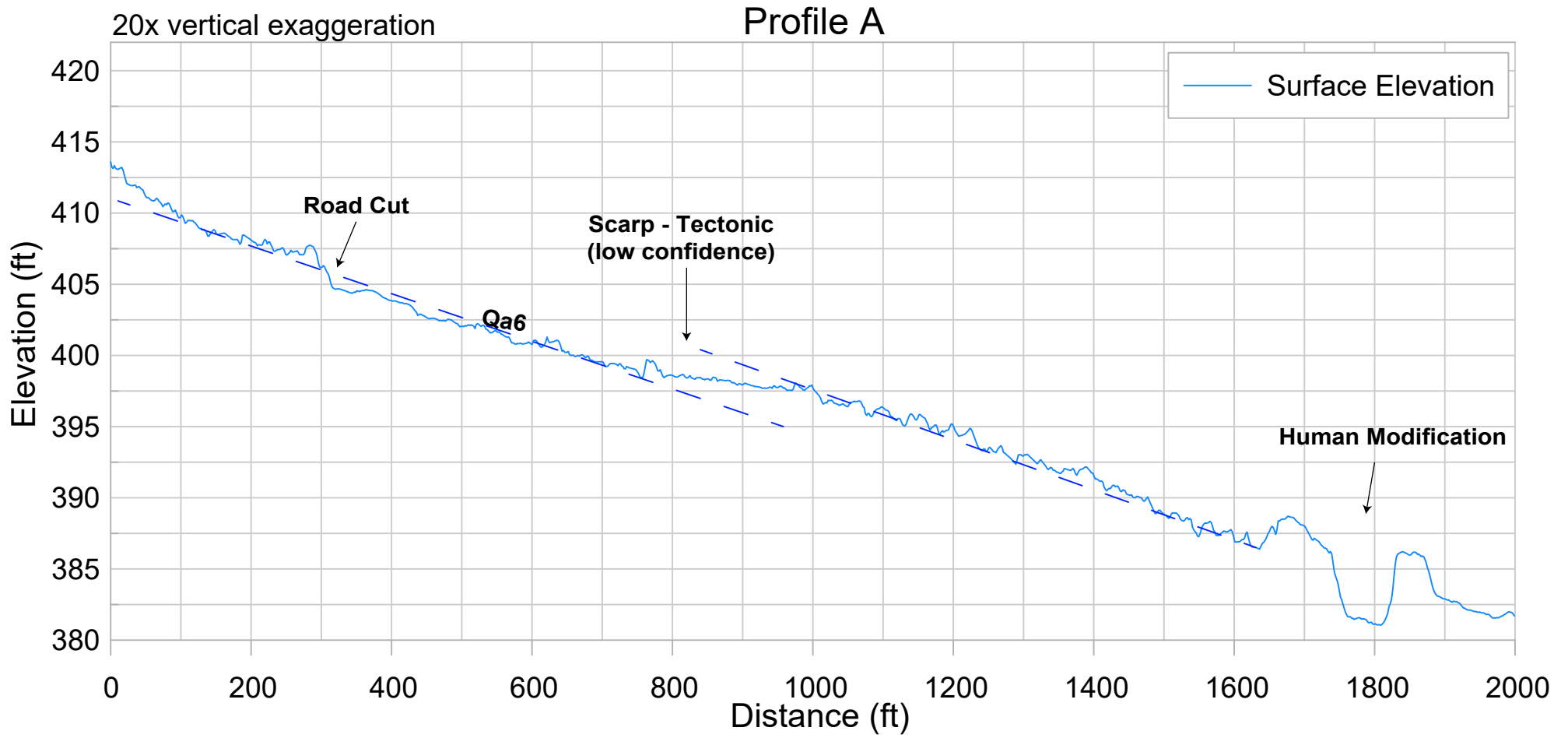


**Notes:**

1. LiDAR is courtesy of WA DNR, WA Geologic Society and the USGS; Olympics North OPSW 2018 and Olympics South OPSW 2019.



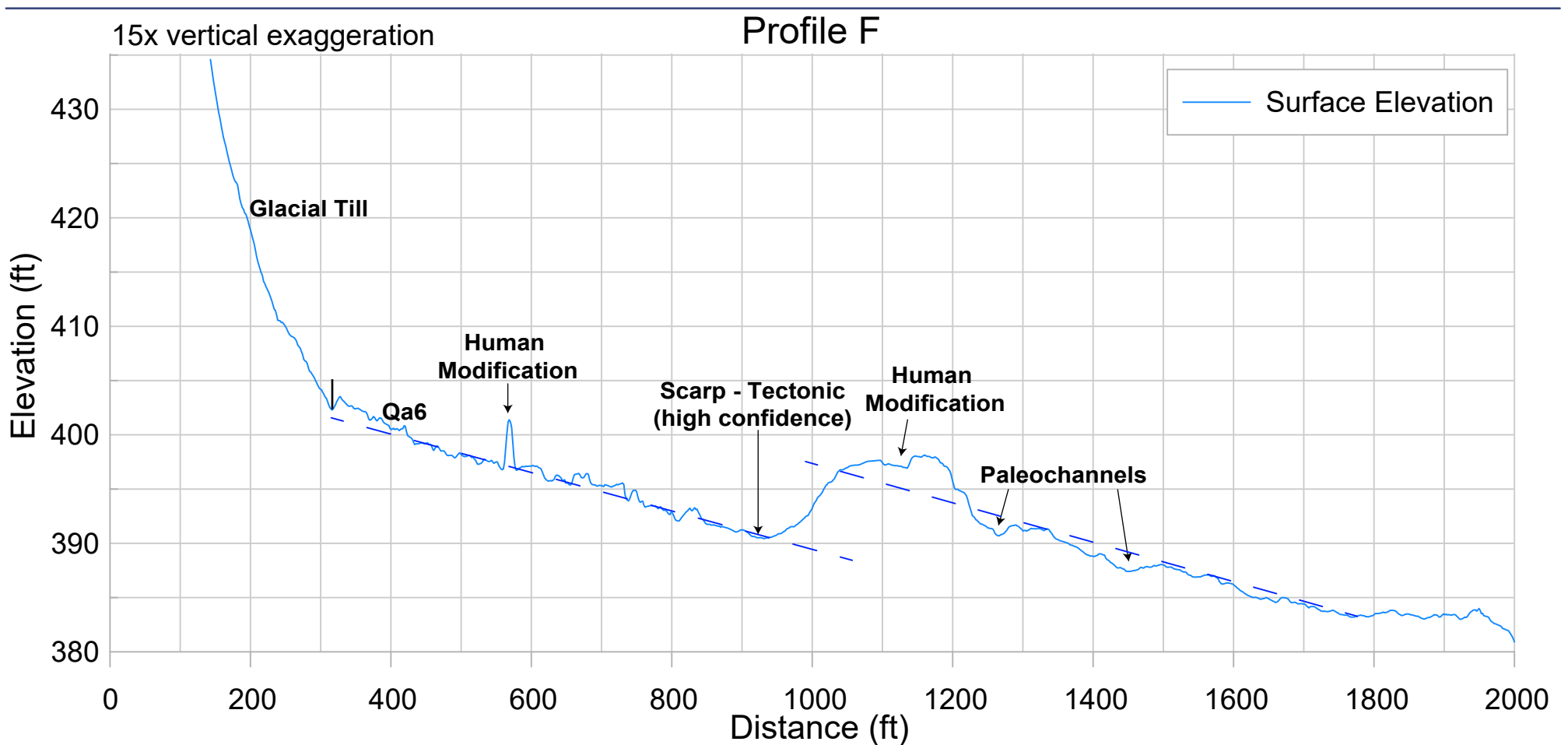
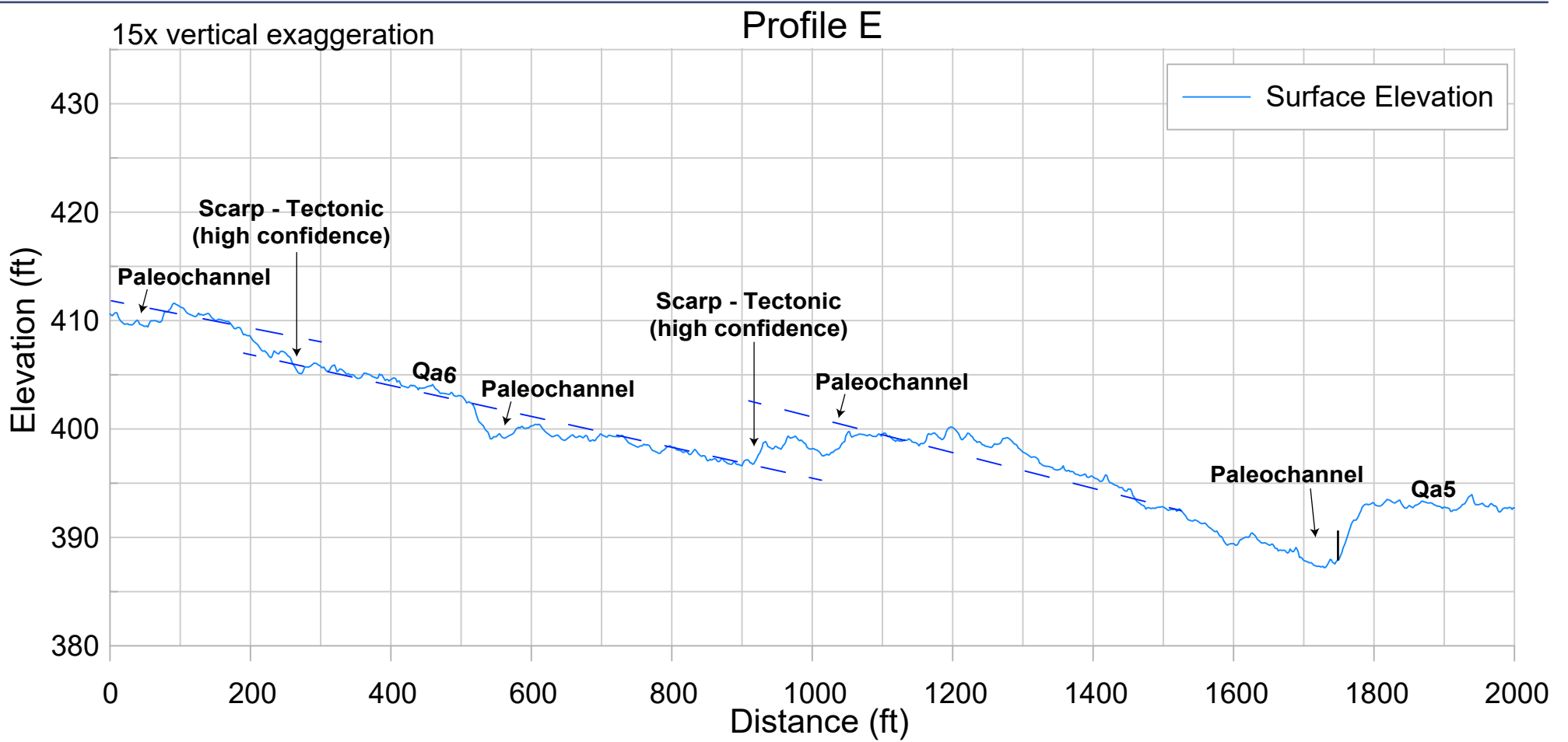
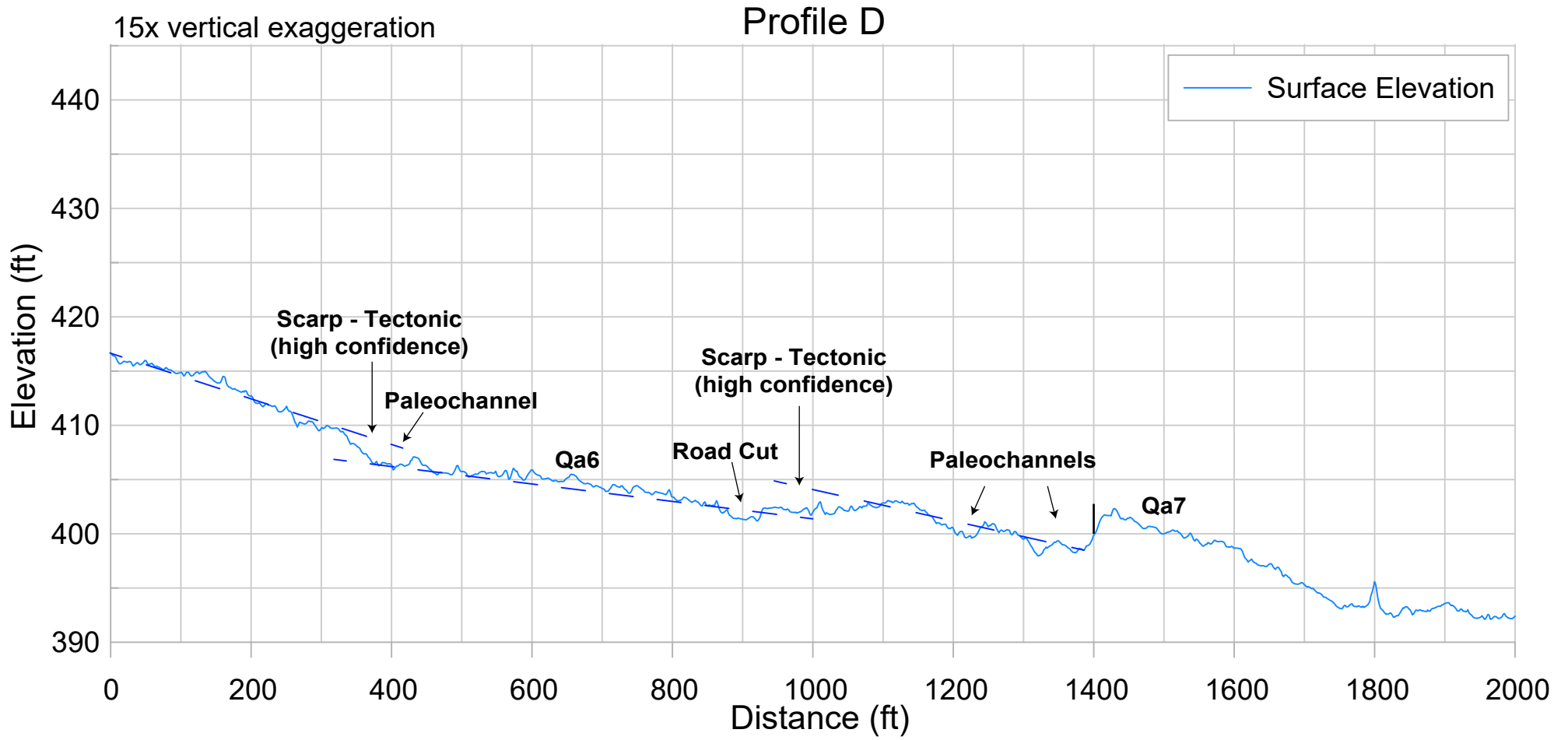




Notes:

1. Fault scarp lineament locations are approximate.
2. Surficial geologic contacts are from this study.
3. Dark blue dashed lines represent a trendline of the surface.

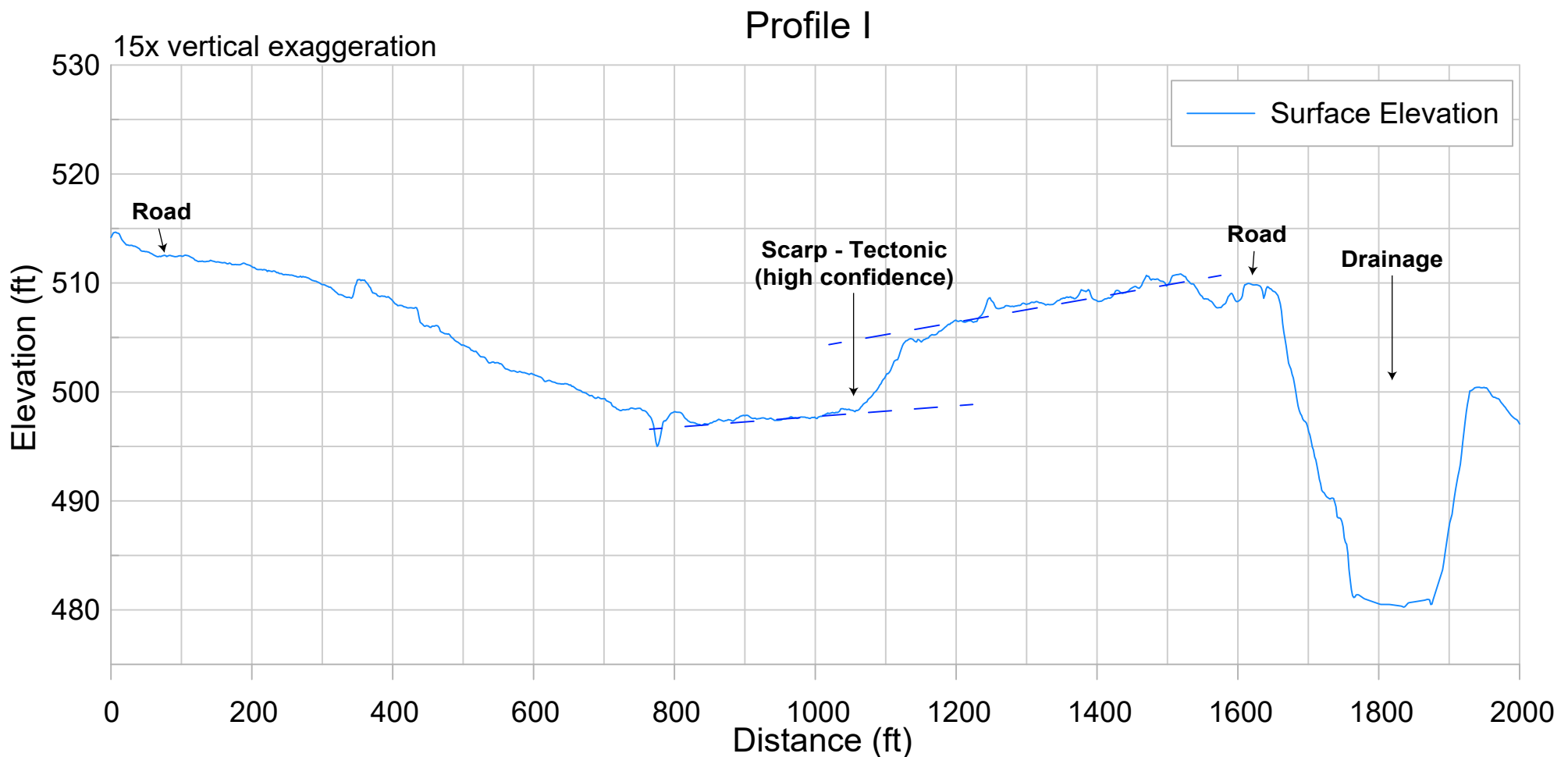
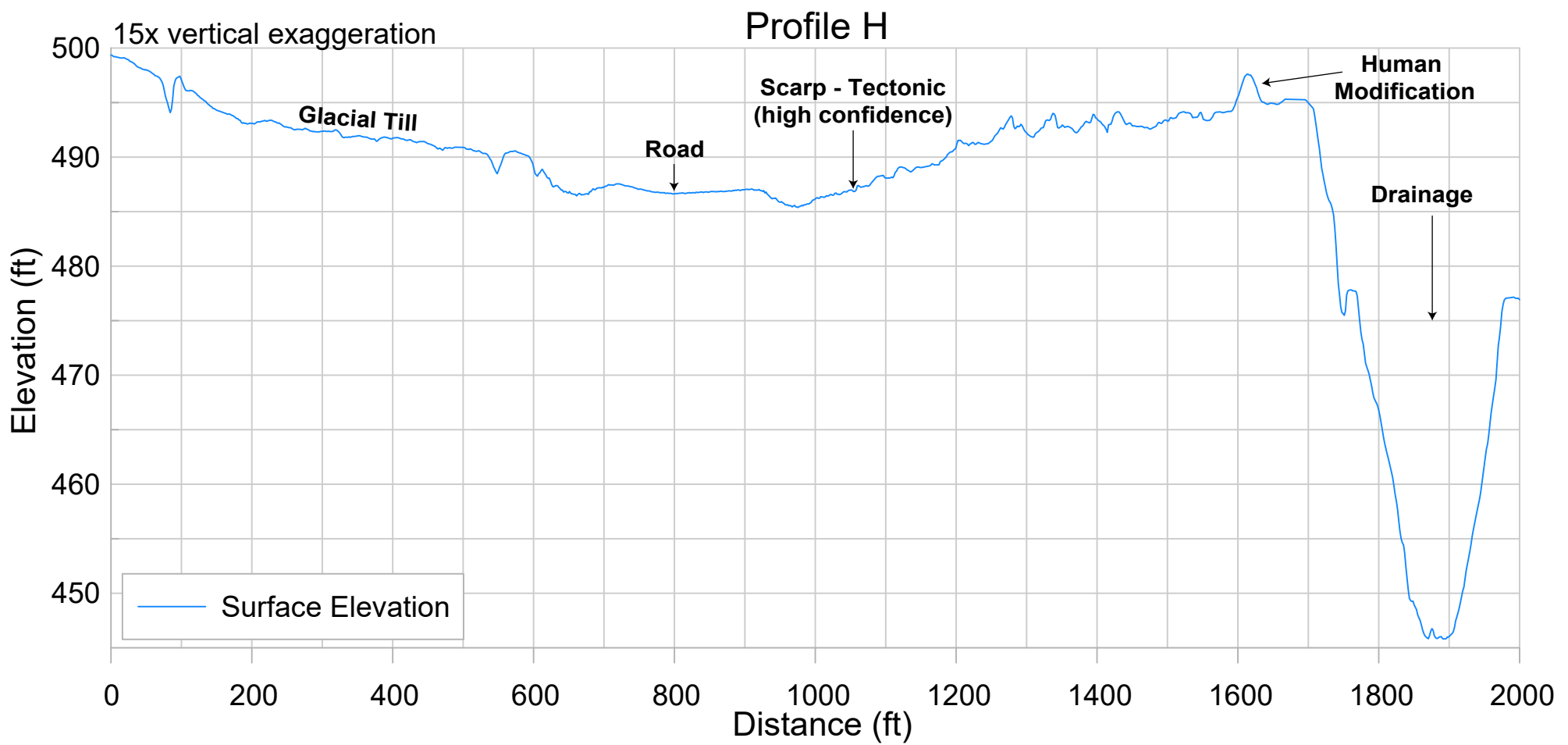
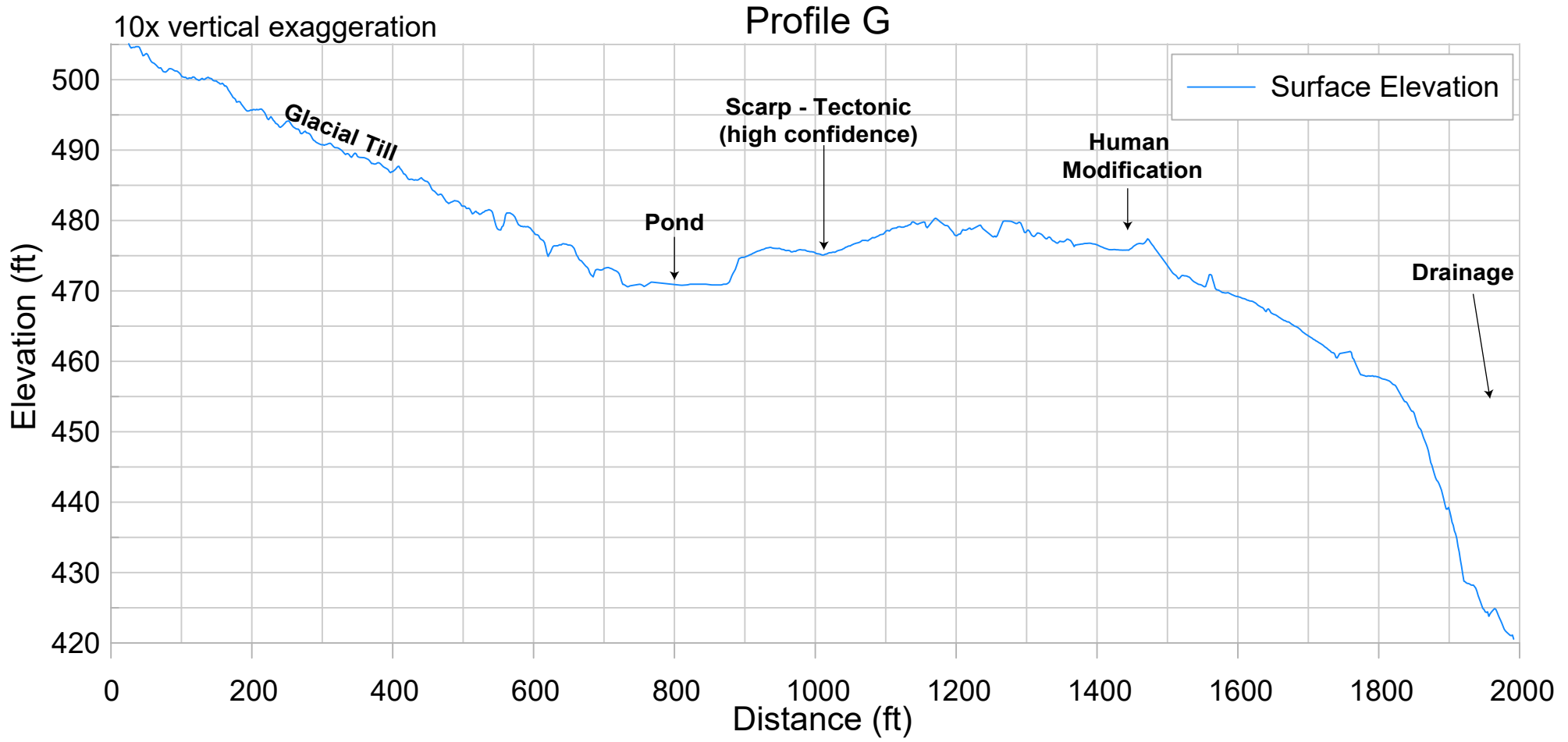
March 2024



Notes:

1. Fault scarp and lineament locations are approximate.
2. Alluvial surficial geologic contacts are from this study and other surficial geology is from Schasse and Wegmann (2000).
3. Dark blue dashed lines represent a trendline of the surface.

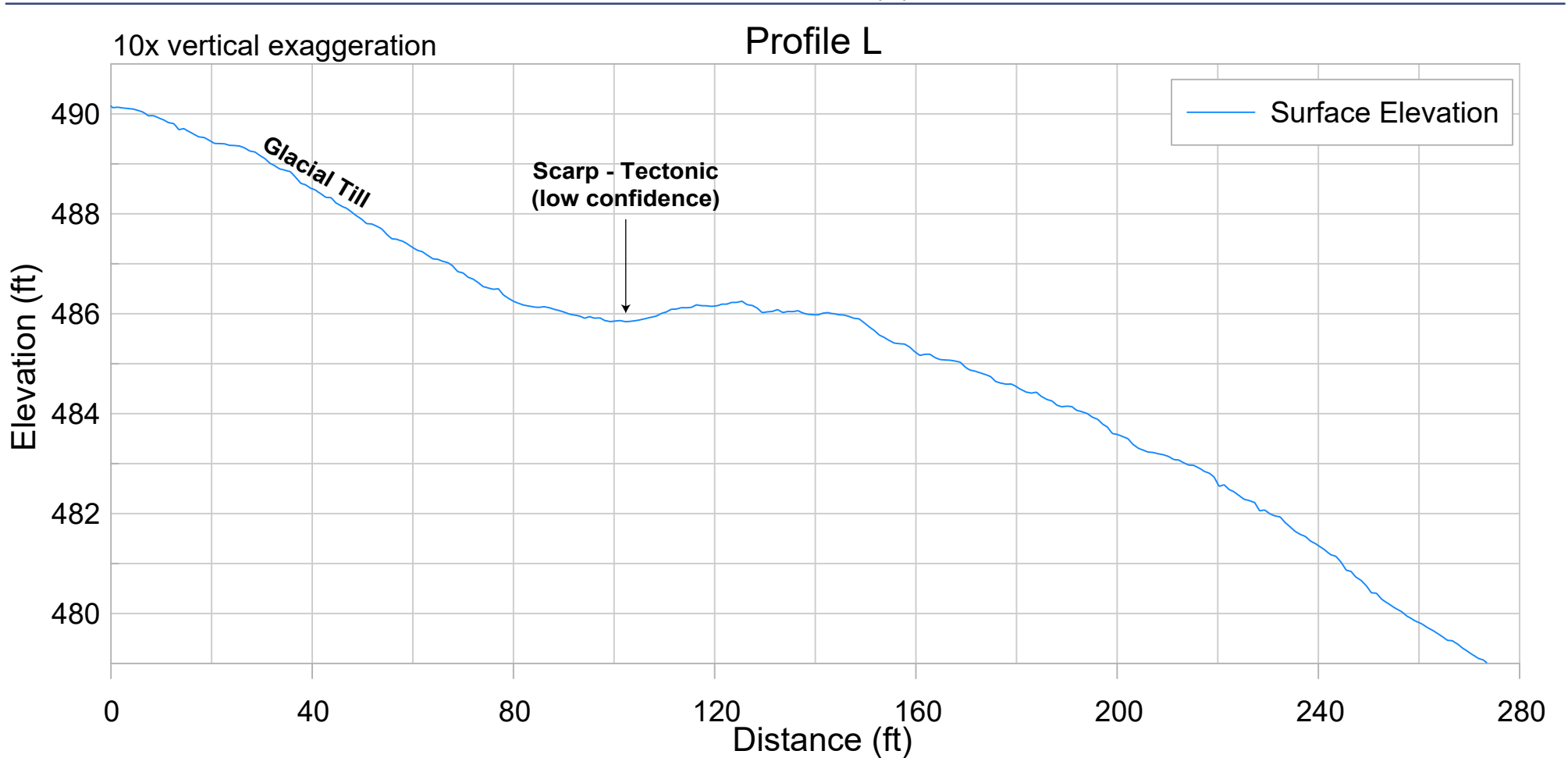
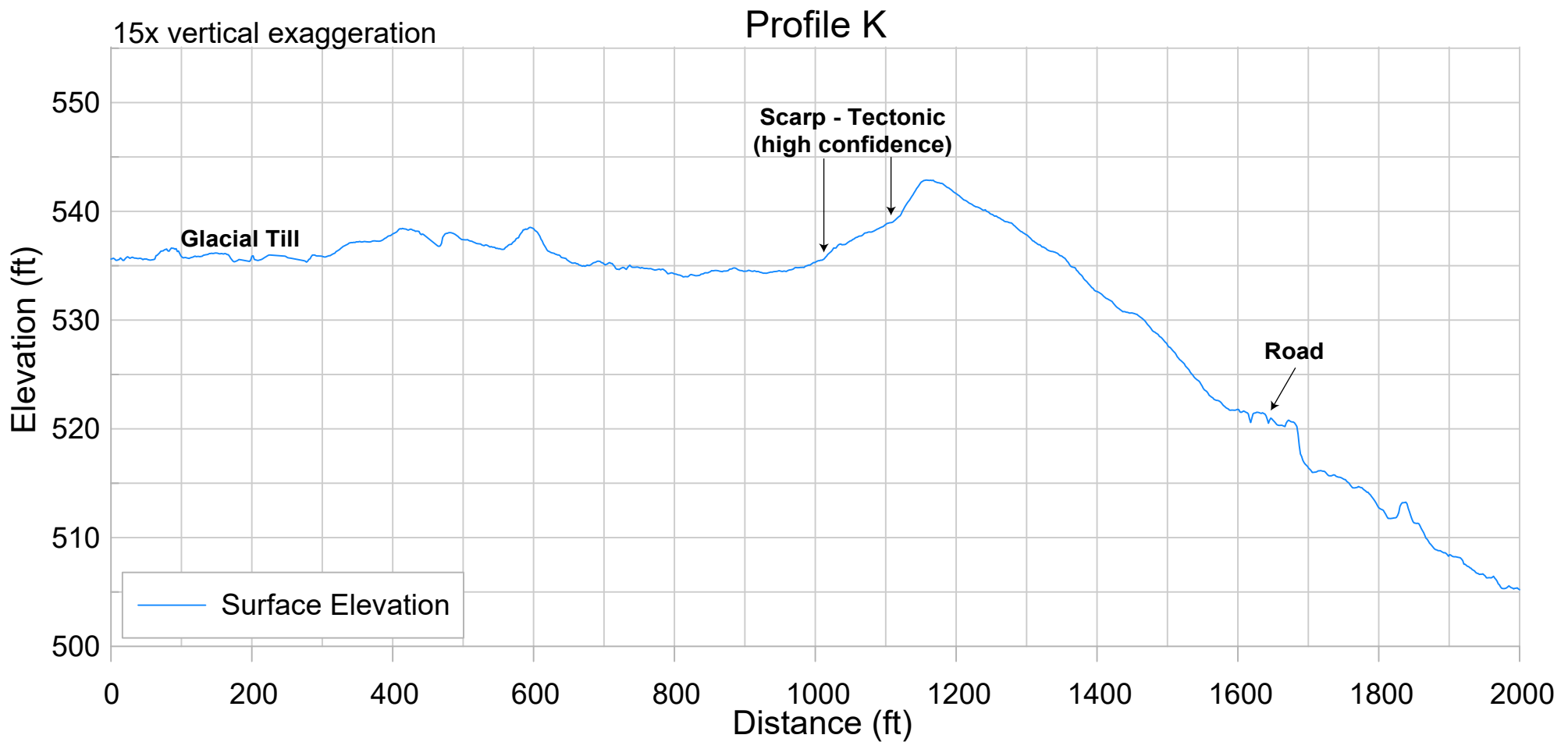
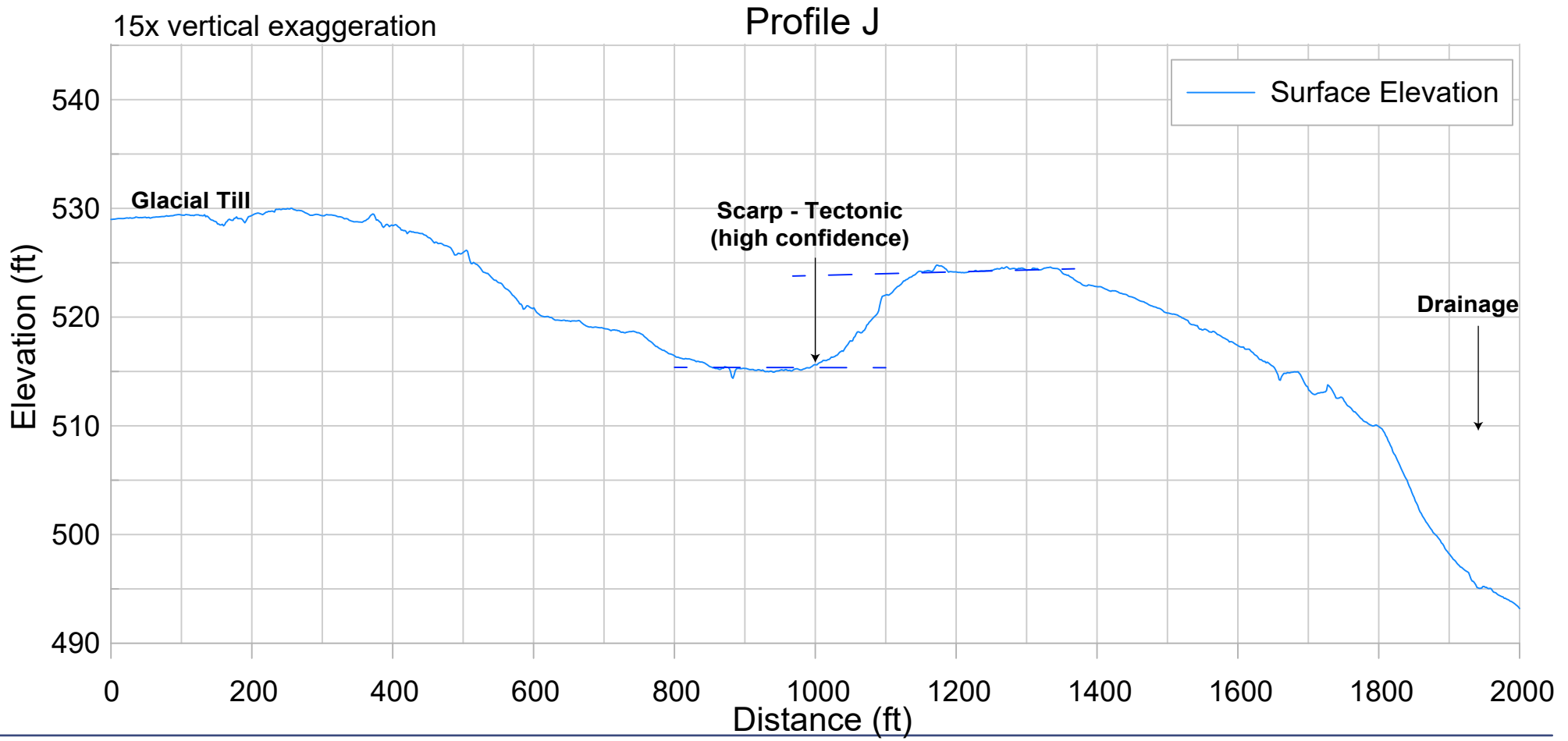
March 2024



Notes:

1. Fault scarp and lineament locations are approximate.
2. Surficial geology is from Schasse and Logan (1998) and Schasse and Wegmann (2000).
3. Dark blue dashed lines represent a trendline of the surface.

March 2024

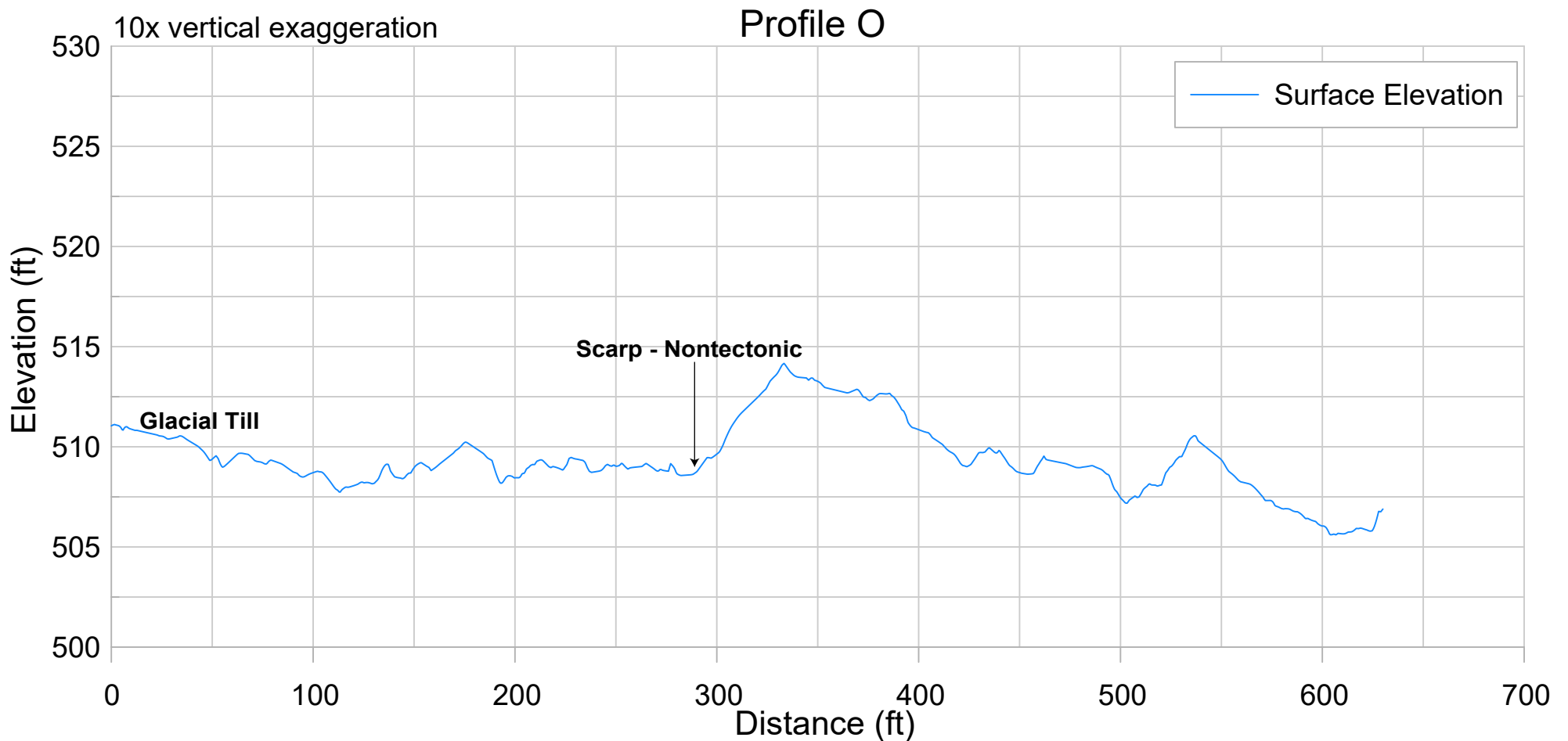
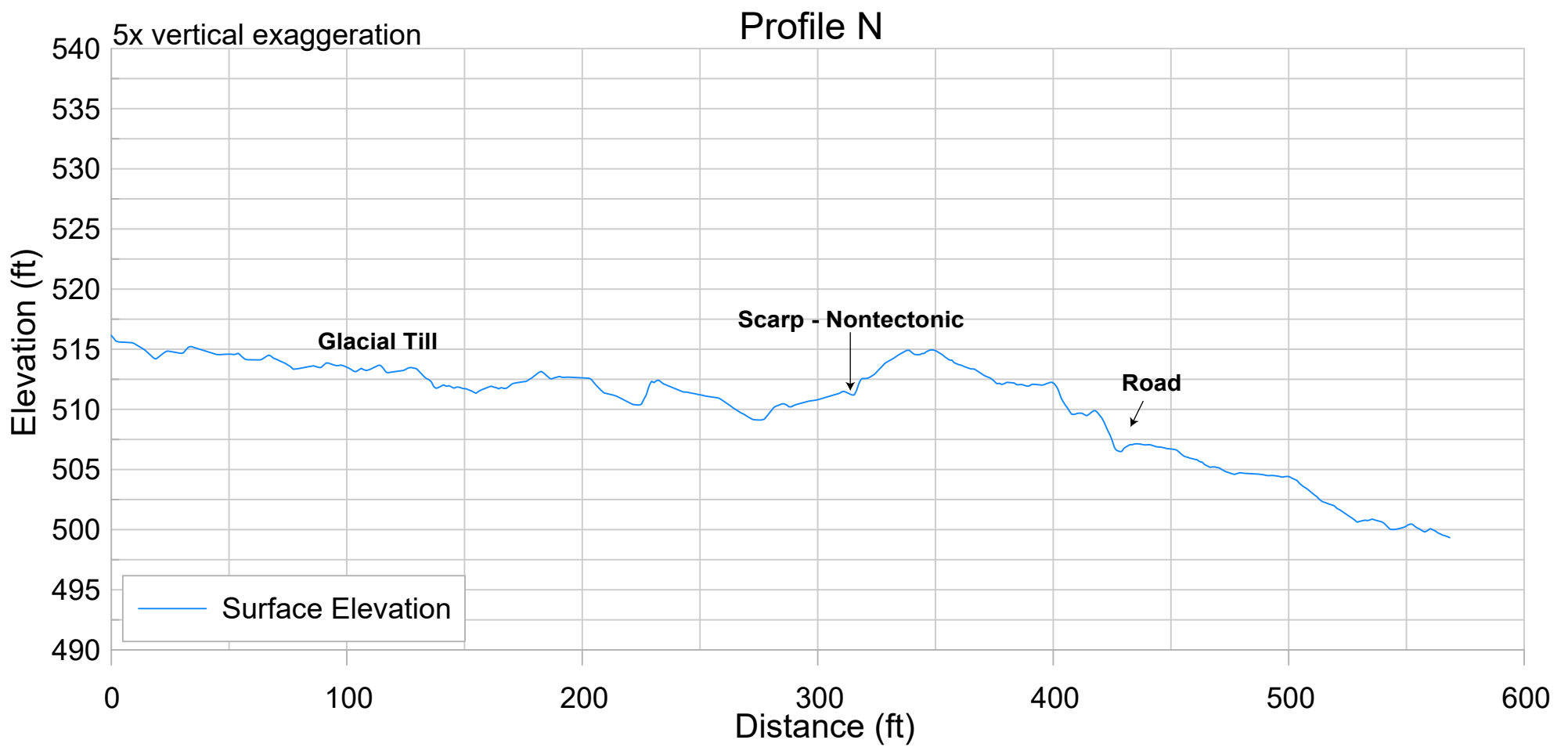
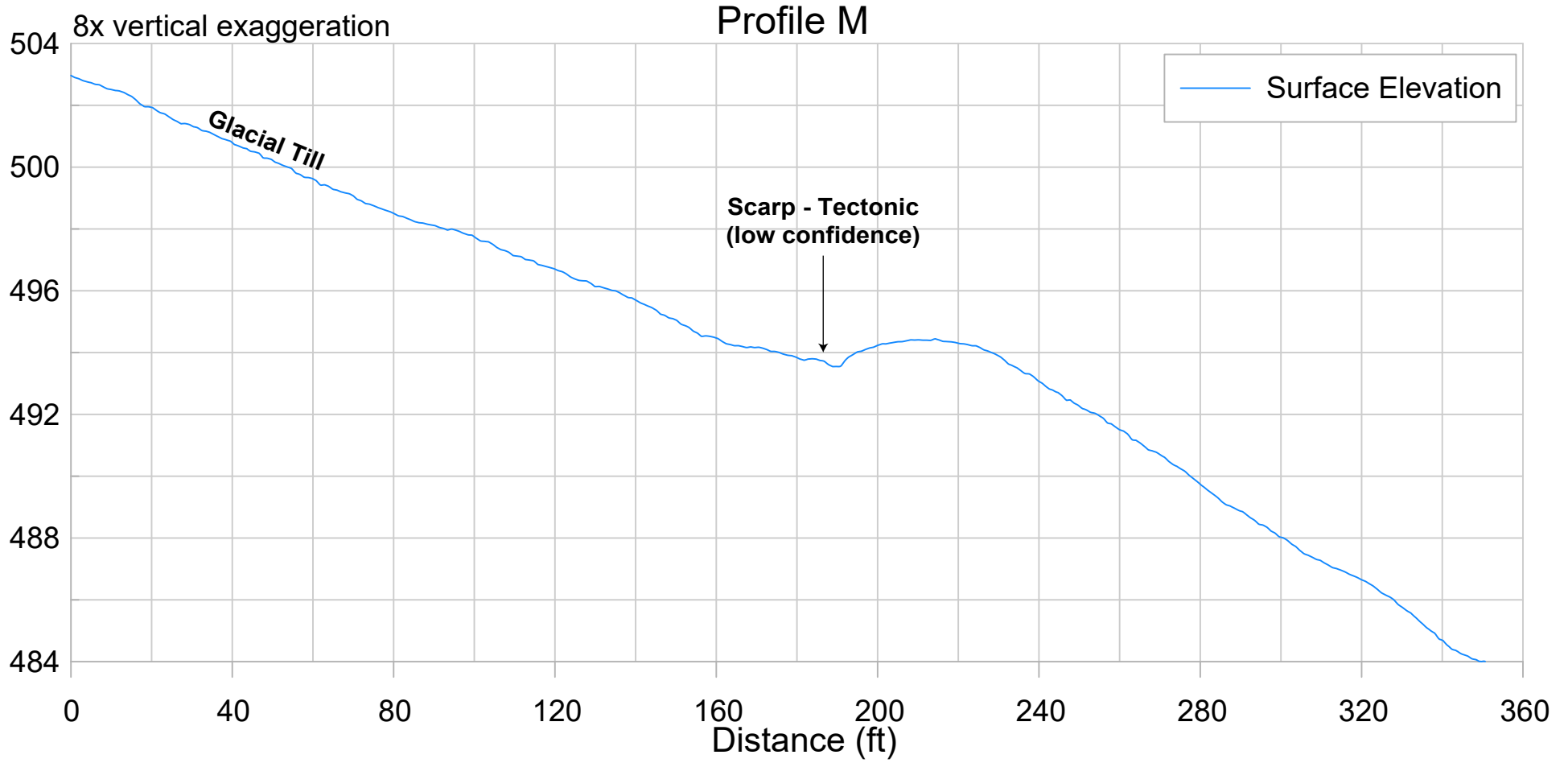


Notes:

1. Fault scarp and lineament locations are approximate.
2. Surficial geology is from Schasse and Logan (1998).
3. Dark blue dashed lines represent a trendline of the surface.

March 2024

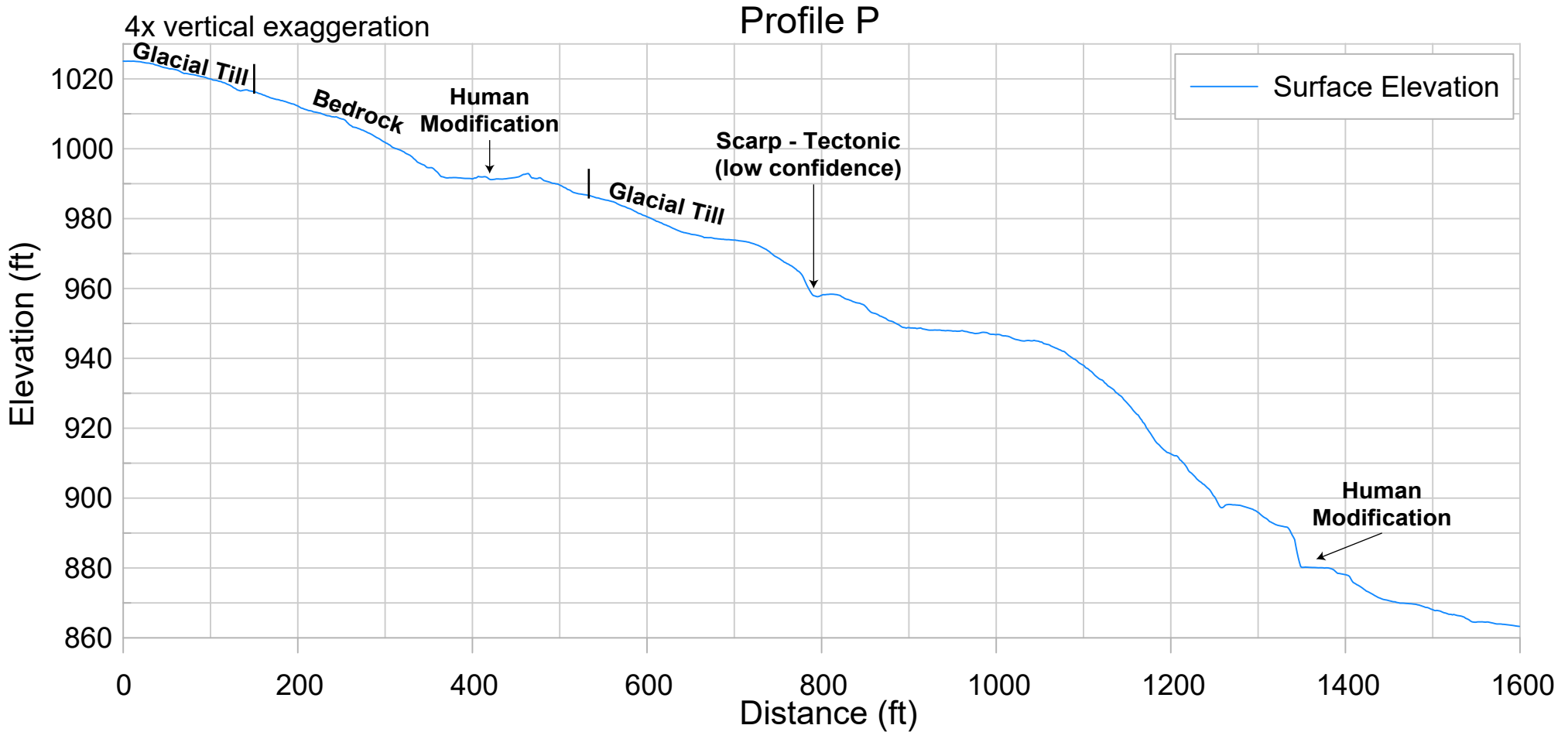




Notes:

1. Fault scarp and lineament locations are approximate.
2. Surficial geology is from Schasse and Logan (1998).

March 2024

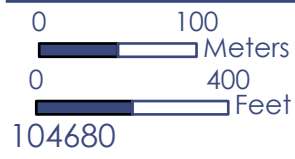
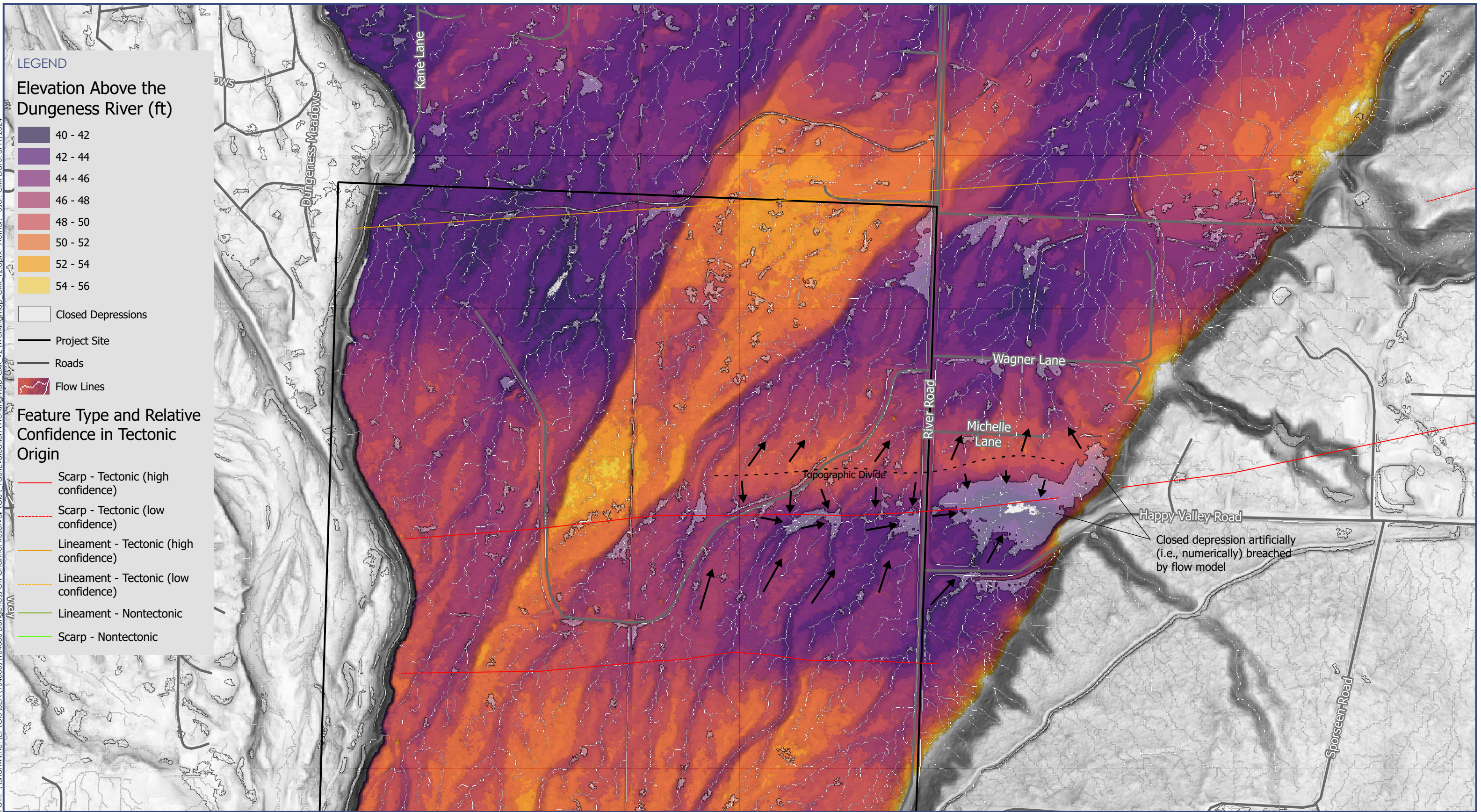


Notes:

1. Fault scarp and lineament locations are approximate.
2. Surficial geology is from Schasse and Logan (1998).

March 2024





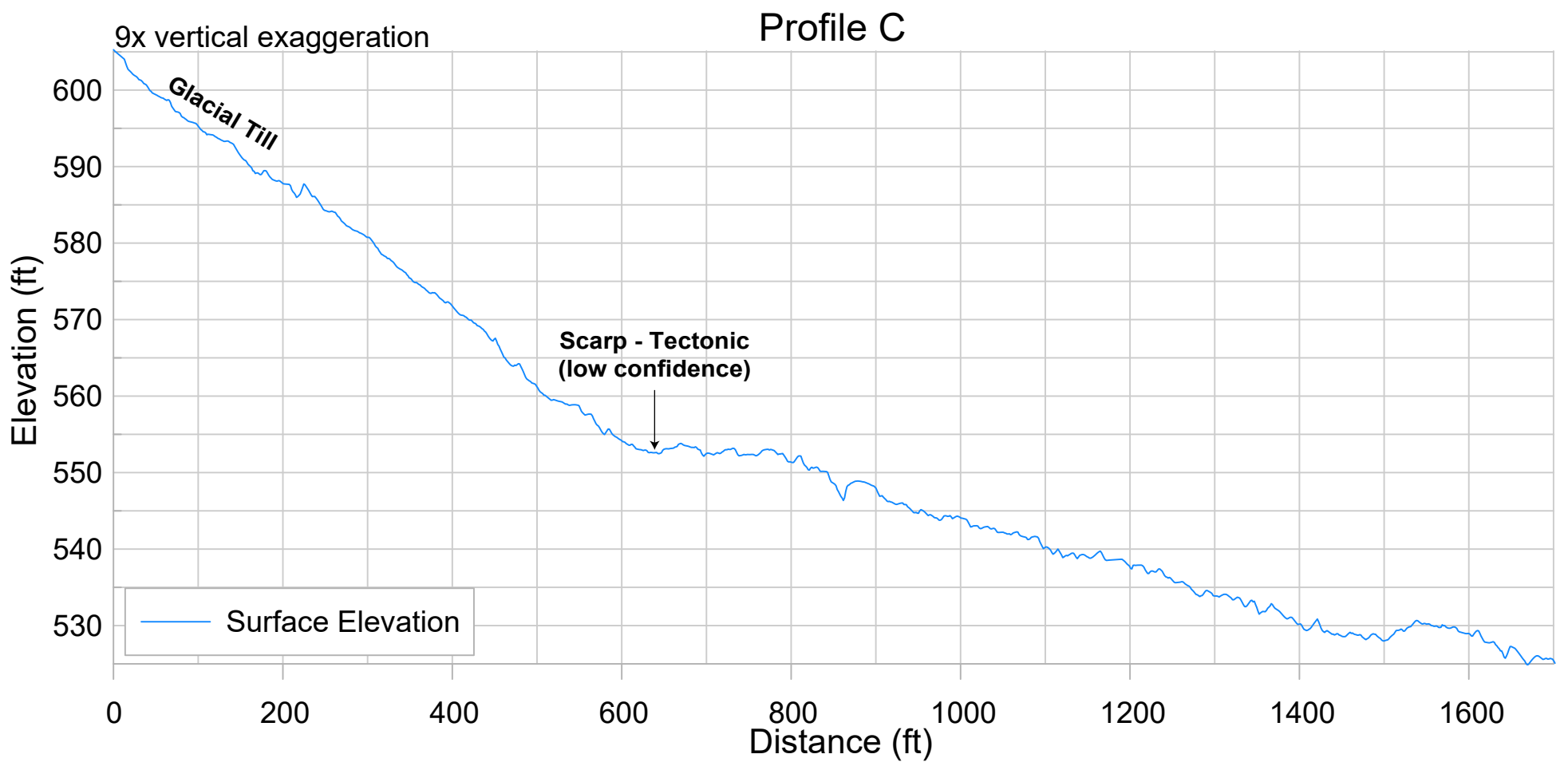
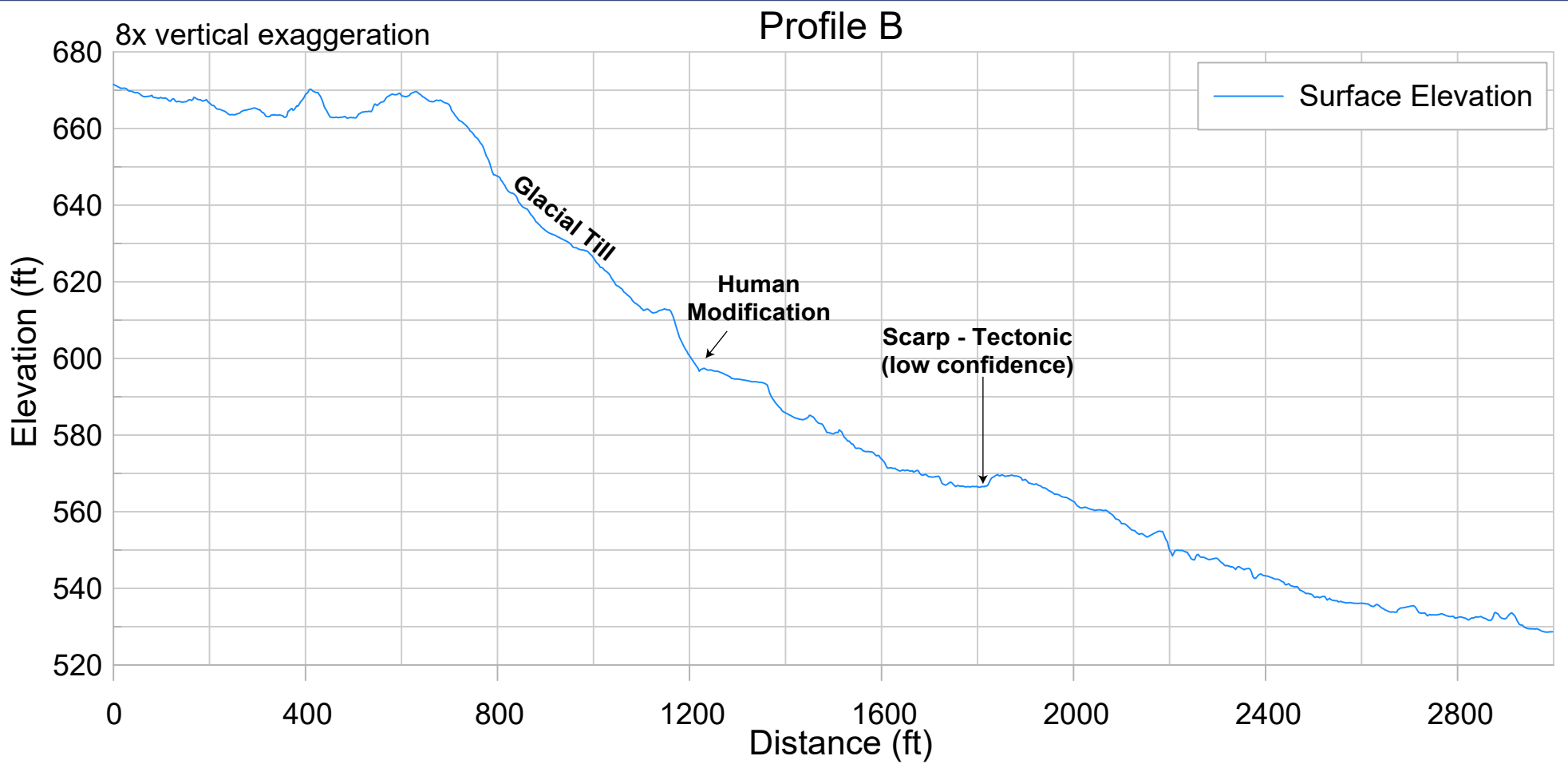
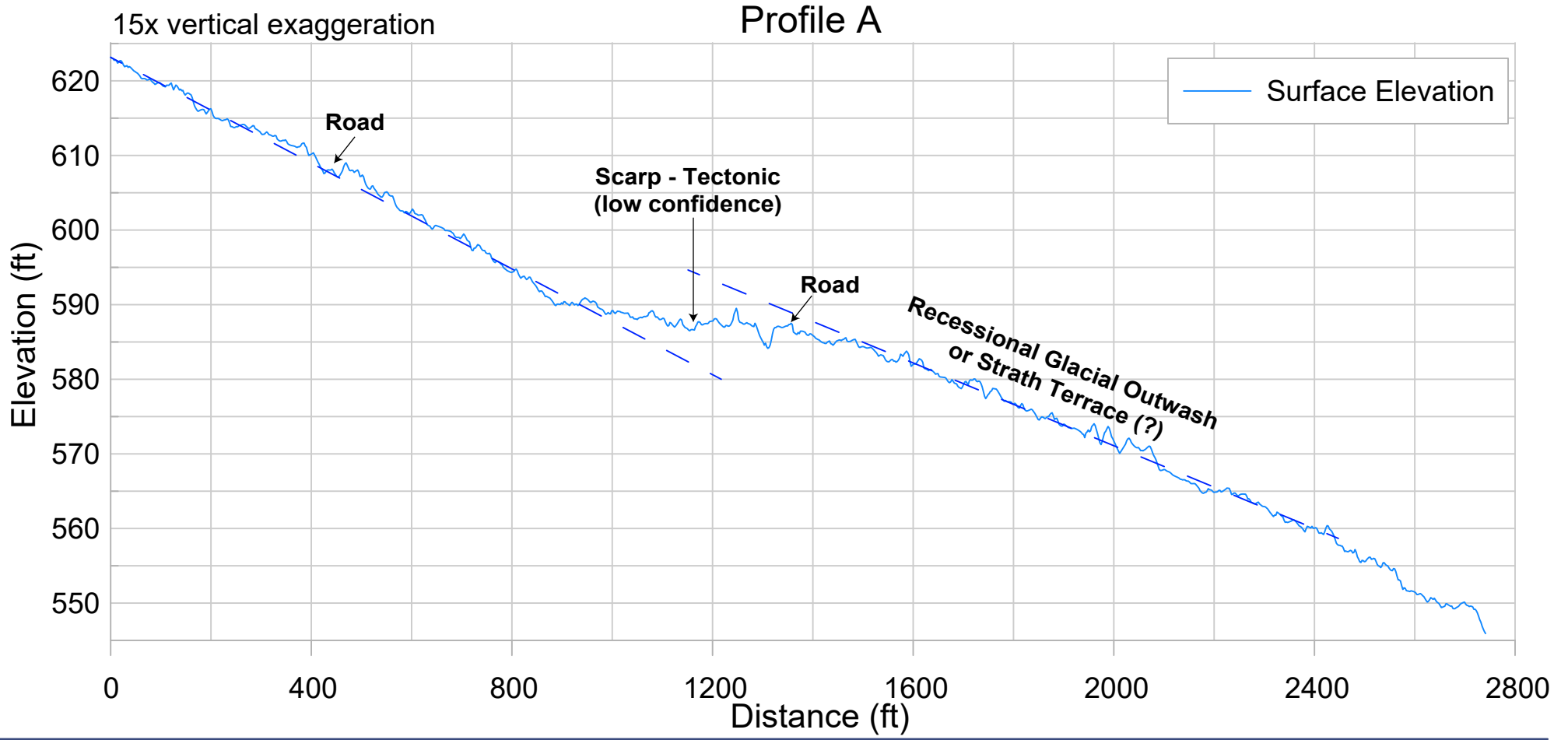
**Notes:**  
1. LiDAR is courtesy of WA DNR, WA Geologic Society and the USGS; Olympics North OPSW 2018 and Olympics South OPSW 2019.











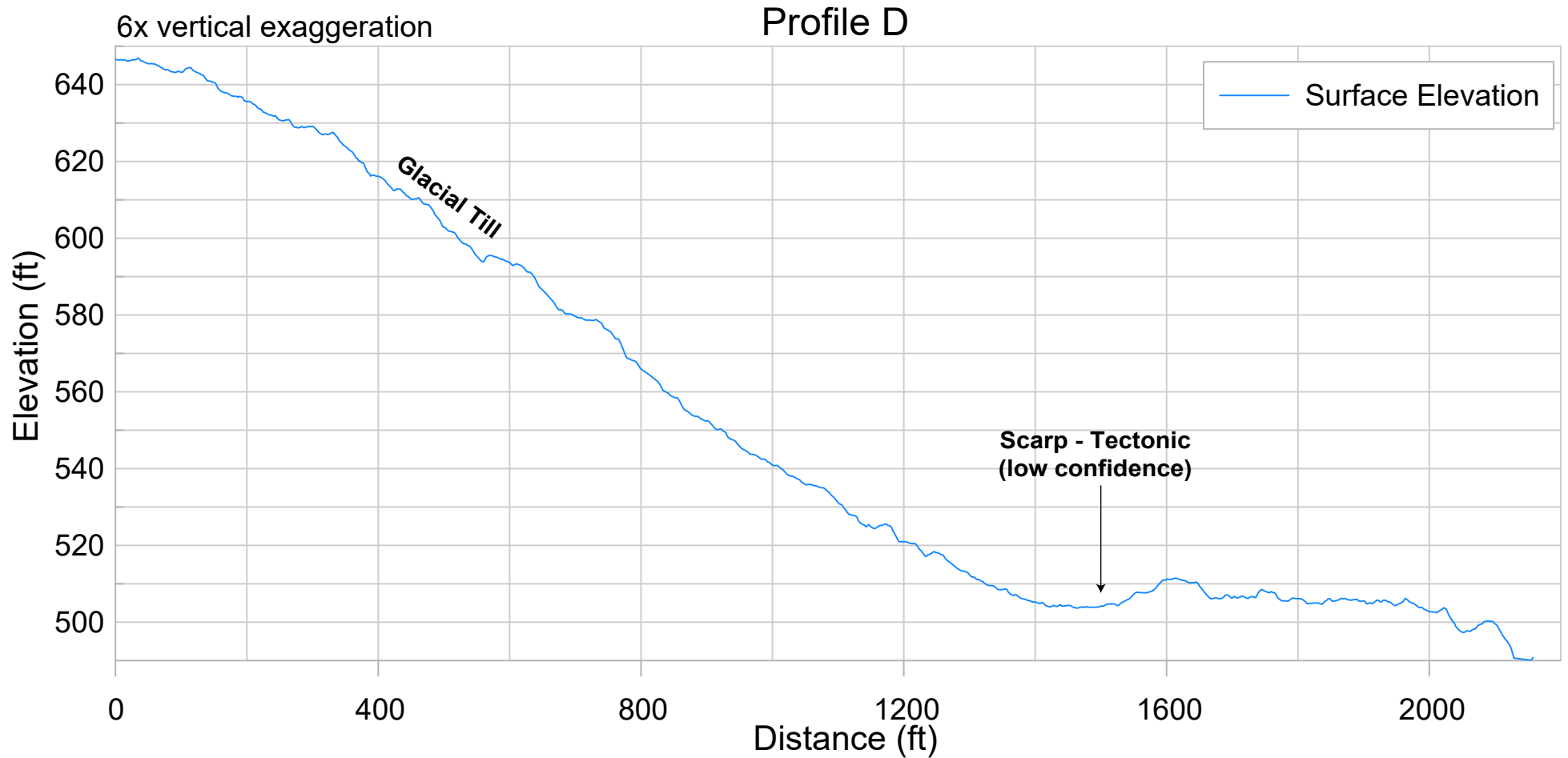
Notes:

1. Fault scarp and lineament locations are approximate.
2. Surficial geology is from Schasse (2003).
3. Dark blue dashed lines represent a trendline of the surface.

March 2024

**WESTERN UPLAND SURFACE TOPOGRAPHIC PROFILES**

**Figure 22 A - C**



Notes:

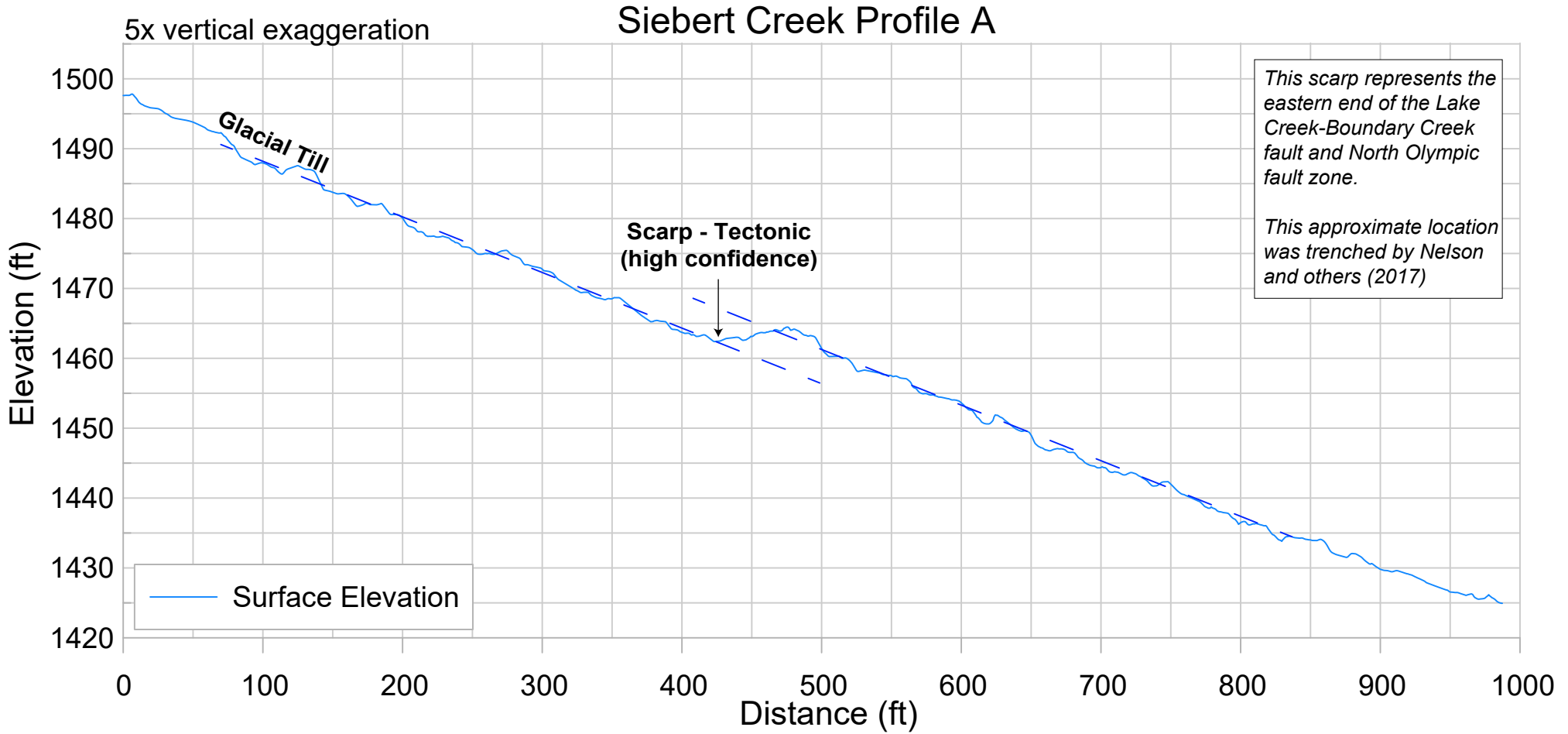
- 1. Fault scarp and lineament locations are approximate.
- 2. Surficial geology is from Schasse (2003).

March 2024

WESTERN UPLAND SURFACE TOPOGRAPHIC PROFILES

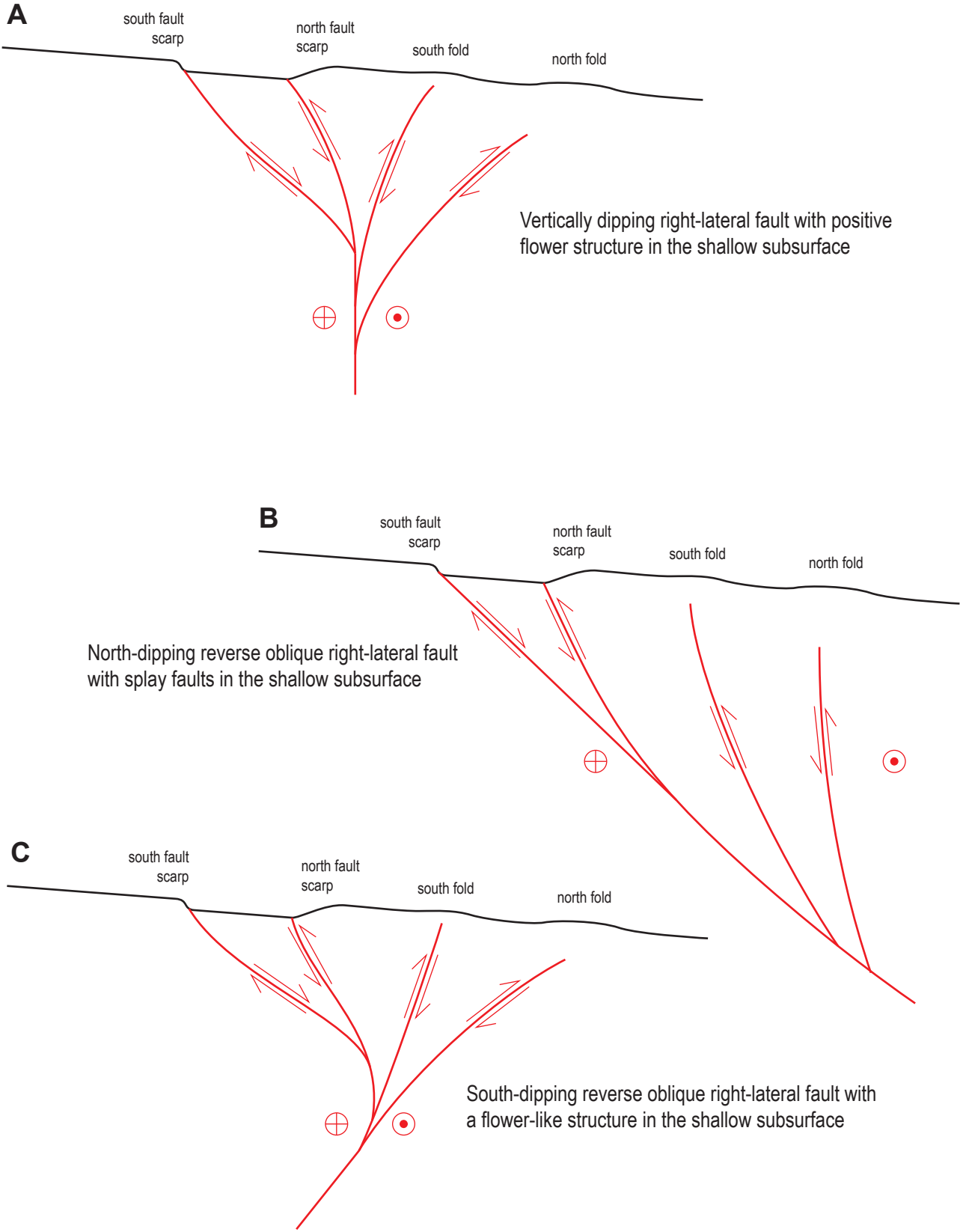
Figure 22 D



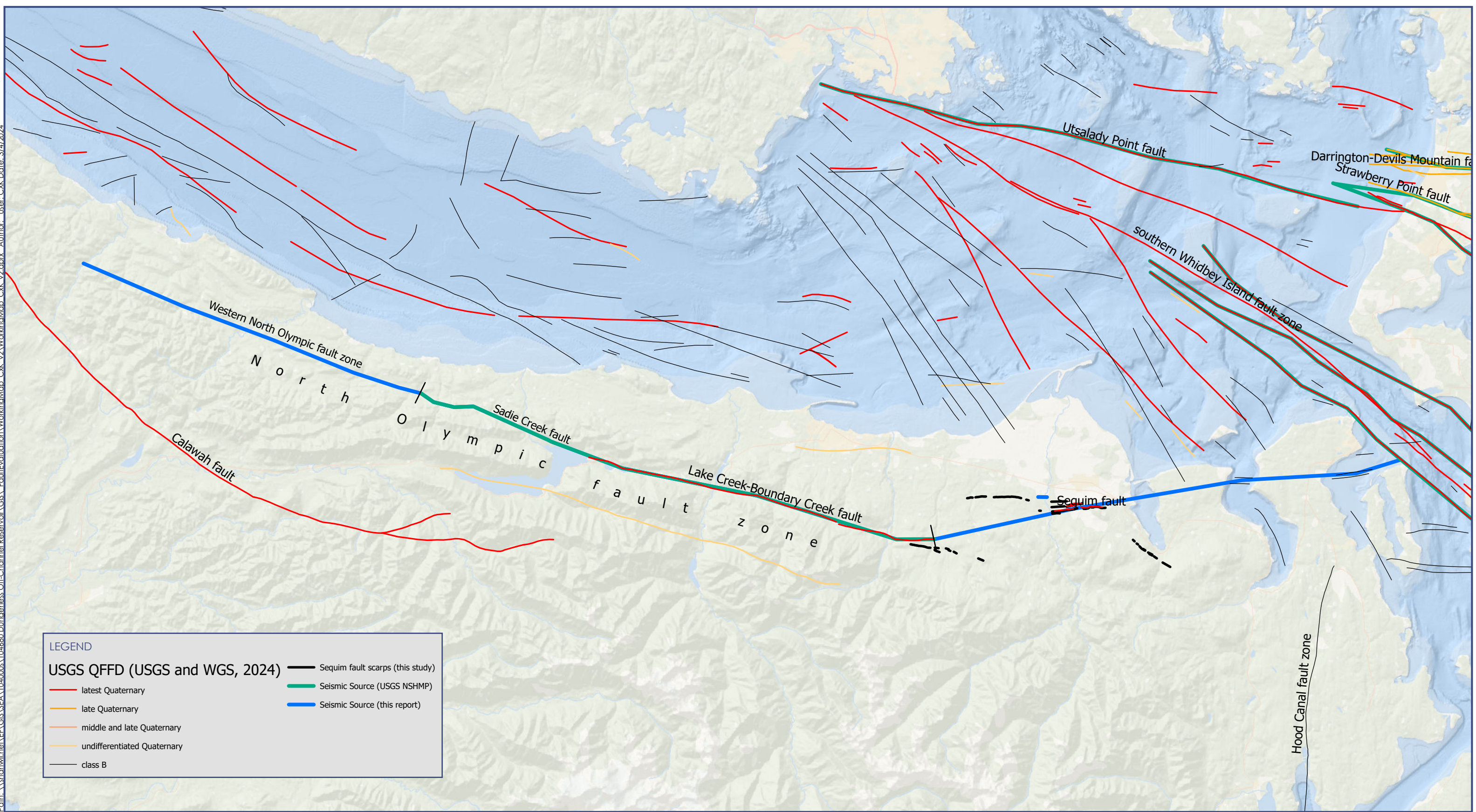


Notes:

1. Fault scarp and lineament locations are approximate.
2. Geologic units are from Schasse (2003).
3. Dark blue dashed lines represent a trendline of the surface.





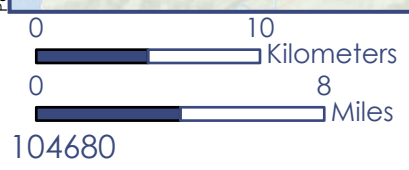


**LEGEND**

**USGS QFFD (USGS and WGS, 2024)**

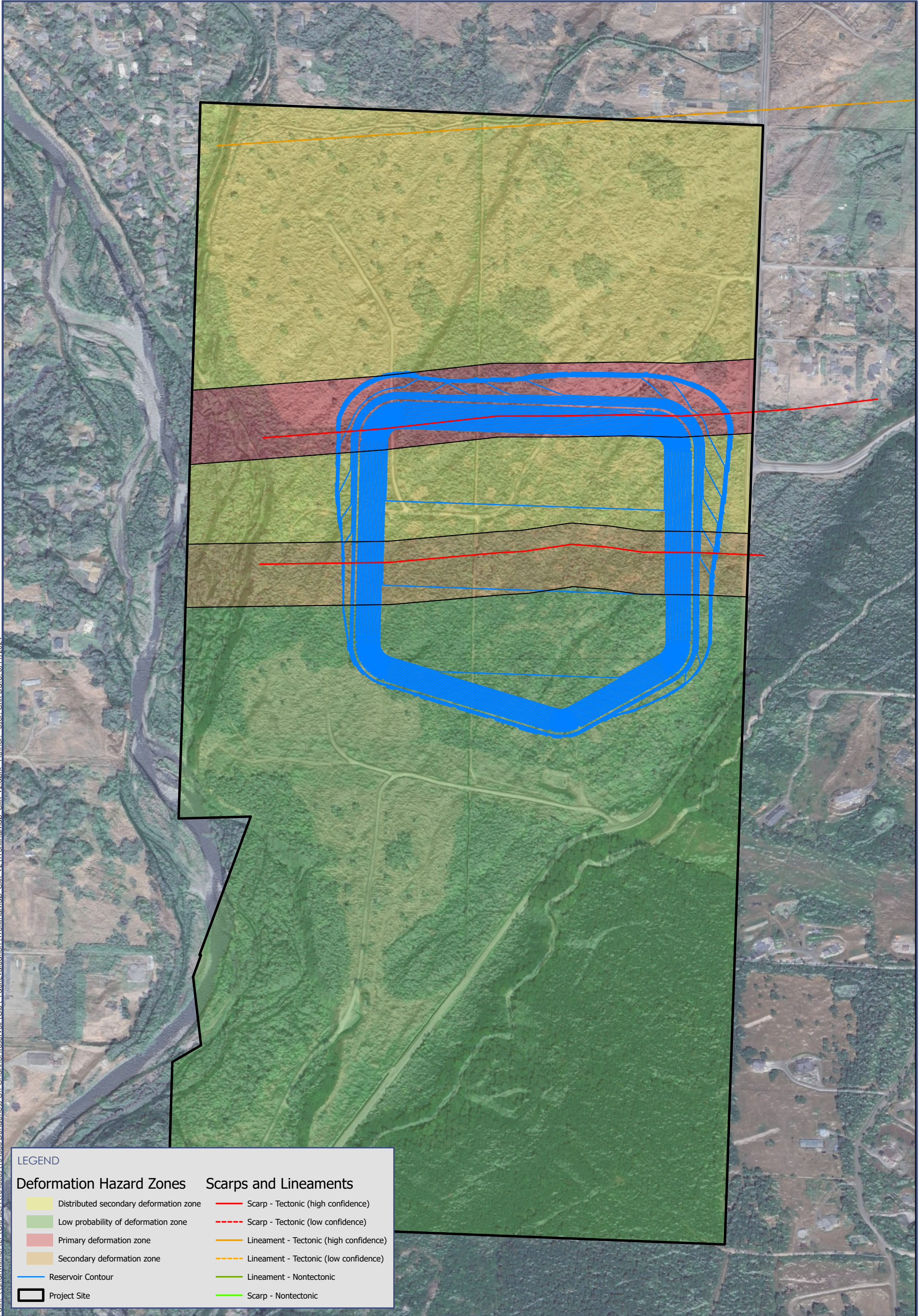
- latest Quaternary
- late Quaternary
- middle and late Quaternary
- undifferentiated Quaternary
- class B

- Sequim fault scarps (this study)
- Seismic Source (USGS NSHMP)
- Seismic Source (this report)



Path: \\shannonwilson\EE\GIS\SEA\104680\Dungeness Off-Channel Reservoir\GIS\FaultEvolution\WorkingMap\_CxK\_v2.aprx Author: User\_CXK Date: 3/14/2024

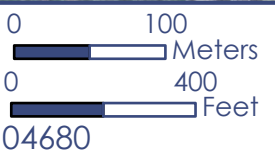




Path: \\shannonwilson\efs\SEA\104680\Dungeness Off-Channel Reservoir\CAD\Fault\Evaluation\WorkingMap\_CxK\_v2.aprx Author: User: CXK Date: 3/11/2024

**LEGEND**

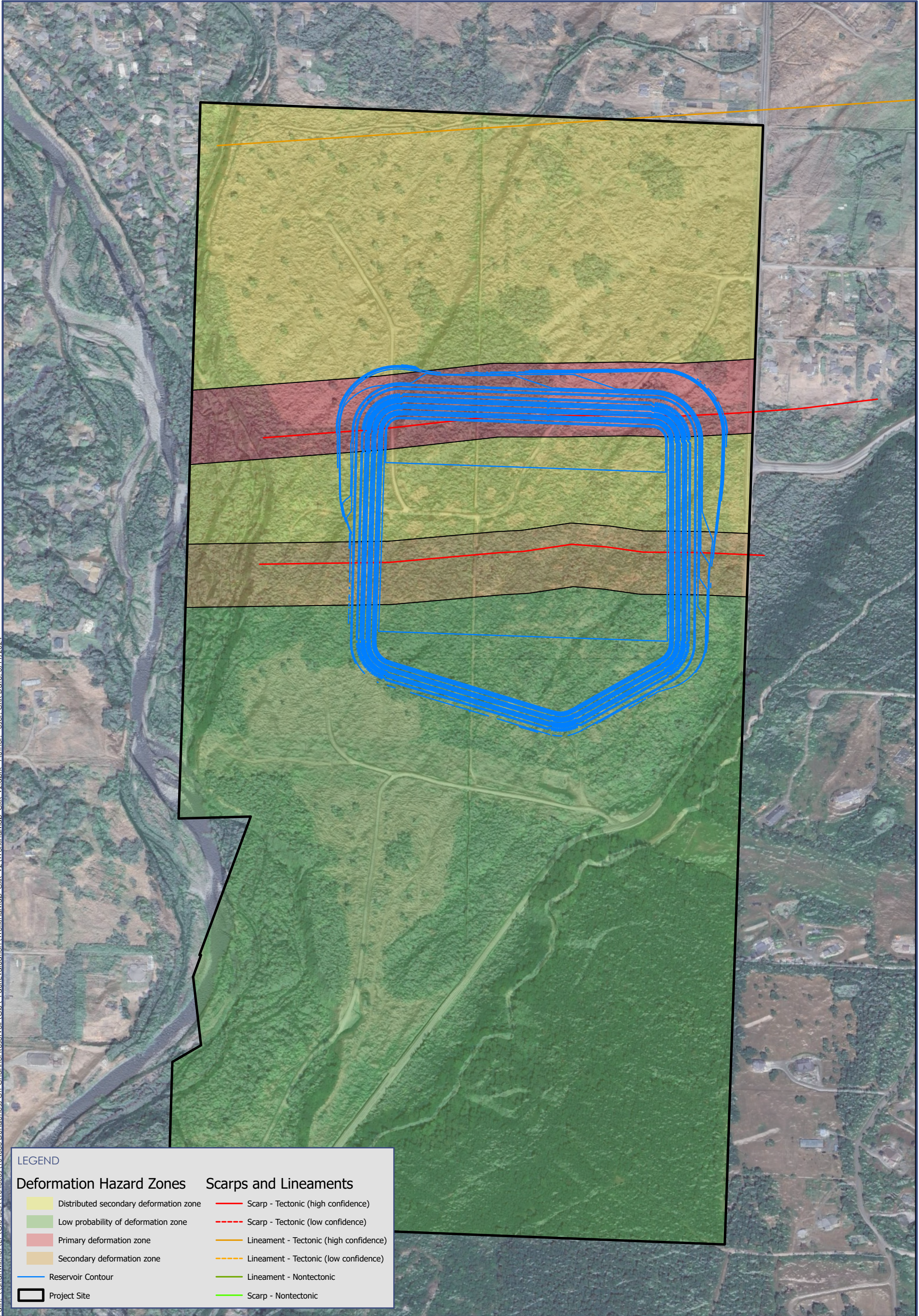
<b>Deformation Hazard Zones</b>	<b>Scarps and Lineaments</b>
<span style="display:inline-block; width:15px; height:10px; background-color:yellow; border:1px solid black;"></span> Distributed secondary deformation zone	<span style="display:inline-block; width:15px; border-bottom:2px solid red;"></span> Scarp - Tectonic (high confidence)
<span style="display:inline-block; width:15px; height:10px; background-color:lightgreen; border:1px solid black;"></span> Low probability of deformation zone	<span style="display:inline-block; width:15px; border-bottom:2px dashed red;"></span> Scarp - Tectonic (low confidence)
<span style="display:inline-block; width:15px; height:10px; background-color:lightcoral; border:1px solid black;"></span> Primary deformation zone	<span style="display:inline-block; width:15px; border-bottom:2px solid orange;"></span> Lineament - Tectonic (high confidence)
<span style="display:inline-block; width:15px; height:10px; background-color:lightgoldenrod; border:1px solid black;"></span> Secondary deformation zone	<span style="display:inline-block; width:15px; border-bottom:2px dashed orange;"></span> Lineament - Tectonic (low confidence)
<span style="display:inline-block; width:15px; border-bottom:2px solid blue;"></span> Reservoir Contour	<span style="display:inline-block; width:15px; border-bottom:2px solid green;"></span> Lineament - Nontectonic
<span style="display:inline-block; width:15px; border-bottom:2px solid black;"></span> Project Site	<span style="display:inline-block; width:15px; border-bottom:2px solid lime;"></span> Scarp - Nontectonic



Notes:  
1. Aerial image courtesy of Google



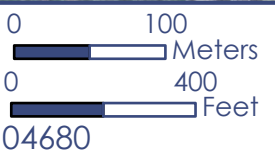




Path: \\shannonwilson\efs\SEA\104680\Dungeness Off-Channel Reservoir\CAD\Fault\Evaluation\WorkingMap\_Cxk\_v2.aprx Author: User: CXK Date: 3/11/2024

**LEGEND**

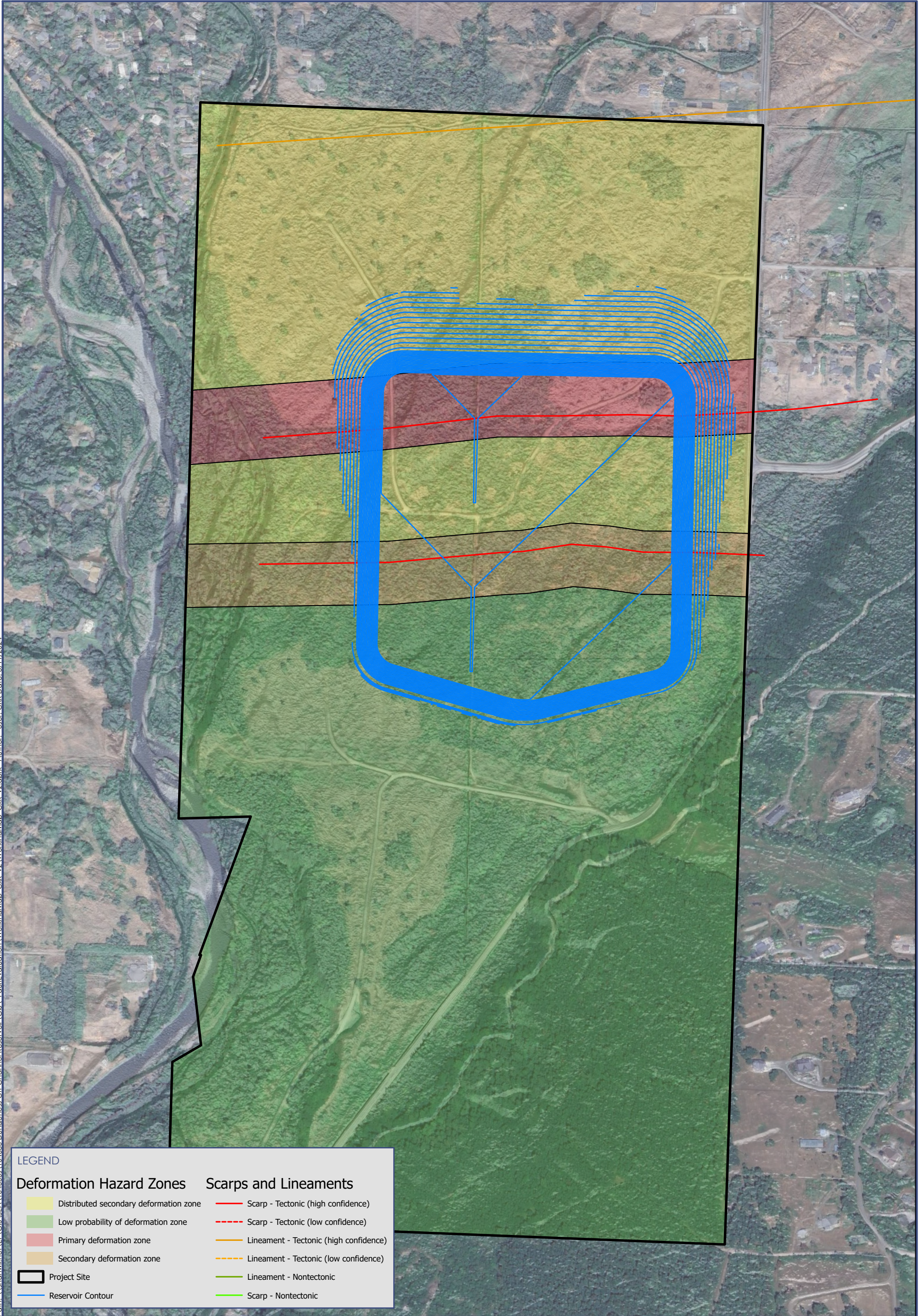
<b>Deformation Hazard Zones</b>	<b>Scarps and Lineaments</b>
<span style="display:inline-block; width:15px; height:10px; background-color:yellow; border:1px solid black;"></span> Distributed secondary deformation zone	<span style="display:inline-block; width:15px; border-bottom:2px solid red;"></span> Scarp - Tectonic (high confidence)
<span style="display:inline-block; width:15px; height:10px; background-color:lightgreen; border:1px solid black;"></span> Low probability of deformation zone	<span style="display:inline-block; width:15px; border-bottom:2px dashed red;"></span> Scarp - Tectonic (low confidence)
<span style="display:inline-block; width:15px; height:10px; background-color:lightcoral; border:1px solid black;"></span> Primary deformation zone	<span style="display:inline-block; width:15px; border-bottom:2px solid orange;"></span> Lineament - Tectonic (high confidence)
<span style="display:inline-block; width:15px; height:10px; background-color:lightgoldenrod; border:1px solid black;"></span> Secondary deformation zone	<span style="display:inline-block; width:15px; border-bottom:2px dashed orange;"></span> Lineament - Tectonic (low confidence)
<span style="display:inline-block; width:15px; border-bottom:2px solid blue;"></span> Reservoir Contour	<span style="display:inline-block; width:15px; border-bottom:2px solid green;"></span> Lineament - Nontectonic
<span style="display:inline-block; width:15px; border-bottom:2px solid black;"></span> Project Site	<span style="display:inline-block; width:15px; border-bottom:2px solid lime;"></span> Scarp - Nontectonic



**Notes:**  
1. Aerial image courtesy of Google







Path: \\shannonwil\ne\VEE\CIS\SEA\104680\Dungeness Off-Channel Reservoir\CIS\Fault\Evaluation\WorkingMap\_CxK\_v2.aprx Author: User: CXK Date: 3/11/2024

**LEGEND**

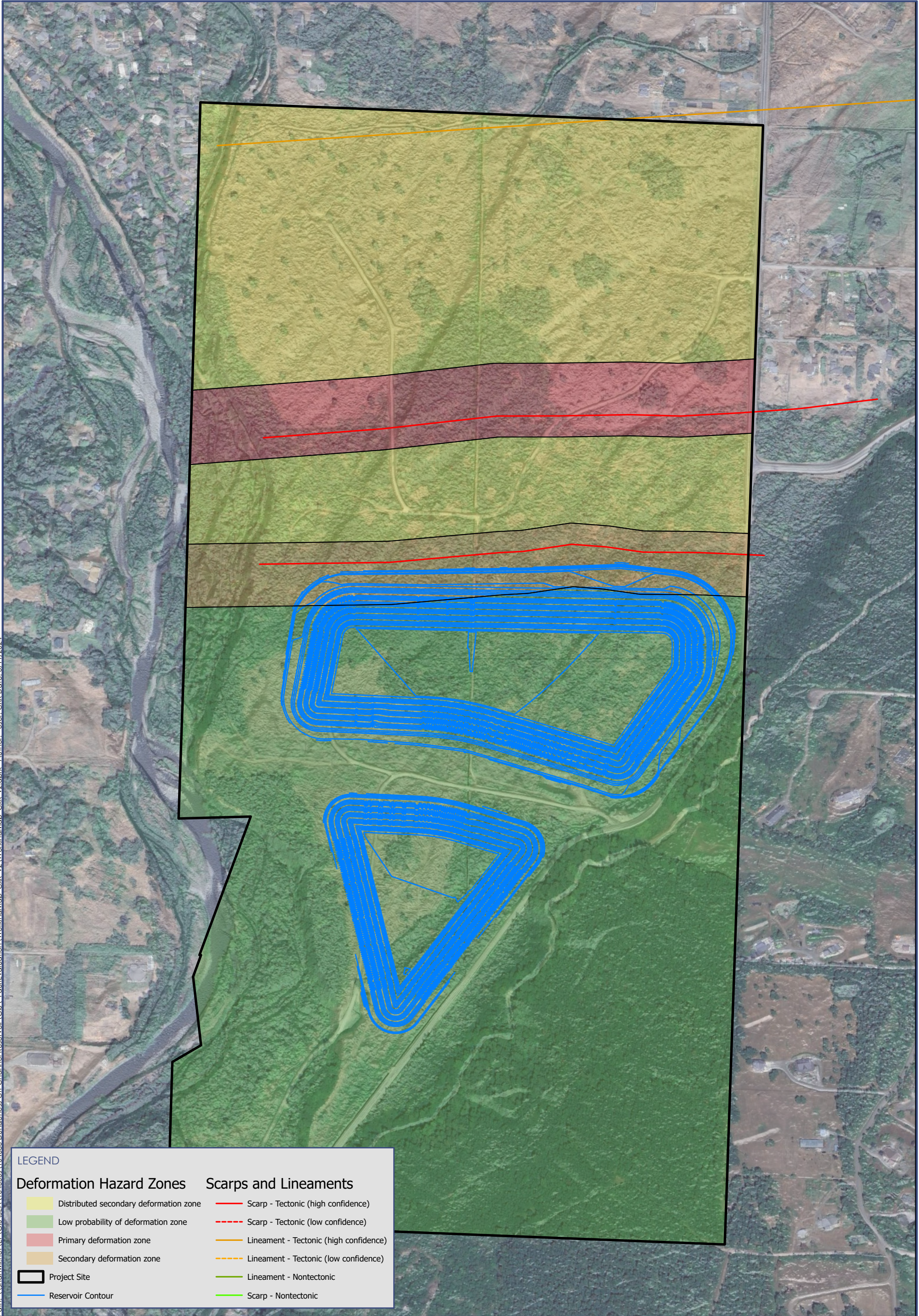
<b>Deformation Hazard Zones</b>	<b>Scarps and Lineaments</b>
<span style="display:inline-block; width:15px; height:10px; background-color:yellow; border:1px solid black;"></span> Distributed secondary deformation zone	<span style="display:inline-block; width:15px; border-bottom:2px solid red;"></span> Scarp - Tectonic (high confidence)
<span style="display:inline-block; width:15px; height:10px; background-color:lightgreen; border:1px solid black;"></span> Low probability of deformation zone	<span style="display:inline-block; width:15px; border-bottom:2px dashed red;"></span> Scarp - Tectonic (low confidence)
<span style="display:inline-block; width:15px; height:10px; background-color:red; border:1px solid black;"></span> Primary deformation zone	<span style="display:inline-block; width:15px; border-bottom:2px solid orange;"></span> Lineament - Tectonic (high confidence)
<span style="display:inline-block; width:15px; height:10px; background-color:tan; border:1px solid black;"></span> Secondary deformation zone	<span style="display:inline-block; width:15px; border-bottom:2px dashed orange;"></span> Lineament - Tectonic (low confidence)
<span style="display:inline-block; width:15px; height:10px; border:2px solid black;"></span> Project Site	<span style="display:inline-block; width:15px; border-bottom:2px solid green;"></span> Lineament - Nontectonic
<span style="display:inline-block; width:15px; border-bottom:2px solid blue;"></span> Reservoir Contour	<span style="display:inline-block; width:15px; border-bottom:2px solid lightblue;"></span> Scarp - Nontectonic

0 100  
Meters  
0 400  
Feet  
104680

Notes:  
1. Aerial image courtesy of Google







Path: \\shannonwilson\efs\SEA\104680\Dungeness Off-Channel Reservoir\CAD\Fault\Evaluation\WorkingMap\_CxK\_v2\WorkingMap\_CxK\_v2.aprx\_Author: User: CXK Date: 3/11/2024

0 100  
Meters  
0 400  
Feet  
104680

Notes:  
1. Aerial image courtesy of Google





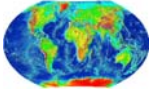
Appendix A

# Geophysical Report

## CONTENTS

- Report for Multichannel Analysis of Surface Wave Survey for the Proposed Dungeness Off-Channel Reservoir, Sequim, WA (Global Geophysics, 2023)





## Global Geophysics

P.O. Box 2229  
Redmond, WA 98073-2229

Tel: 425-890-4321  
Fax: 206-5820-0838

---

January 6, 2023

Our ref: 112-1027.000

Anchor QEA, LLC  
1201 3rd Avenue, Suite 2600  
Seattle, WA 98101

Attention: Mr. David Rice, P.E.

**RE: REPORT FOR MULTICHANNEL ANALYSIS OF SURFACE WAVE SURVEY FOR THE PROPOSED DUNGENESS OFF-CHANNEL RESERVOIR, SEQUIM, WA**

Dear Mr. Rice:

Global Geophysics LLC. conducted multichannel analysis of surface wave (MASW) survey with a field assistant from Shannon & Wilson for the proposed Dungeness Off-Channel Reservoir, Sequim, WA in November and December 2022. The objective of the study is to determine the depths to the top of the till encountered in the previous borings.

### **GEOPHYSICAL METHODS AND FIELD PROCEDURES**

Multi-channel analysis of surface wave (MASW) was used for this project. The following paragraphs describe the method and field procedure.

#### **Multi-channel analysis of surface wave**

The Multichannel Analysis of Surface Waves (MASW) method determines variations in surface wave velocities with increasing distances and wavelengths. The data from these measurements are used to model the shear wave velocities of the subsurface. This information can then be used to infer rock/soil types, stratigraphy and soil conditions.

The MASW survey requires a seismic source, to generate surface-waves, and at least 24 geophones, to measure the ground response at increasing distances from the source. Surface waves are a special type of seismic wave whose propagation is confined to the near surface medium. The depth of subsurface penetration of a surface-wave is directly proportional to its wavelength. In a non-homogeneous medium, surface-waves are dispersive, i.e. each wavelength has a characteristic velocity stemming from subsurface heterogeneities. The relationship between surface-wave velocity and wavelength is used to calculate the shear-wave velocity of the medium with increasing depth.

The seismic source can be either active or passive, depending on the application and location of the survey. Examples of active sources include explosives, weight-drops, and vibrating pads. Examples of passive sources are drill rigs, road traffic, micro-tremors, and water-wave action (in near-shore environments). Geophone measures the arrival time of the various components of the surface wave-train traveling from the seismic source.

The surface-wave velocity with respect to frequency (called the ‘dispersion curve’) is determined by measuring the delay time in wave propagation between the geophones. The dispersion curve is then matched to a theoretical dispersion curve using an iterative forward-modeling procedure. The result is a profile of shear-wave velocity versus depth. This shear wave profile can be with used other parameters such as density, to estimate the dynamic shear modulus of the medium as a function of depth.

The MASW survey was conducted using Geometrics Geode 48-channel digital seismographs. The sensors were Geospace geophones placed at 5 ft spacing. The seismic energy sources were a 20 lb sledgehammer.

## **RESULTS**

The surface wave data were collected along nine transects (Lines 1, 2, 3, 5, 6, 8, 9, 10 and 11). Due to the budget constrain, data were not collected along Lines 4 and 7. The approximate line locations are shown in Figure 1. The s-wave velocity profiles are presented in Figures 2-8.

The data was collected every 20 ft along Line 1 using moving geophone array. Fixed geophone array was used at end of the lines. The data were processed with SeisImager.

- Line 1 (Figure 2): The interpreted depth to top of the till varies between 0 and 42 ft. The localized relative low velocity zones below 40 ft bgs between stations 1100 and 2200 (green color) are likely related to the meandering of the stream bed.
- Line 2 (Figure 3): The interpreted depth to top of the till varies between 0 and 25 ft.
- Line 3 (Figure 4): The interpreted depth to top of the till varies between 18 and 55 ft.
- Line 5 (Figure 5): The interpreted depth to top of the till varies between 19 and 48 ft.
- Line 6 (Figure 6): The interpreted depth to top of the till varies between 25 and 50 ft.
- Line 8 (Figure 7): The interpreted depth to top of the till varies between 16 and 38 ft.
- Line 9 (Figure 7): The interpreted depth to top of the till varies between 10 and 38 ft.
- Line 10 (Figure 8): The interpreted depth to top of the till varies between 16 and 40 ft.
- Line 11 (Figure 8): The interpreted depth to top of the till varies between 19 and over 60 ft.



## **LIMITATION OF GEOPHYSICAL METHODS**

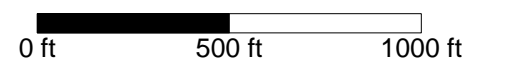
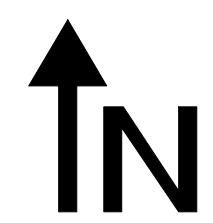
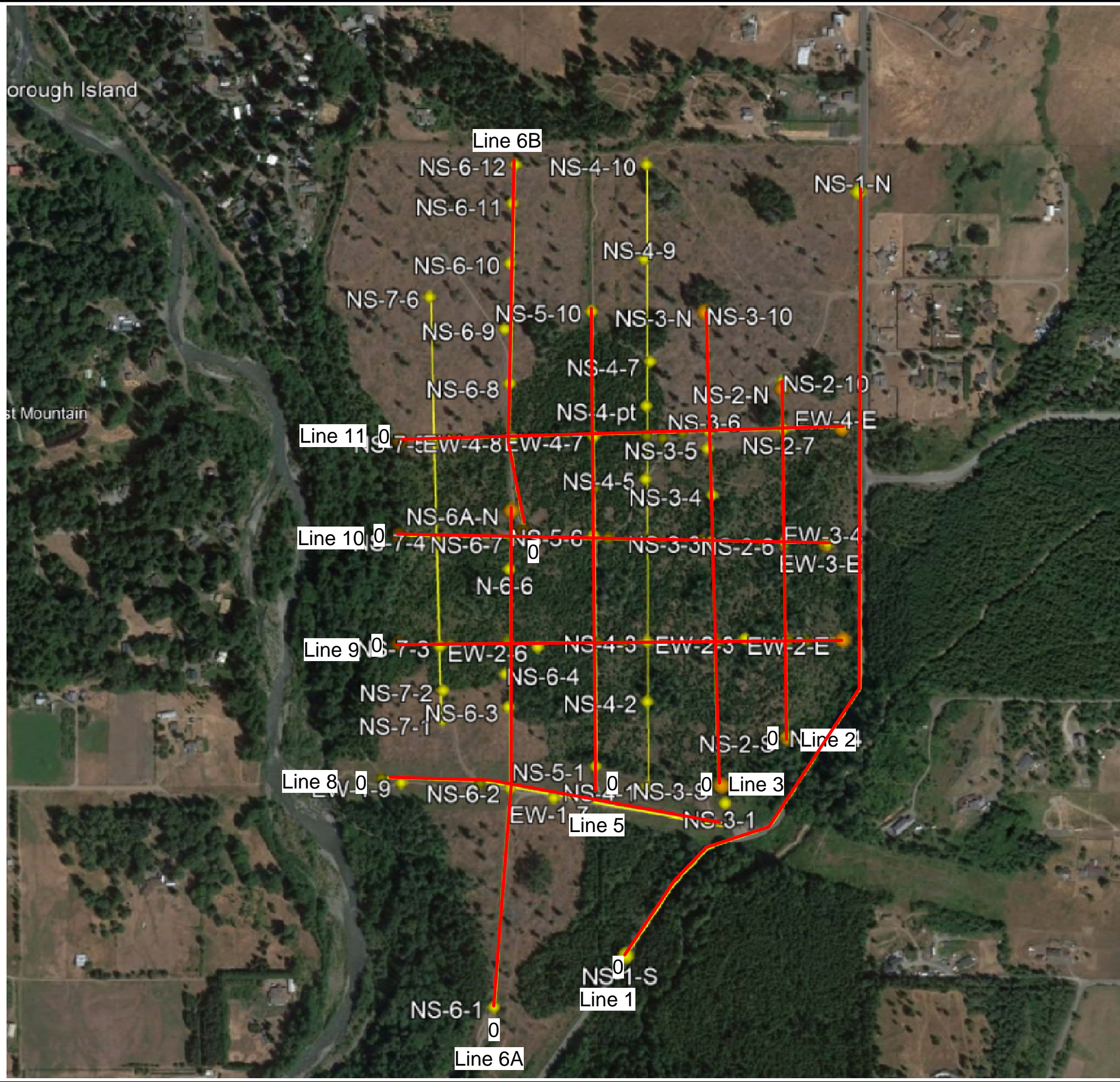
Global geophysics services are conducted in a manner consistent with the level of care and skill ordinarily exercised by other members of the geophysical community currently practicing under similar conditions subject to the time limits and financial and physical constraints applicable to the services. MASW is a remote sensing geophysical method that may not detect all subsurface conditions due to the limitations of the methods, soil conditions, size of the features and their depths. In general, the errors in the interpreted depths and velocities, dependent on the resolution of the technique, are estimated to be approximately  $\pm 15\%$  of the true depths and velocities.

Sincerely,

**Global Geophysics**

A handwritten signature in black ink, appearing to read "John Liu", with a stylized flourish at the end.

John Liu, Ph.D., R.G.  
Principal Geophysicist

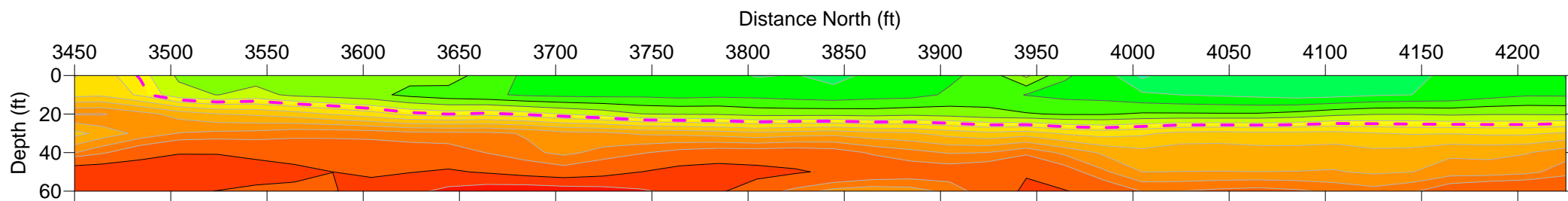
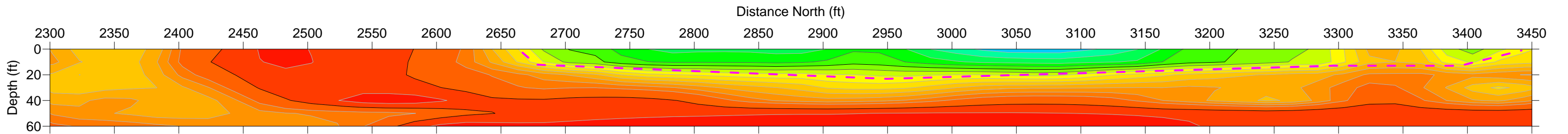
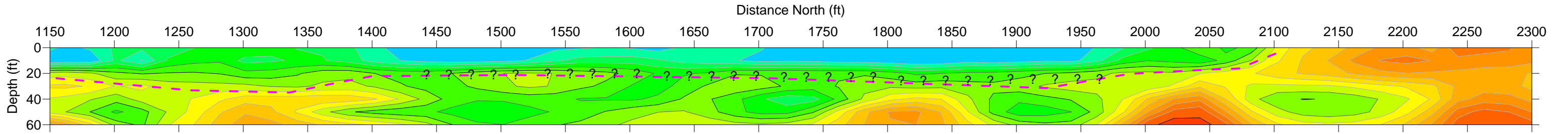
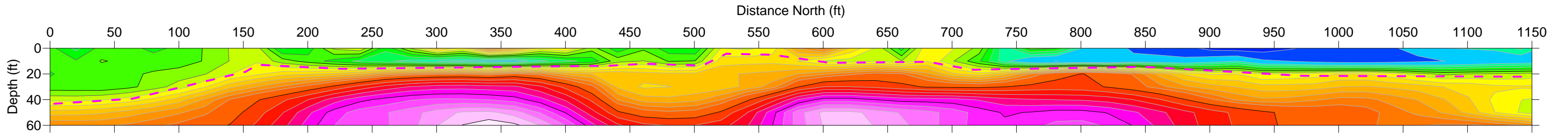


Note: No data were collected along proposed Line 4 and Line 7

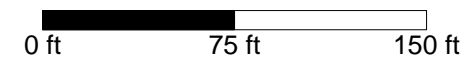
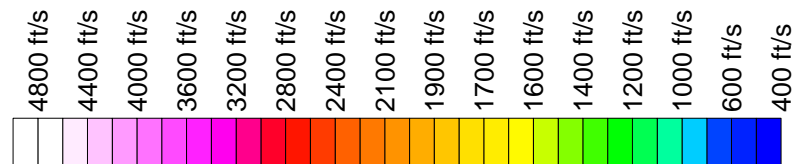
PROJECT			<b>Dungeness Off-Channel Reservoir Sequim, Washington</b>	
TITLE			<b>Site Map</b>	
<b>Global Geophysics</b> P.O. Box 2229 Redmond, WA 98073-2229 Tel: 425-890-4321	Project #:		FILE No.	
	DESIGN	--	SCALE	AS SHOWN   REV.
	CADD	EJ		
	CHECK	JL		
	REVIEW	--		<b>FIGURE 1</b>



Line 1

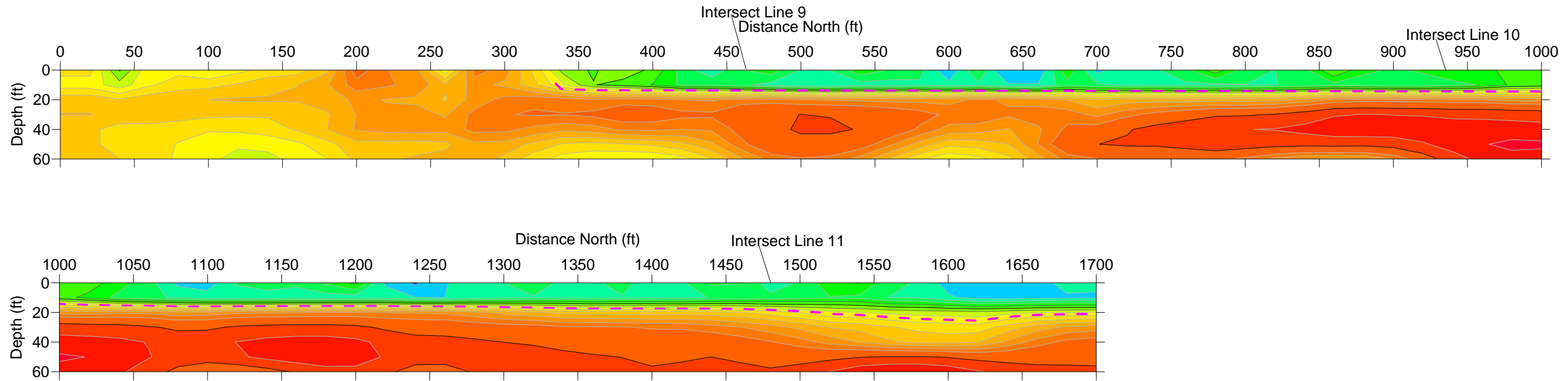


Legend:  
 - - - - - Interpreted top of the till



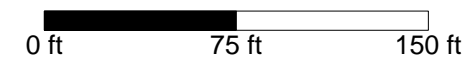
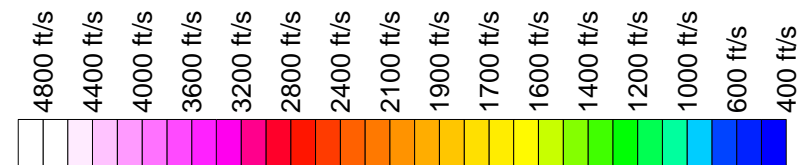
PROJECT			<b>Dungeness Off-Channel Reservoir Sequim, Washington</b>	
TITLE				
<b>Line 1 S-Wave Profile</b>				
Global Geophysics P.O. Box 2229 Redmond, WA 98073-2229 Tel: 425-890-4321	Project #:		FILE No.:	
	DESIGN	--	SCALE	AS SHOWN [REV]
	CADD	EJ		
	CHECK	JL		
	REVIEW	--		<b>FIGURE 2</b>

Line 2



Legend:

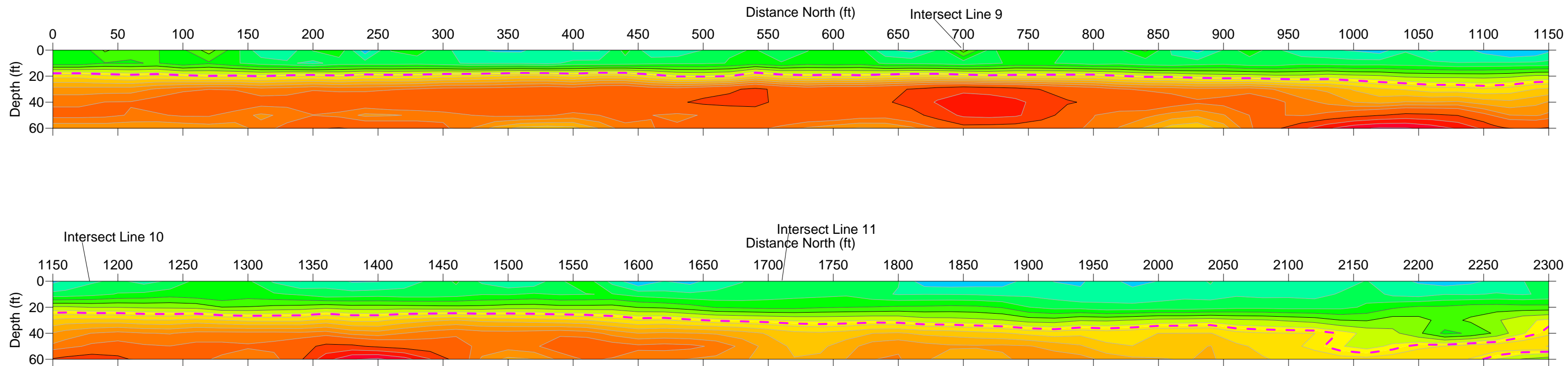
--- Interpreted top of the till



PROJECT		
<b>Dungeness Off-Channel Reservoir Sequim, Washington</b>		
TITLE		
<b>Line 2 S-Wave Profile</b>		
Global Geophysics	Project #:	FILE No.
P.O. Box 2229	DESIGN --	SCALE AS SHOWN
Redmond, WA 98073-2229	CADD EJ	REV.
Tel: 425-890-4321	CHECK JL	<b>FIGURE 3</b>
	REVIEW --	

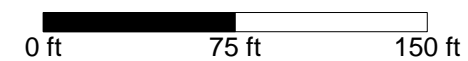
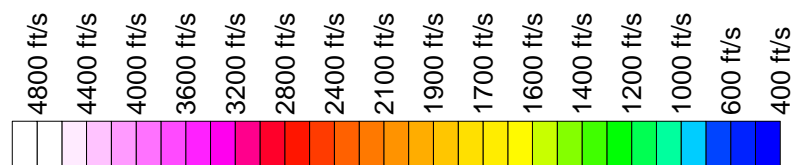


Line 3



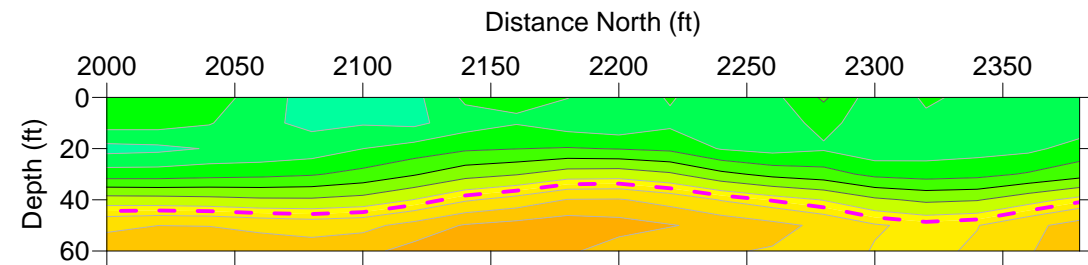
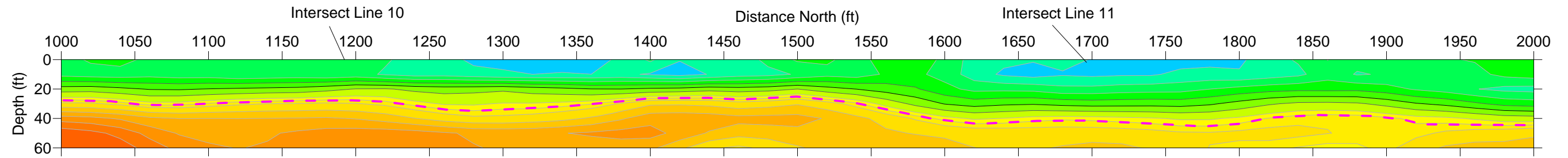
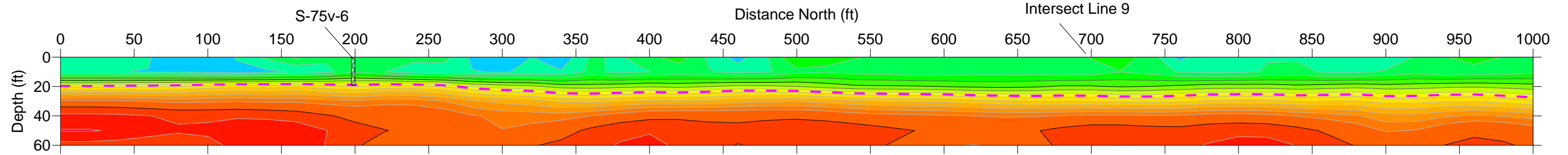
Legend:

--- Interpreted top of the till



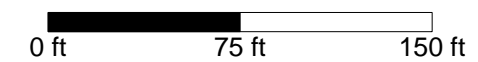
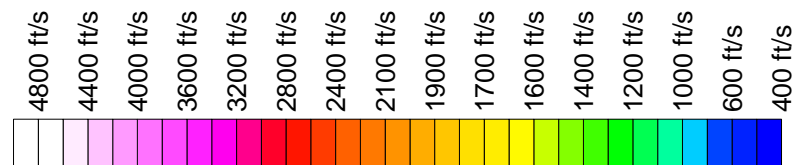
PROJECT		
<b>Dungeness Off-Channel Reservoir Sequim, Washington</b>		
TITLE		
<b>Line 3 S-Wave Profile</b>		
Global Geophysics P.O. Box 2229 Redmond, WA 98073-2229 Tel: 425-890-4321	Project #:	FILE No.
	DESIGN --	SCALE AS SHOWN REV.
	CADD EJ	
	CHECK JL	
REVIEW --		<b>FIGURE 4</b>

Line 5



Legend:

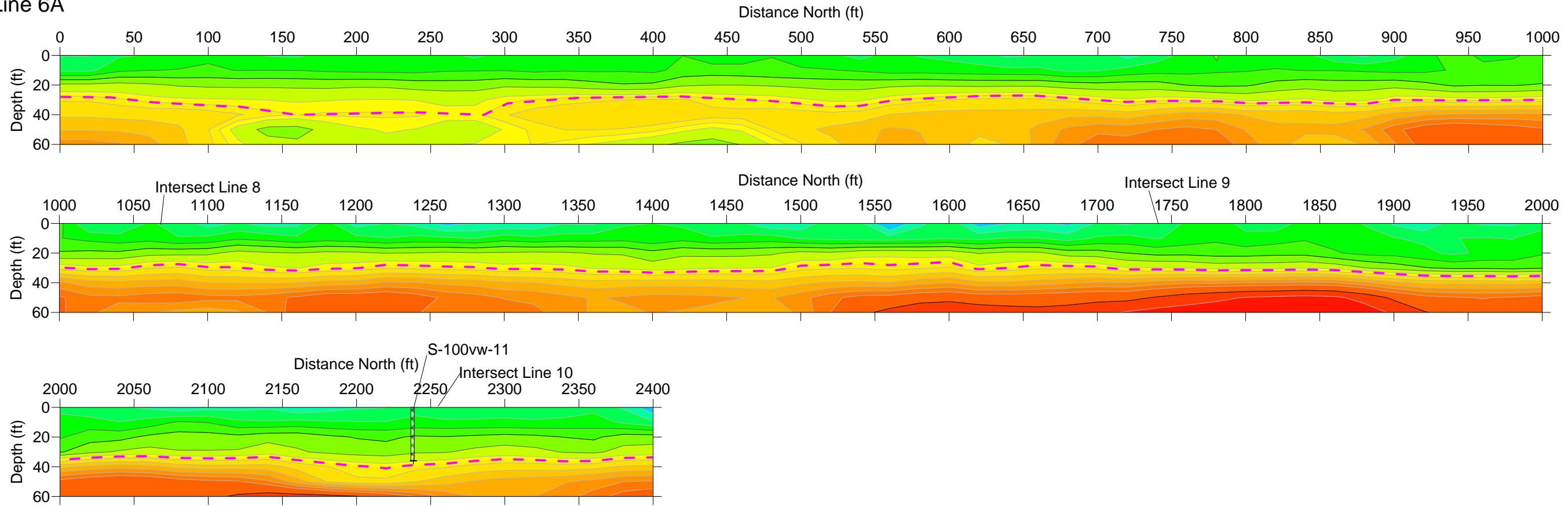
--- Interpreted top of the till



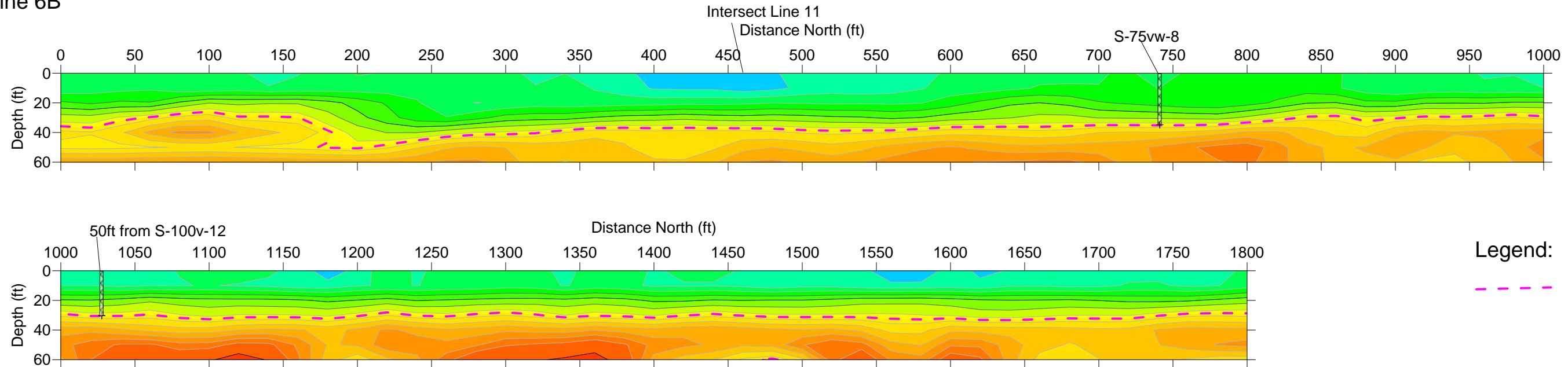
PROJECT			<b>Dungeness Off-Channel Reservoir Sequim, Washington</b>	
TITLE			<b>Line 5 S-Wave Profile</b>	
Global Geophysics P.O. Box 2229 Redmond, WA 98073-2229 Tel: 425-890-4321	Project #:		FILE No.:	
	DESIGN	--	SCALE	AS SHOWN   REV.
	CADD	EJ		
	CHECK	JL		
	REVIEW	--		<b>FIGURE 5</b>



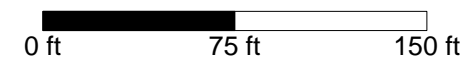
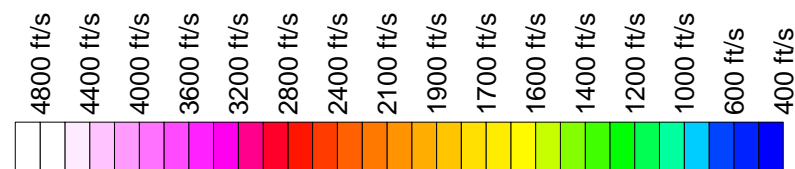
Line 6A



Line 6B

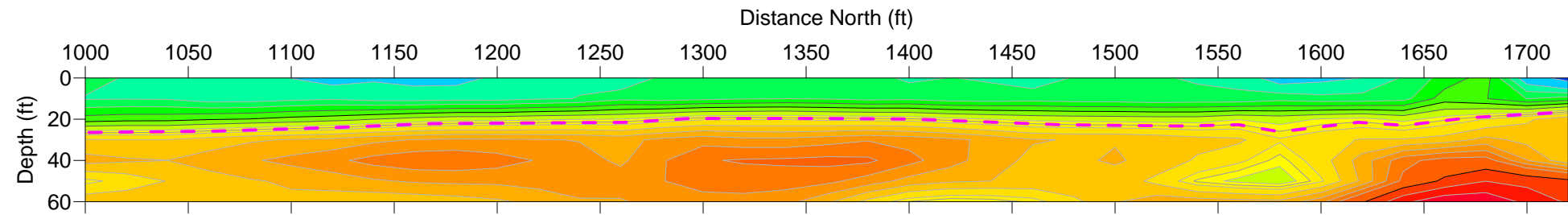
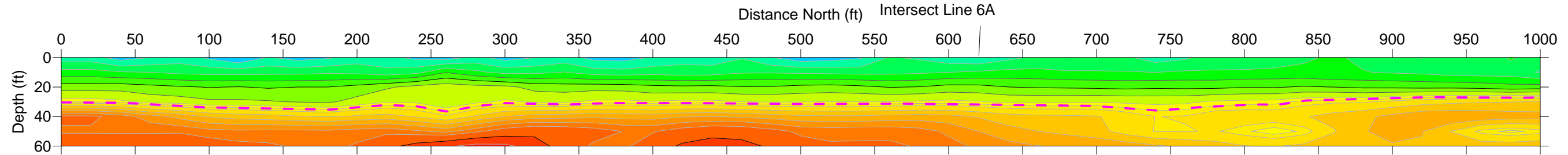


**Legend:**  
 - - - - - Interpreted top of the till

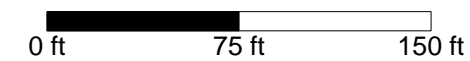
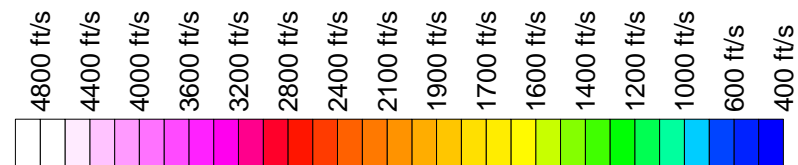
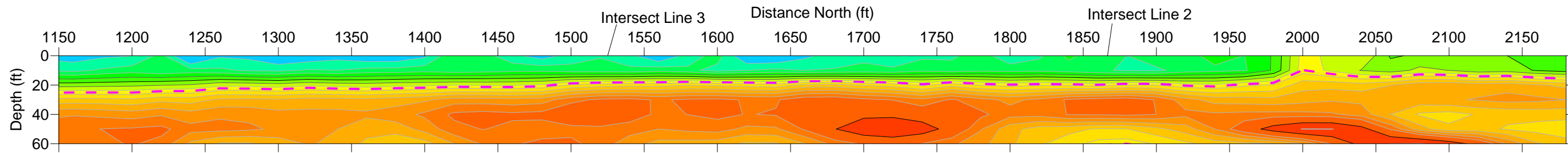
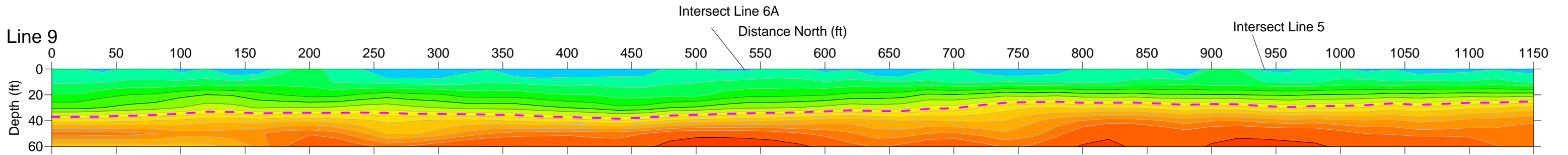


PROJECT			<b>Dungeness Off-Channel Reservoir Sequim, Washington</b>	
TITLE			<b>Lines 6A and 6B S-Wave Profiles</b>	
Global Geophysics P.O. Box 2229 Redmond, WA 98073-2229 Tel: 425-890-4321	Project #:		FILE No.:	
	DESIGN:	--	SCALE:	AS SHOWN   REV.
	CADD:	EJ		
	CHECK:	JL		
	REVIEW:	--		<b>FIGURE 6</b>

Line 8



Line 9



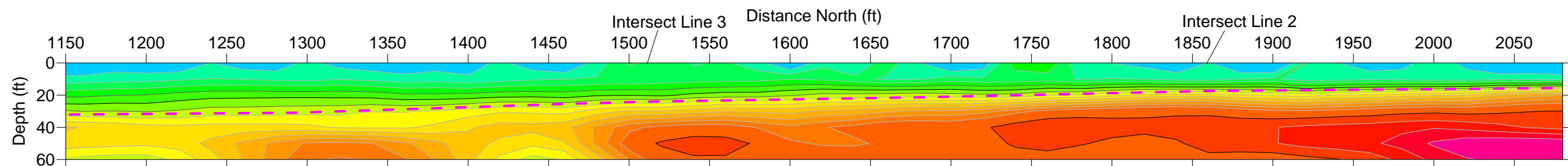
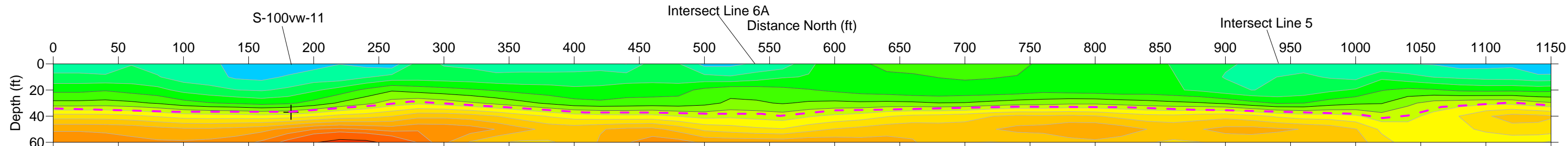
Legend:

--- Interpreted top of the till

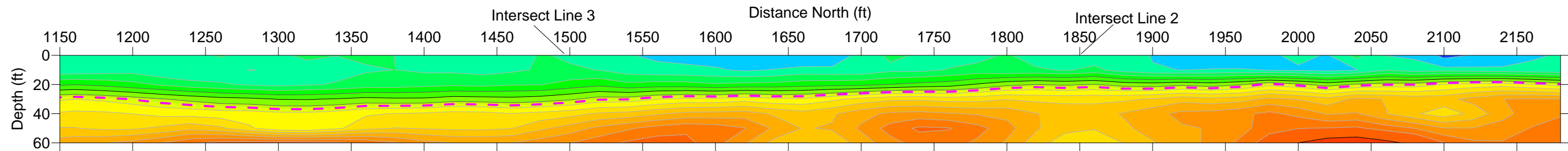
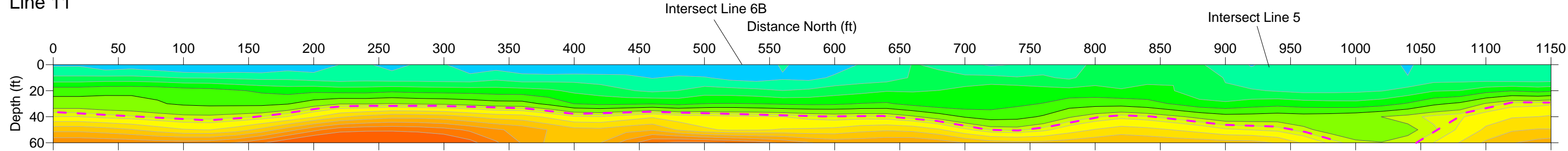
PROJECT			
<b>Dungeness Off-Channel Reservoir Sequim, Washington</b>			
TITLE			
<b>Lines 8 and 9 S-Wave Profiles</b>			
Global Geophysics P.O. Box 2229 Redmond, WA 98073-2229 Tel: 425-890-4321	Project #:	FILE No.	
	DESIGN --	SCALE AS SHOWN	REV.
	CADD EJ		
	CHECK JL		
	REVIEW --		<b>FIGURE 7</b>



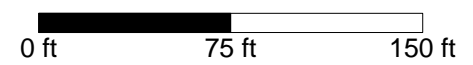
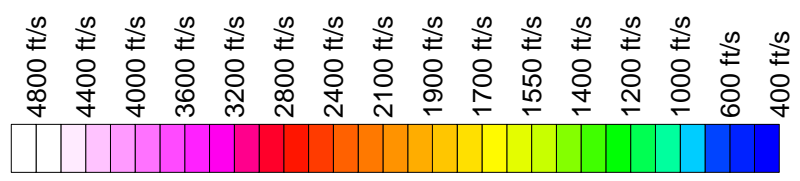
Line 10



Line 11



Legend:  
 - - - - - Interpreted top of the till



PROJECT			
<b>Dungeness Off-Channel Reservoir Sequim, Washington</b>			
TITLE			
<b>Lines 10 and 11 S-Wave Profiles</b>			
Global Geophysics P.O. Box 2229 Redmond, WA 98073-2229 Tel: 425-890-4321	Project #:	FILE No.:	
	DESIGN --	SCALE AS SHOWN	REV.
	CADD EJ		
	CHECK JL		
	REVIEW --		<b>FIGURE 8</b>

# Important Information

About Your Geotechnical/Environmental Report

IMPORTANT INFORMATION



## CONSULTING SERVICES ARE PERFORMED FOR SPECIFIC PURPOSES AND FOR SPECIFIC CLIENTS.

Consultants prepare reports to meet the specific needs of specific individuals. A report prepared for a civil engineer may not be adequate for a construction contractor or even another civil engineer. Unless indicated otherwise, your consultant prepared your report expressly for you and expressly for the purposes you indicated. No one other than you should apply this report for its intended purpose without first conferring with the consultant. No party should apply this report for any purpose other than that originally contemplated without first conferring with the consultant.

## THE CONSULTANT'S REPORT IS BASED ON PROJECT-SPECIFIC FACTORS.

A geotechnical/environmental report is based on a subsurface exploration plan designed to consider a unique set of project-specific factors. Depending on the project, these may include the general nature of the structure and property involved; its size and configuration; its historical use and practice; the location of the structure on the site and its orientation; other improvements such as access roads, parking lots, and underground utilities; and the additional risk created by scope-of-service limitations imposed by the client. To help avoid costly problems, ask the consultant to evaluate how any factors that change subsequent to the date of the report may affect the recommendations. Unless your consultant indicates otherwise, your report should not be used (1) when the nature of the proposed project is changed (for example, if an office building will be erected instead of a parking garage, or if a refrigerated warehouse will be built instead of an unrefrigerated one, or chemicals are discovered on or near the site); (2) when the size, elevation, or configuration of the proposed project is altered; (3) when the location or orientation of the proposed project is modified; (4) when there is a change of ownership; or (5) for application to an adjacent site. Consultants cannot accept responsibility for problems that may occur if they are not consulted after factors that were considered in the development of the report have changed.

## SUBSURFACE CONDITIONS CAN CHANGE.

Subsurface conditions may be affected as a result of natural processes or human activity. Because a geotechnical/environmental report is based on conditions that existed at the time of subsurface exploration, construction decisions should not be based on a report whose adequacy may have been affected by time. Ask the consultant to advise if additional tests are desirable before construction starts; for example, groundwater conditions commonly vary seasonally.

Construction operations at or adjacent to the site and natural events such as floods, earthquakes, or groundwater fluctuations may also affect subsurface conditions and, thus, the continuing adequacy of a geotechnical/environmental report. The consultant should be kept apprised of any such events and should be consulted to determine if additional tests are necessary.

## MOST RECOMMENDATIONS ARE PROFESSIONAL JUDGMENTS.

Site exploration and testing identifies actual surface and subsurface conditions only at those points where samples are taken. The data were extrapolated by your consultant, who then applied judgment to render an opinion about overall subsurface conditions. The actual interface between materials may be far more gradual or abrupt than your report indicates. Actual conditions in areas not sampled may differ from those predicted in your report. While nothing can be done to prevent such situations, you and your consultant can work together to help reduce their impacts. Retaining

your consultant to observe subsurface construction operations can be particularly beneficial in this respect.

### A REPORT'S CONCLUSIONS ARE PRELIMINARY.

The conclusions contained in your consultant's report are preliminary, because they must be based on the assumption that conditions revealed through selective exploratory sampling are indicative of actual conditions throughout a site. Actual subsurface conditions can be discerned only during earthwork; therefore, you should retain your consultant to observe actual conditions and to provide conclusions. Only the consultant who prepared the report is fully familiar with the background information needed to determine whether or not the report's recommendations based on those conclusions are valid and whether or not the contractor is abiding by applicable recommendations. The consultant who developed your report cannot assume responsibility or liability for the adequacy of the report's recommendations if another party is retained to observe construction.

### THE CONSULTANT'S REPORT IS SUBJECT TO MISINTERPRETATION.

Costly problems can occur when other design professionals develop their plans based on misinterpretation of a geotechnical/environmental report. To help avoid these problems, the consultant should be retained to work with other project design professionals to explain relevant geotechnical, geological, hydrogeological, and environmental findings, and to review the adequacy of their plans and specifications relative to these issues.

### BORING LOGS AND/OR MONITORING WELL DATA SHOULD NOT BE SEPARATED FROM THE REPORT.

Final boring logs developed by the consultant are based upon interpretation of field logs (assembled by site personnel), field test results, and laboratory and/or office evaluation of field samples and data. Only final boring logs and data are customarily included in geotechnical/environmental reports. These final logs should not, under any circumstances, be redrawn for inclusion in architectural or other design drawings, because drafters may commit errors or omissions in the transfer process.

To reduce the likelihood of boring log or monitoring well misinterpretation, contractors should be given ready access to the complete geotechnical engineering/environmental report prepared or authorized for their use. If access is provided only to the report prepared for you, you should advise contractors of the report's limitations, assuming that a contractor was not one of the specific persons for whom the report was prepared, and that developing construction cost estimates was not one of the specific purposes for which it was prepared. While a contractor may gain important knowledge from a report prepared for another party, the contractor should discuss the report with your consultant and perform the additional or alternative work believed necessary to obtain the data specifically appropriate for construction cost estimating purposes. Some clients hold the mistaken impression that simply disclaiming responsibility for the accuracy of subsurface information always insulates them from attendant liability. Providing the best available information to contractors helps prevent costly construction problems and the adversarial attitudes that aggravate them to a disproportionate scale.



## READ RESPONSIBILITY CLAUSES CLOSELY.

Because geotechnical/environmental engineering is based extensively on judgment and opinion, it is far less exact than other design disciplines. This situation has resulted in wholly unwarranted claims being lodged against consultants. To help prevent this problem, consultants have developed a number of clauses for use in their contracts, reports, and other documents. These responsibility clauses are not exculpatory clauses designed to transfer the consultant's liabilities to other parties; rather, they are definitive clauses that identify where the consultant's responsibilities begin and end. Their use helps all parties involved recognize their individual responsibilities and take appropriate action. Some of these definitive clauses are likely to appear in your report, and you are encouraged to read them closely. Your consultant will be pleased to give full and frank answers to your questions.

**The preceding paragraphs are based on information provided by the ASFE/Association of Engineering Firms Practicing in the Geosciences, Silver Spring, Maryland.**

IMPORTANT INFORMATION